Unnatural MUC1 based glycopeptides in early stage breast cancer biomarkers discovery

(非天然型 MUC1 糖ペプチドによる乳がん早期バイオマーカーの探索)

Doctoral Dissertation

2021 March

Pablo Adrián Guillén Poza

Laboratory of Advanced Chemical Biology

Graduate School of Life Science, Hokkaido University

Table of Contents

Abstract

Mucin 1 (MUC1) is a highly glycosylated *O*-glycoprotein that experiences alterations in cancer cells and assists the tumor progression. In many human carcinomas and, in particular in breast cancer, MUC1 is overexpressed and aberrantly glycosylated. As a consequence, previously covered antigens are now exposed and accessible to the immune system. This results in the production of antibodies towards these neoepitopes, providing an exploitable divergence between healthy individuals and cancer patients antibody profiles. In order to properly differentiate and develop specific diagnostic tools for early breast cancer detection, we require of the appropriate chemical probes.

In this thesis, we have focused on the MUC1 tumor-associated carbohydrate Tn antigen (*α*-*O*-GalNAc-Ser/Thr) because of its tumor high specificity, well-defined chemical structure and starting point role for more complex tumor antigens. Previous studies report the use of autoantibodies as potential cancer biosensors. With the intention of developing a more effective and robust sensing device we considered the substitution of GalNAc monosaccharides by stable glycomimic units. To investigate our hypothesis, two different glycopeptide libraries presenting the natural Tn antigen or the sp^2-iminosugar-derived unnatural analog were produced through microwave assisted solid-phase peptide synthesis. The whole glycopeptide collection was then evaluated with anti-MUC1 (SM3, VU-3C6, and VU-11E2) monoclonal antibodies (mAbs) in a microarray platform. The most promising candidates were tested with healthy, stage I and stage IV breast cancer sera with the aim of discovering serological autoantibodies (autoAbs) as stage-dependent breast cancer diagnostic biomarkers.

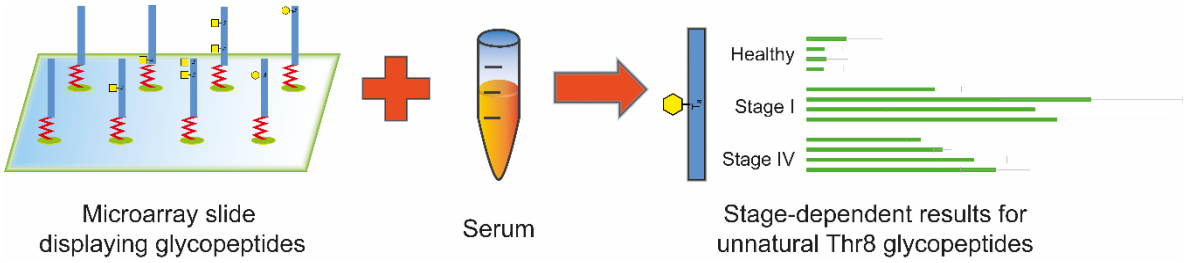

Despite the variability between mAbs, the suitability of the glycopeptides bearing the unnatural sp^2-iminosugar-based Tn antigen mimic to detect anti-MUC1 antibodies was demonstrated. The present results also revealed that the glycopeptide mimic-antibody interactions are glycosylation pattern-specific and underlined the crucial contribution of the PDTR epitope embedded in the glycopeptide backbone to mAbs binding. Furthermore, stage I breast cancer serum experiments clearly showed autoAbs binding with a specific sp^2-iminosugar glycopeptide with almost no interaction with healthy serum, results which will promote further studies on their function as early cancer biomarkers.

Abbreviations

Ac_2O	Acetic anhydride
ACN	Acetonitrile
autoAbs	Autoantibodies
DCM	Dichloromethane
DHB	2,5-Dihydroxybenzoic acid
DIEA	*N*,*N*-Diisopropylethylamine
DMF	*N*,*N*-dimethylformamide
eq	Equivalent
HBTU	2-(1H-benzotriazole-1-yl)-1,1,3,3-tetramethyluronium hexafluorophosphate
HOAt	1-hydroxy-7-azabenzotriazole
HOBt	1-hydroxybenzotriazole monohydrate
IgG	Immunoglobulin G
Ketone linker	5-Oxohexanoic acid
mAbs	Monoclonal antibodies
MALDI-TOF	Matrix-assisted laser desorption/ionization-time of flight
MeOH	Methanol
MS	Mass spectrometry
MTBE	Methyl *tert*-butyl ether
MUC1	Mucin 1

MW	Microwave
***N*-protected AO/PC-copolymer**	(2-methacryloyloxyethylphosphorylcholinecyclohexylmethacrylate-*N*-[2-[2-[2-(t-butoxycarbonylaminooxyacetylamino) ethoxy]ethoxy]ethyl]-methacrylamido
PEG	Polyethylene glycol
PEG linker	Fmoc-NH-(PEG)-COOH (9 atoms)
PyBOP	Benzotriazol-1-yl-oxy tris-pyrrolidino-phosphonium hexafluorophosphate
Pyr	Pyridine
RFU	Reference fluorescence unit
RP-HPLC	Reversed-phase high performance liquid chromatography
RP-UPLC	Reversed-phase ultra-performance liquid chromatography
SPPS	Solid-phase peptide synthesis
TACA	Tumor-associated carbohydrate antigens
TFA	2,2,2-trifluoroacetic acid
Tn antigen	α-*O*-GalNAc-Ser/Thr
VNTR	Variable number tandem repeat

Additional materials

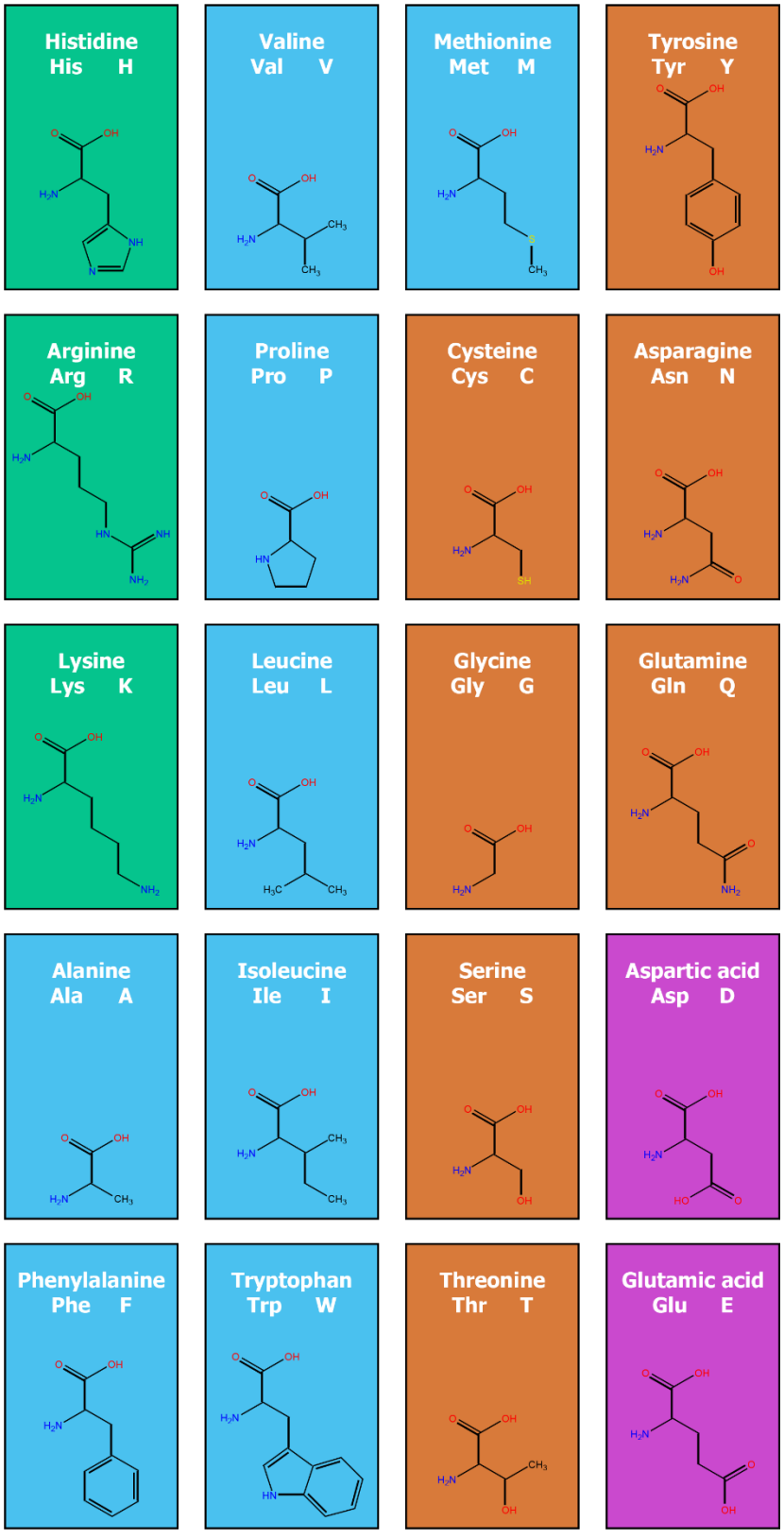

Chapter 1.
General introduction

1.1. Cancer

Advances in modern medicine like the improvement of sanitation, along with vaccination, the discovery of new antibiotics and the development of new diagnostic tools have greatly decreased the mortality caused by infectious diseases. In addition, prevention programs have raised the awareness of cardiovascular diseases, providing information about healthier lifestyles and reducing the impact of associated pathologies. This healthcare background has led to cancer as one of the leading causes of death worldwide, altering its position from the first to the sixth place depending on different socioeconomic factors (Figure 1).[1–4]

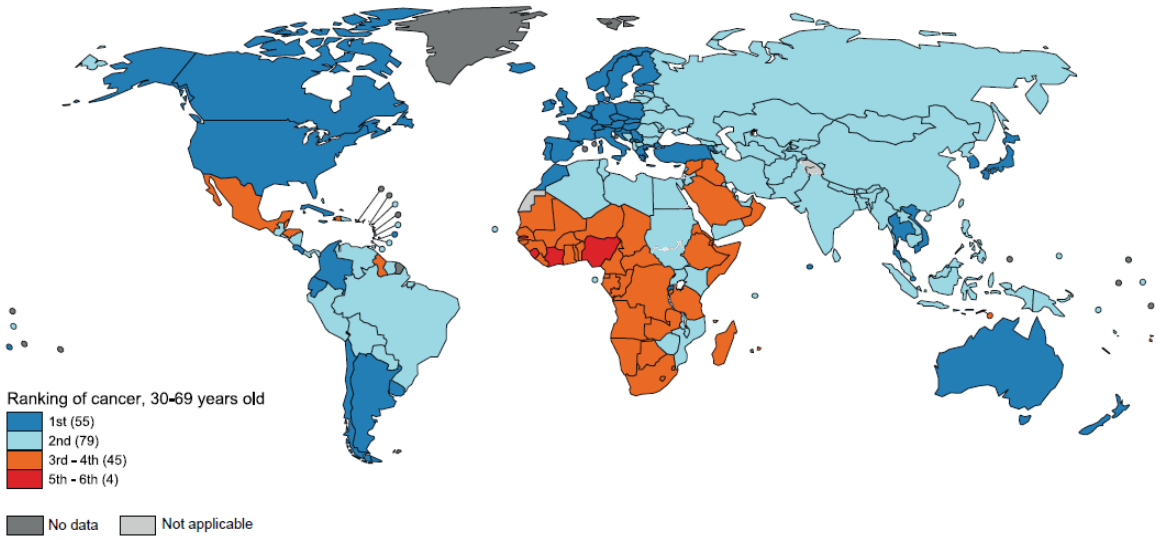

Figure 1. Global map of cancer as a leading cause of premature death at ages 30-69 years.[4]

We define cancer as the abnormal proliferation of cells and the spread of those cells through almost any part of the body, beginning with nearby tissue invasion and culminating in distant organs metastasis. Based on immune evasion, we can describe cancer evolution in three different phases: elimination, equilibrium and escape. The immune system possesses a

sophisticated defense network that allows cancer cells detection and eradication. During the elimination phase, the tumor progression can be contained by the immune system. In the equilibrium phase, new resistant cancer cell variants emerge, increasing survival and leading to the escape phase, where the immune system defense mechanisms are surpassed and tumor development will proceed (Figure 2).[5]

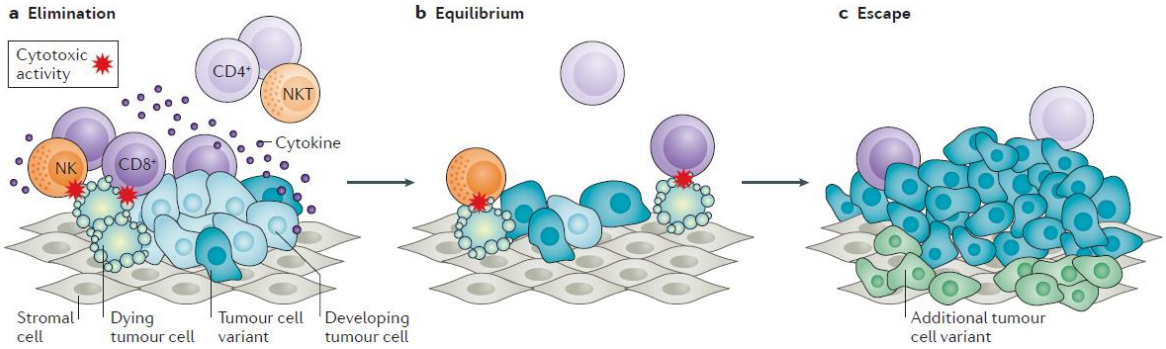

Figure 2. Tumor immune escape progression.[5]

Its etiology is extremely diverse, including factors such as age, diet, nutrition, alcoholism, infectious agents, physical activity, contamination, genetic and epigenetic modifications, among a long list of causes.[6–8] There are many types of cancer depending on their origin, giving rise to breast, lung, prostate, ovarian and numerous other cancer pathologies. Therefore, cancer is a complex term that shouldn't be conceived as just one disease but as combination of similar diseases with growth, spread and behavior differences. Only understanding the relevant differences between them will allow us to develop specific methodologies to properly diagnose and prescribe a suitable treatment.[9]

Breast cancer is actually considered the most frequent malignancy in women worldwide, presenting a great morphological and molecular heterogeneity. Metastatic breast cancer is nowadays considered as a non-curable disease. Unfortunately, the available

therapies for this advanced stage have the purposes of maintaining the quality of life of the patient and elongating the life expectancy. By contrast, early breast cancer that presents no cancer cells spread outside the breast can be treated with actual therapies. Although the importance of a treatment possibility is reassuring, the best approach to avoid tumor growth and health deterioration is early detection.[10–14] Thus, the first step to approach this intricate disease is to discern healthy cells from tumor cells. With that purpose, we have focused our attention in MUC1, one of the most studied breast cancer hallmarks.[15–18]

1.2. Breast cancer and MUC1 relationship

MUC1, also known as cancer antigen 15-3 (CA15-3), cluster of differentiation 227 (CD227), and Krebs von den Lungen-6 (KL-6), is a high molecular weight *O*-glycoprotein expressed on the apical surface of epithelial cells. It is composed of a 20 amino acids variable number tandem repeat (VNTR) (30-100) that includes 5 potential glycosylation positions (GV<u>T</u><u>S</u>APD<u>T</u>RPAPG<u>S</u><u>T</u>APPAH; glycosylation positions underlined) and presents a high glycosylation degree in normal tissues.[19] Similar to other mucins, it is responsible for epithelial barrier protection, lubrication, and cellular adhesion, among other functions. However, it also plays a critical role in tumor malignancy processes, such as proliferation, metastasis, and invasion.[20–23] MUC1 has been previously reported as an overexpressed protein in most carcinomas and in particular in breast cancer, becoming a noteworthy biomarker. Therefore, MUC1 is directly related with breast cancer, and the biomolecular reason for this situation is not only its remarkable overexpression but also the singular aberrant glycosylation phenomenon that undergoes in the majority of breast carcinomas.[24]

The glycosylation process can be considered as one of the most important lipid and protein post translational modifications, with an estimation of around a 95% of cell surface proteins being covered by glycans. It takes part in multiple biological structural and recognition roles such as solubility, physical and enzymatic protection, lubrication, new glycoproteins folding control, and subsequent three-dimensional configuration modification and stability, tissue development, intracellular signaling, cell-cell recognition, and molecular recognition for immune activation or pathological processes infection.[25–27] In addition, several glycans have been already identified as mediators for tumor progression events like proliferation, adhesion, neovascularization, dissemination and invasion (Figure 3).[22,23,28]

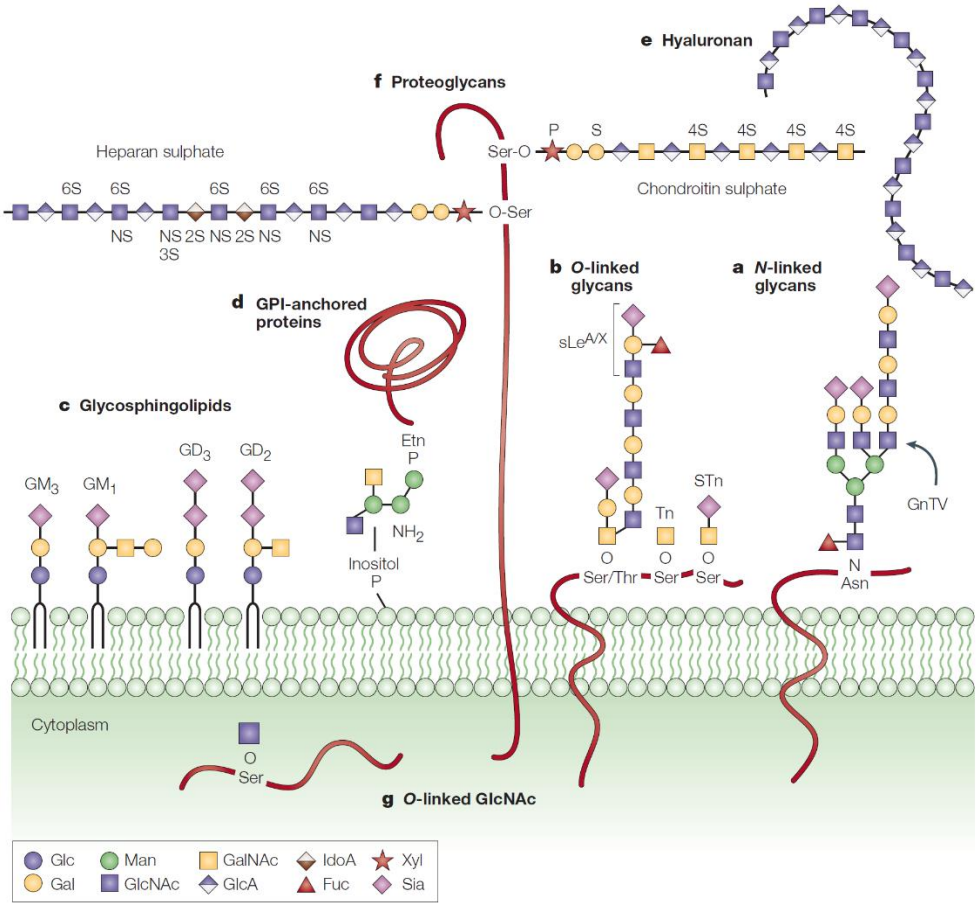

Figure 3. Examples of glycans involved in tumor progression.[28]

Cell glycosylation status can suffer alterations by oncogenesis, giving rise to aberrant glycosylation in cancer cells.[18,29] In breast cancer, the mechanisms responsible for this anomaly find their origin in changes in the expression of glycosyltransferases, relocalisation of *N*-acetylgalactosaminyltransferases from the Golgi apparatus to the endoplasmic reticulum and alteration of the normal glycosidase activity.[30,31] Dysregulation in the precise glycan production machinery provokes the shortening of normal long glycan chains that cover MUC1 thus, giving rise to previously covered *O*-glycans truncated neoepitopes exhibition (Figure 4).[18,32] In breast cancer, this altered glycosylation profile is widely accepted as a hallmark of cancer.[33]

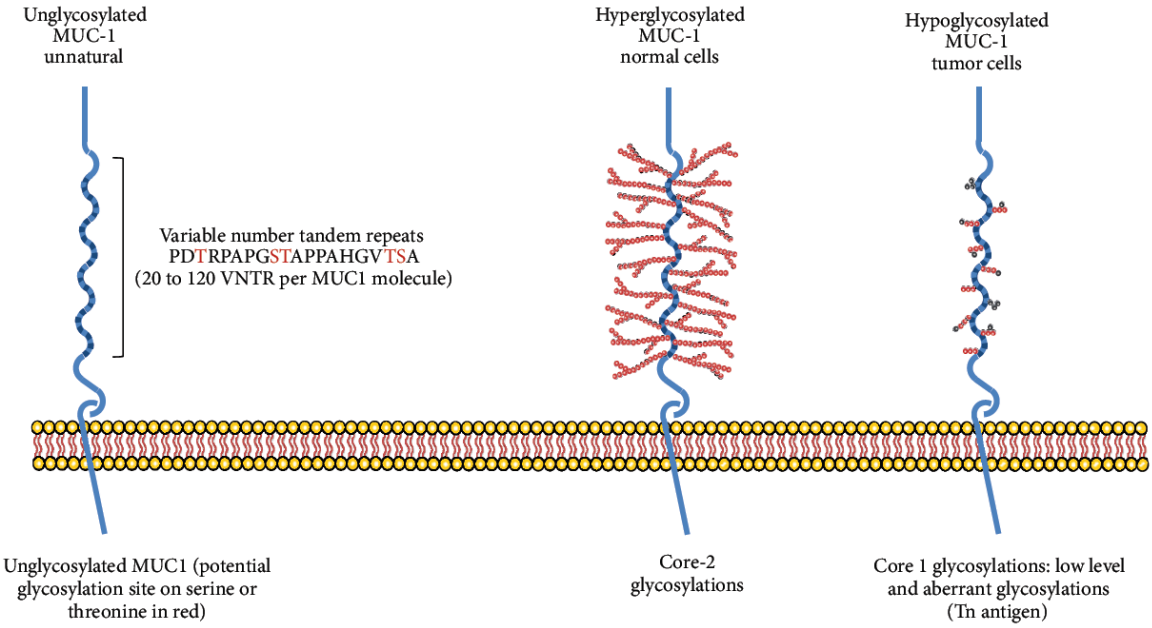

Figure 4. MUC1 in normal cells compared with MUC1 in cancer cells with neoepitopes exhibition.[32]

1.3. Tumor-associated carbohydrate antigens

These unexpected neoantigens are known as tumor-associated carbohydrate antigens (TACAs) and can be used to distinguish normal cells from tumor cells.[34,35] Those components can be organized in two different glycoconjugates groups. Glycolipids, which are lipids that present a carbohydrate covalently attached and are directly anchored through the lipid region to the lipid bilayer on the cell surface.[36] Glycoproteins, which carry glycans covalently attached to the peptide backbone are usually integrated in the cell surface as transmembrane proteins but they can also appear in a secreted form. In a similar way, glycoproteins also present subcategories in function of the glycosylated amino acid residue. Therefore, *N*-glycoproteins present glycans attached through an amide bond with Asn residues and *O*-glycoproteins have the glycans amide bond linked through mainly the hydroxyl group of Ser or Thr residues, and exceptionally Tyr residues.[37] One important feature of glycoproteins is that they are non-template driven. This implies that the information for the glycans addition is not encoded at the DNA level, but monosaccharides or sugar building blocks are assembled through complex enzymatic processes.[38] As mentioned, MUC1 is an *O*-glycoprotein which means that the glycans attached will only be located in the threonine and serine residues of the peptide backbone. In normal conditions, MUC1 is highly glycosylated but in cancer cells, previous cited alterations inhibit the correct formation of the natural glycan structures. Thus, TACAs emerge because of the enzymatic machinery malfunction, responsible for the glycan addition to the protein domain (Figure 5). In this context, the most immature and shortest structure that we can find linked to the peptide backbone is the Tn antigen.[39]

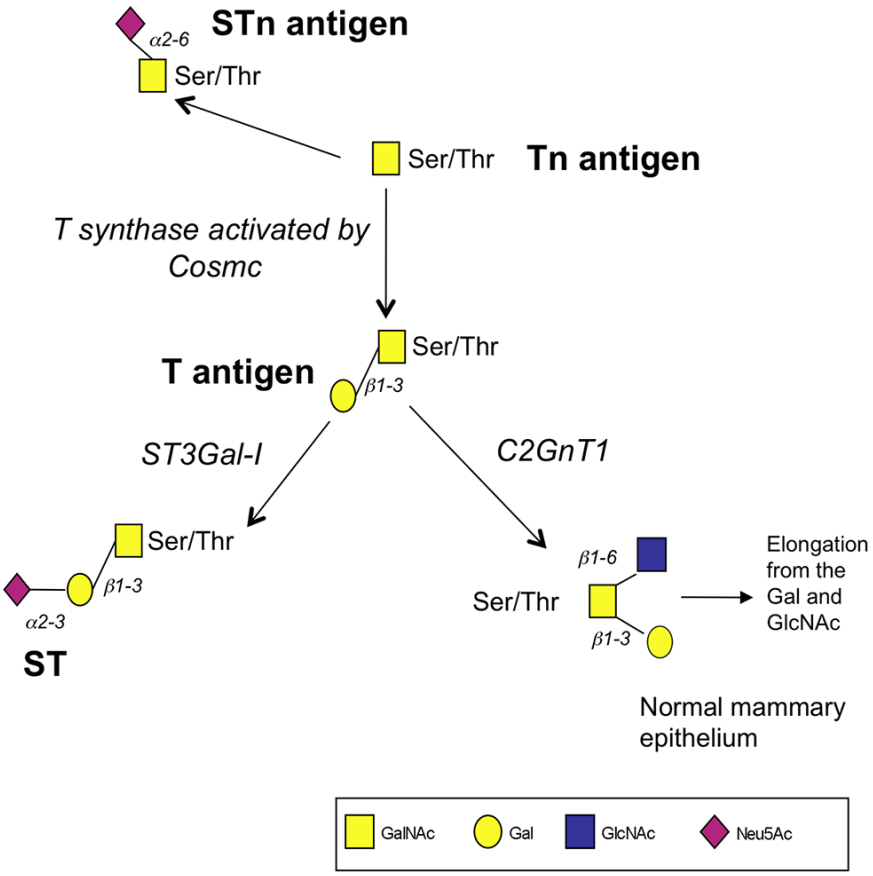

Figure 5. Representation of MUC1 early stage *O*-linked glycosylation pathway.[40]

The 'T antigen nouvelle' or just Tn antigen gets its name from Moreau *et al*. in 1957 and makes reference to a *N*-acetylgalactosamine monosaccharide linked to a Ser or Thr residue though an α-*O*-glycosidic bond (α-*O*-GalNAc-Ser/Thr).[41] It is the initial structure for the glycan chain elongation pathway in normal conditions but constitute part of the essential machinery for inducing metastasis and invasiveness.[42] Its tumor specificity makes the Tn antigen very little or no expressed at all in normal tissues while it is expressed in several tumor types such as breast, ovarian, prostate, colon, stomach and lung carcinomas, a feature that makes it a promising biomarker.[43,44]

1.4. References

(1) World Health Organization. Global Status Report On Noncommunicable Diseases 2014. **2014**.

(2) Bray, F.; Ferlay, J.; Soerjomataram, I.; Siegel, R. L.; Torre, L. A.; Jemal, A. Global Cancer Statistics 2018: GLOBOCAN Estimates of Incidence and Mortality Worldwide for 36 Cancers in 185 Countries. *CA. Cancer J. Clin.* **2018**, *68* (6), 394–424. https://doi.org/10.3322/caac.21492.

(3) Siegel, R. L.; Miller, K. D.; Jemal, A. Cancer Statistics, 2019. *CA. Cancer J. Clin.* **2019**, *69* (1), 7–34. https://doi.org/10.3322/caac.21551.

(4) Christopher, P. W.; Weiderpass, E.; Bernard, W. S. *World Cancer Report Cancer Research for Cancer Prevention*; 2020.

(5) Van Der Burg, S. H.; Arens, R.; Ossendorp, F.; Van Hall, T.; Melief, C. J. M. Vaccines for Established Cancer: Overcoming the Challenges Posed by Immune Evasion. *Nat. Rev. Cancer* **2016**, *16* (4), 219–233. https://doi.org/10.1038/nrc.2016.16.

(6) Wei, E. K.; Wolin, K. Y.; Colditz, G. A. Time Course of Risk Factors in Cancer Etiology and Progression. *J. Clin. Oncol.* **2010**, *28* (26), 4052–4057. https://doi.org/10.1200/JCO.2009.26.9324.

(7) Wicki, A.; Hagmann, J. Diet and Cancer. *Swiss Med. Wkly.* **2011**, *141* (SEPTEMBER), 1–8. https://doi.org/10.4414/smw.2011.13250.

(8) Blackadar, C. B. Historical Review of the Causes of Cancer. *World J. Clin. Oncol.* **2016**, *7* (1), 54–86. https://doi.org/10.5306/wjco.v7.i1.54.

(9) Hassanpour, S. H.; Dehghani, M. Review of Cancer from Perspective of Molecular. *J. Cancer Res. Pract.* **2017**, *4* (4), 127–129. https://doi.org/10.1016/j.jcrpr.2017.07.001.

(10) Harbeck, N.; Gnant, M. Breast Cancer. *Lancet* **2017**, *389* (10074), 1134–1150. https://doi.org/10.1016/S0140-6736(16)31891-8.

(11) Turashvili, G.; Brogi, E. Tumor Heterogeneity in Breast Cancer. *Front. Med.* **2017**, *4* (DEC). https://doi.org/10.3389/fmed.2017.00227.

(12) Harbeck, N.; Penault-Llorca, F.; Cortes, J.; Gnant, M.; Houssami, N.; Poortmans, P.; Ruddy, K.; Tsang, J.; Cardoso, F. Breast Cancer. *Nat. Rev. Dis. Prim.* **2019**, *5* (1), 66. https://doi.org/10.1038/s41572-019-0111-2.

(13) Januškevičienė, I.; Petrikaitė, V. Heterogeneity of Breast Cancer: The Importance of Interaction between Different Tumor Cell Populations. *Life Sci.* **2019**, *239*, 117009. https://doi.org/10.1016/j.lfs.2019.117009.

(14) Waks, A. G.; Winer, E. P. Breast Cancer Treatment. *JAMA* **2019**, *321* (3), 288–300. https://doi.org/10.1001/jama.2018.19323.

(15) Taylor-Papadimitriou, J.; Burchell, J.; Miles, D. W.; Dalziel, M. MUC1 and Cancer. *Biochim. Biophys. Acta* **1999**, *1455* (2–3), 301–313. https://doi.org/10.1016/s0925-4439(99)00055-1.

(16) Bon, G. G.; Van Kamp, G. J.; Verstraeten, R. A.; Von Mensdorff-Pouilly, S.; Hilgers, J.; Kenemans, P. Quantification of MUC1 in Breast Cancer Patients: A Method Comparison Study. *Eur. J. Obstet. Gynecol. Reprod. Biol.* **1999**, *83* (1), 67–75. https://doi.org/10.1016/S0301-2115(98)00302-9.

(17) Rahn, J. J.; Dabbagh, L.; Pasdar, M.; Hugh, J. C. The Importance of MUC1 Cellular Localization in Patients with Breast Carcinoma. *Cancer* **2001**, *91* (11), 1973–1982. https://doi.org/10.1002/1097-0142(20010601)91:11<1973::AID-CNCR1222>3.0.CO;2-A.

(18) Gendler, S. J. MUC1, The Renaissance Molecule. *J. Mammary Gland Biol. Neoplasia* **2001**, *6* (3), 339–353. https://doi.org/10.1023/A:1011379725811.

(19) Apostolopoulos, V.; Stojanovska, L.; Gargosky, S. E. MUC1 (CD227): A Multi-Tasked Molecule. *Cell. Mol. Life Sci.* **2015**, *72* (23), 4475–4500. https://doi.org/10.1007/s00018-015-2014-z.

(20) Hollingsworth, M. A.; Swanson, B. J. Mucins in Cancer: Protection and Control of the Cell Surface. *Nat. Rev. Cancer* **2004**, *4* (1), 45–60. https://doi.org/10.1038/nrc1251.

(21) Kufe, D. W. Mucins in Cancer: Function, Prognosis and Therapy. *Nat. Rev. Cancer* **2009**, *9* (12), 874–885. https://doi.org/10.1038/nrc2761.

(22) Bhatia, R.; Gautam, S. K.; Cannon, A.; Thompson, C.; Hall, B. R.; Aithal, A.; Banerjee, K.; Jain, M.; Solheim, J. C.; Kumar, S.; Batra, S. K. Cancer-Associated Mucins: Role in Immune Modulation and Metastasis. *Cancer Metastasis Rev.* **2019**, *38* (1–2), 223–236. https://doi.org/10.1007/s10555-018-09775-0.

(23) Reynolds, I. S.; Fichtner, M.; McNamara, D. A.; Kay, E. W.; Prehn, J. H. M.; Burke, J. P. Mucin Glycoproteins Block Apoptosis; Promote Invasion, Proliferation, and Migration; and Cause Chemoresistance through Diverse Pathways in Epithelial Cancers. *Cancer Metastasis Rev.* **2019**, *38* (1–2), 237–257. https://doi.org/10.1007/s10555-019-09781-w.

(24) Duffy, M. J.; Evoy, D.; McDermott, E. W. CA 15-3: Uses and Limitation as a Biomarker for Breast Cancer. *Clin. Chim. Acta* **2010**, *411* (23–24), 1869–1874. https://doi.org/10.1016/j.cca.2010.08.039.

(25) Varki, A. Biological Roles of Glycans. *Glycobiology* **2017**, *27* (1), 3–49. https://doi.org/10.1093/glycob/cww086.

(26) Zhou, D.; Xu, L.; Huang, W.; Tonn, T. Epitopes of MUC1 Tandem Repeats in Cancer as Revealed by Antibody Crystallography: Toward Glycopeptide Signature-Guided Therapy. *Molecules* **2018**, *23* (6), 1326. https://doi.org/10.3390/molecules23061326.

(27) Valverde, P.; Ardá, A.; Reichardt, N.-C.; Jiménez-Barbero, J.; Gimeno, A. Glycans in Drug Discovery. *Medchemcomm* **2019**, *10* (10), 1678–1691. https://doi.org/10.1039/C9MD00292H.

(28) Fuster, M. M.; Esko, J. D. The Sweet and Sour of Cancer: Glycans as Novel Therapeutic Targets. *Nat. Rev. Cancer* **2005**, *5* (7), 526–542. https://doi.org/10.1038/nrc1649.

(29) Wang, M.; Zhu, J.; Lubman, D. M.; Gao, C. Aberrant Glycosylation and Cancer Biomarker Discovery: A Promising and Thorny Journey. *Clin. Chem. Lab. Med.* **2019**, *57* (4), 407–416. https://doi.org/10.1515/cclm-2018-0379.

(30) Pinho, S. S.; Reis, C. A. Glycosylation in Cancer: Mechanisms and Clinical Implications. *Nat. Rev. Cancer* **2015**, *15* (9), 540–555. https://doi.org/10.1038/nrc3982.

(31) Burchell, J. M.; Beatson, R.; Graham, R.; Taylor-Papadimitriou, J.; Tajadura-Ortega, V. O-Linked Mucin-Type Glycosylation in Breast Cancer. *Biochem. Soc. Trans.* **2018**,

46 (4), 779–788. https://doi.org/10.1042/BST20170483.

(32) Lakshminarayanan, V.; Thompson, P.; Wolfert, M. A.; Buskas, T.; Bradley, J. M.; Pathangey, L. B.; Madsen, C. S.; Cohen, P. A.; Gendler, S. J.; Boons, G. J. Immune Recognition of Tumor-Associated Mucin MUC1 Is Achieved by a Fully Synthetic Aberrantly Glycosylated MUC1 Tripartite Vaccine. *Proc. Natl. Acad. Sci. U. S. A.* **2012**, *109* (1), 261–266. https://doi.org/10.1073/pnas.1115166109.

(33) Ludwig, J. A.; Weinstein, J. N. Biomarkers in Cancer Staging, Prognosis and Treatment Selection. *Nat. Rev. Cancer* **2005**, *5* (11), 845–856. https://doi.org/10.1038/nrc1739.

(34) Springer, G. F. T and Tn, General Carcinoma Autoantigens. *Science (80-.).* **1984**, *224* (4654), 1198–1206. https://doi.org/10.1126/science.6729450.

(35) Xu, Y.; Sette, A.; Sidney, J.; Gendler, S. J.; Franco, A. Tumor-Associated Carbohydrate Antigens: A Possible Avenue for Cancer Prevention. *Immunol. Cell Biol.* **2005**, *83* (4), 440–448. https://doi.org/10.1111/j.1440-1711.2005.01347.x.

(36) Daniotti, J. L.; Vilcaes, A. A.; Torres Demichelis, V.; Ruggiero, F. M.; Rodriguez-Walker, M. Glycosylation of Glycolipids in Cancer: Basis for Development of Novel Therapeutic Approaches. *Front. Oncol.* **2013**, *3* (December), 1–12. https://doi.org/10.3389/fonc.2013.00306.

(37) Zarschler, K.; Janesch, B.; Pabst, M.; Altmann, F.; Messner, P.; Schäffer, C. Protein Tyrosine O-Glycosylation-A Rather Unexplored Prokaryotic Glycosylation System. *Glycobiology* **2010**, *20* (6), 787–798. https://doi.org/10.1093/glycob/cwq035.

(38) Lopez Aguilar, A.; Briard, J. G.; Yang, L.; Ovryn, B.; Macauley, M. S.; Wu, P. Tools

for Studying Glycans: Recent Advances in Chemoenzymatic Glycan Labeling. *ACS Chem. Biol.* **2017**, *12* (3), 611–621. https://doi.org/10.1021/acschembio.6b01089.

(39) Fu, C.; Zhao, H.; Wang, Y.; Cai, H.; Xiao, Y.; Zeng, Y.; Chen, H. Tumor-Associated Antigens: Tn Antigen, STn Antigen, and T Antigen. *Hla* **2016**, *88* (6), 275–286. https://doi.org/10.1111/tan.12900.

(40) Beatson, R.; Maurstad, G.; Picco, G.; Arulappu, A.; Coleman, J.; Wandell, H. H.; Clausen, H.; Mandel, U.; Taylor-Papadimitriou, J.; Sletmoen, M.; Burchell, J. M. The Breast Cancer-Associated Glycoforms of MUC1, MUC1-Tn and Sialyl-Tn, Are Expressed in COSMC Wild-Type Cells and Bind the C-Type Lectin MGL. *PLoS One* **2015**, *10* (5), 1–21. https://doi.org/10.1371/journal.pone.0125994.

(41) DAUSSET, J.; MOULLEC, J.; BERNARD, J. Acquired Hemolytic Anemia with Polyagglutinability of Red Blood Cells Due to a New Factor Present in Normal Human Serum (Anti-Tn). *Blood* **1959**, *14*, 1079–1093. https://doi.org/10.1182/blood.V14.10.1079.1079.

(42) Wu, X.; Yin, Z.; McKay, C.; Pett, C.; Yu, J.; Schorlemer, M.; Gohl, T.; Sungsuwan, S.; Ramadan, S.; Baniel, C.; Allmon, A.; Das, R.; Westerlind, U.; Finn, M. G.; Huang, X. Protective Epitope Discovery and Design of MUC1-Based Vaccine for Effective Tumor Protections in Immunotolerant Mice. *J. Am. Chem. Soc.* **2018**, *140* (48), 16596–16609. https://doi.org/10.1021/jacs.8b08473.

(43) Ju, T.; Otto, V. I.; Cummings, R. D. The Tn Antigen-Structural Simplicity and Biological Complexity. *Angew. Chemie Int. Ed.* **2011**, *50* (8), 1770–1791. https://doi.org/10.1002/anie.201002313.

(44) Ju, T.; Wang, Y.; Aryal, R. P.; Lehoux, S. D.; Ding, X.; Kudelka, M. R.; Cutler, C.; Zeng, J.; Wang, J.; Sun, X.; Heimburg-Molinaro, J.; Smith, D. F.; Cummings, R. D. Tn and Sialyl-Tn Antigens, Aberrant O-Glycomics as Human Disease Markers. *Proteomics - Clin. Appl.* **2013**, *7* (9–10), 618–631. https://doi.org/10.1002/prca.201300024.

Chapter 2.
Unnatural MUC1 based glycopeptide library synthesis

2.1. Introduction

2.1.1. Cancer immunotherapy

The medical history of cancer began a long time ago and it has evolved from ancient radical surgery to the actual revolutionary oncology research. Surgical procedures, along with treatments like radiotherapy and chemotherapy have experienced major changes and improvements, giving rise to new more specific methodologies. Genetic engineering, monoclonal antibodies, CAR T-cells and immune checkpoint inhibitors, among others have improved pharmacology and clinical oncology. These innovations have allowed an effective treatment for previously considered non-curable tumors. However, still a lot remains to be done in the field of medical oncology.[1,2]

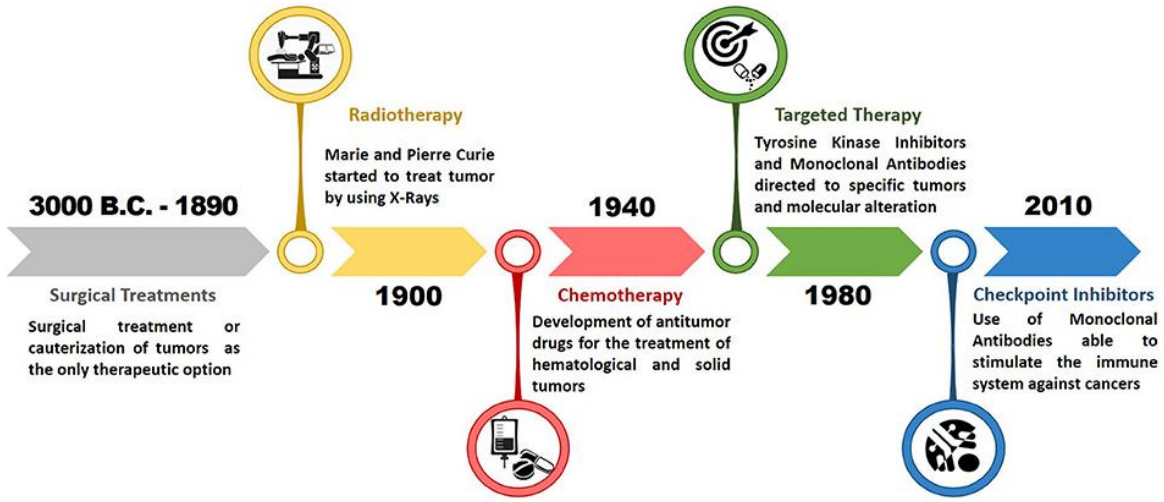

Figure 1. Timeline of cancer treatments.[1]

Currently, MUC1 associated Tn antigen has generated a lot of interest because of its applications in cancer immunotherapy. The core concept of this unique type of therapies is to induce a modification in the immune system to produce an effective response against

tumor cells.[3,4] One of the major strategies for cancer immunotherapy is the production of therapeutic antitumor vaccines. Due to the specificity of the Tn antigen several researchers have worked on the development of vaccines, achieving immune system activation, specific antibodies production and tumor growth control in transgenic mice.[5–8] However, cancer epitopes present low immunogenicity because unlike exogenous antigens originated from bacteria or viruses, they are present in small amounts on normal cells. In addition, there is a certain immunological tolerance against cancer epitopes as TACAs because the immune system perceives them as self-antigens.[9–11]

2.1.2. Glycan mimic selected: *sp*^{2}-iminosugar

The use of glycomimetics, compounds that are able to emulate the bioactive function of carbohydrates, has been successfully confirmed in several medical chemistry areas, opening new paths for drug discovery and allowing better treatments for certain diseases.[12,13] For the design of a novel glycan mimic, it is important to conduct a comprehensive structure-binding analysis to modify only non-critical binding elements.[14,15] Previous studies with mAbs (Anti-MUC1 mAbs VU-3C6[16] and SM3[17]) and MUC1 peptides containing the Tn antigen demonstrated that the *galacto* configuration, the *N*-acetyl group protons and the H2, were essential for the binding (Figure 2 highlighted in grey). Therefore, a functional glycomimic prototype needs to maintain these essential features. Conversely, substituents at positions C5 and C6 can presumably be modified without affecting the binding, allowing the use of these positions for affinity improvement. In this work we have focused our attention on the so-called iminosugars, specifically on *sp*^{2}-iminosugars on account of their structural similarity with the Tn antigen.[17]

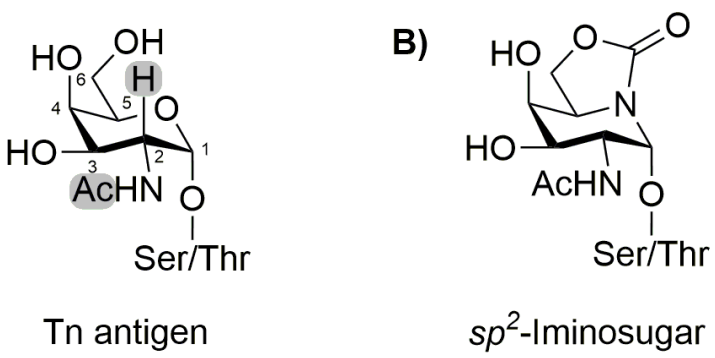

Figure 2. Tn antigen and *sp*^{2}-iminosugar-based unnatural Tn antigen mimic candidate.

Iminosugars are carbohydrate analogs in which the endocyclic oxygen has been substituted for a nitrogen atom.[18] Given the participation of glycans, glycoconjugates, glycosidases and lectins among others, in so many biological processes, the ability to emulate carbohydrates makes iminosugars a very attractive and powerful tool.

From an historical point of view, iminosugars were already used in ancient Chinese phytomedicine yet it wasn't until 1960 when its scientific value started to be recognized. Some of the most relevant events in the timeline of iminosugars are the first publication of 1-deoxynojirimycin (DNJ) synthesis by Paulsen *et al*. in 1966,[19] the isolation of nojirimycin (NJ) from *Streptomyces* by Inouye *et al*.[20] and later isolation from natural sources of DNJ the same year and the first isolation of castanospermine (CS) from *Castanospermum austral* immature seeds in 1981.[21] (Figure 3). As a consequence of these discoveries, a blooming interest for iminosugars was triggered resulting in the development of original analogues and novel synthetic strategies.

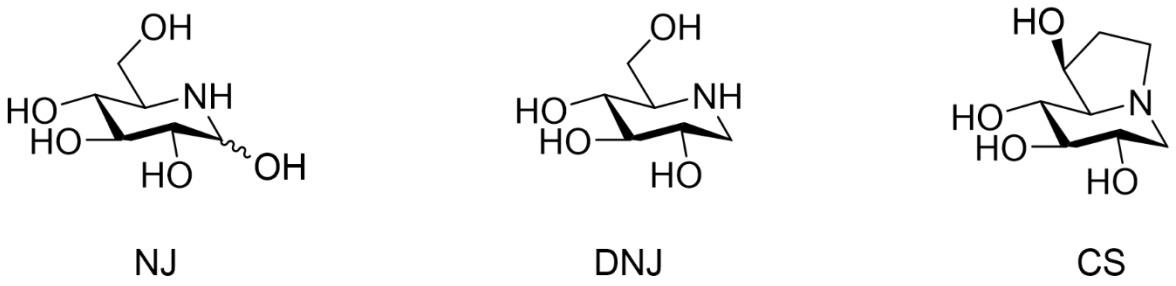

Figure 3. Nojirimycin (NJ), 1-deoxynojirimycin (DNJ) and castanospermine (CS) structures.

Although the apparently simple oxygen substitution for nitrogen opens the way to remarkable biological properties, it also raises many synthetic challenges. For instance, the natural iminosugars nojirimycin (NJ), 1-deoxynojirimycin (DNJ), and castanospermine (CS) initially called our attention because of their structural similarities with the glycone part of the Tn antigen molecule. However, the intrinsic lability of aminoacetal functions prevents the construction of *O*-glycoside analogs. This constraint can be overcome with sp^2-iminosugars, a subclass of azaheterocyclic glycomimetics in which the amine-type nitrogen characteristic of iminosugars is transformed into a pseudo amide functionality.[22] This subtle modification drastically enhances the anomeric effect, imparting chemical stability to axially-oriented anomeric carbon—heteroatom bonds. In consequence, glycosylation reactions present a total α-stereoselectivity, thereby avoiding the troublesome reparation of α and β-anomers that often penalize glycoside synthesis. [23] Furthermore, the five-membered cyclic carbamate ring is an integral part of the sp^2-iminosugar structure that fixes the conformation about the C5—C6 bond in the *gauche-gauche* conformation; it does not affect the key regions for anti-Tn antigen antibody binding and has instead the potential to enhance binding profiles by adding new contact points.[24] Moreover, replacement of the acetal functionality in the natural Tn antigen into an isosteric aminoacetal segment may convey

chemical and metabolic stability, a key advantage for the development of robust diagnostic devices. A previous communication provided a proof of concept of the suitability of sp^2-iminosugars to prepare chemically stable α-*O*-linked glycopeptide surrogates with total anomeric selectivity, which are critical issues for biological applications.[23] Several studies assessing the therapeutic capabilities of different sp^2-iminosugar-type analogues have already been published suggesting remarkably positive results in the treatment of an extensive list of disorders. For instance, we can find bibliography referring to lysosomal storage diseases,[25] inhibitory properties of α-galactosidases and α-glucosidases,[26,27] antileishmanial (*Leishmania donovani*) activity,[28] anti-inflammatory activity,[29] antiviral activity against human influenza A virus[30] and anti-tumoral activity.[31,32]

2.1.3. Glycopeptide library synthesis

Our aim is the development of glycomimics to emulate the functional properties of glycans and glycoconjugates which has proven to be very successful in several fields, including the search for carbohydrate active enzyme inhibitors and immune response regulators.[13,14,22,26,33] Sugar analogs of the sp^2-iminosugar family have proven particularly useful to access α-linked glycoside equivalents.[34,35]

In the present study, two MUC1 VNTR-based glycopeptide libraries bearing either the Natural (N) Tn antigen or an Unnatural (U) glycomimic where the α-linked GalNAc monosaccahride motif has been replaced into a sp^2-iminosugar motif with an identical substitution and configurational profile were synthesized through chemical synthesis.[36,37]

2.1.4. Microwave assisted solid-phase peptide synthesis

Peptides are short sequences of amino acids interconnected through amide bonds. Peptides, similar to proteins, participate in multiple essential biological events which evokes a big interest in them for medicinal and pharmaceutical purposes. They can be obtained from natural sources isolation, recombinant expression techniques or chemical synthesis. However, when post translational modifications are involved, the obtention of a reasonable yield quantity poses an arduous challenge. In order to get satisfactory results, chemical synthesis is the method of choice to address these complex situations. Solid-phase peptide synthesis (SPPS) allows successful production of customized peptides already carrying out post translational changes. Bruce Merrifield introduced in 1963 the innovative concept of peptide production on an insoluble resin that allows purification by simple washing followed by a cleavage step to separate the desired peptide from the resin.[38] Although this methodology requires certain considerations such as resin material, linkers, swelling and amino acid protecting groups among others, this process is characterized for its simplicity and efficiency.[39–41]

The most common general process for SPPS starts with the activation of the *C*-terminal position of the first amino acid and linkage through that position to the resin (a polymeric support). Then, the system is washed, the temporary *N*-terminal Fmoc protecting group is removed, followed by another washing step and *C*-terminal activation of the second residue, allowing the coupling of the second component to the sequence. This cycle has to be repeated until the whole peptide is completed to finish with all the protecting groups removal and cleavage from the resin (Figure 4).[36,37] Furthermore, the implementation of microwave

(MW) technology to heat the reaction during couplings and deprotections has provided significant synthesis time reductions and a notable increase in the product purity.[42–45]

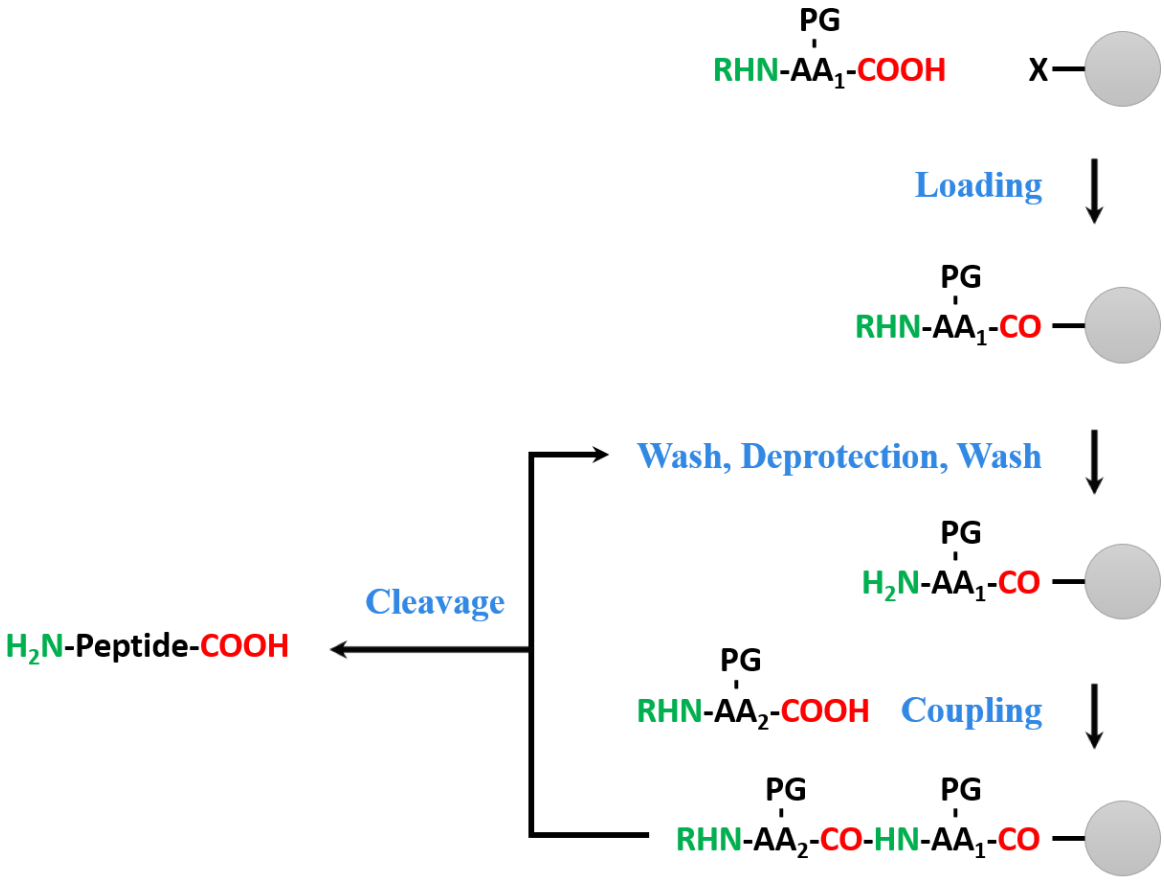

Figure 4. SPPS general cyclic scheme. [36]

2.2. Results and discussion

To accurately mimic nature and boost recognition, natural and unnatural glycans were both attached to the VNTR of MUC1, generating multiple combinations due to the 5 different *O*-glycosylation points present in the peptide sequence. To study the mimetic capabilities of the sp^2-iminosugar motif in the next chapter, a library composed of 27 MUC1 (glyco)peptides was synthesized. The selected peptide sequence (Figure 5) corresponds to the MUC1 20-amino acid VNTR, three additional amino acids were added to the sequence, a PEG linker to act as spacer and a ketone linker to attach the peptide to the microarray slide surface. Five potential *O*-glycosylation sites were within the VNTR sequence of MUC1, allowing different glycosylation patterns.

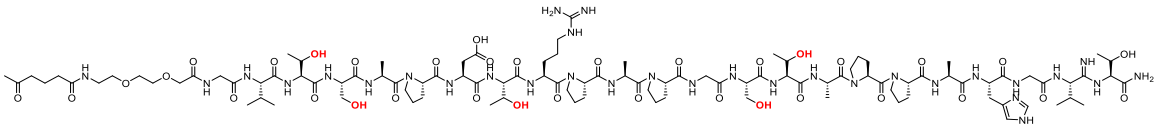

1 3 4 5 8 14 15 23

5-oxo-hexanoyl-PEG(9a)-GVTSAPDTRPAPGSTAPPAHGVT-NH_2

Figure 5. MUC1 VNTR based peptide sequence synthesized (glycosylation points in red).

A previous MUC1 library with the natural Tn antigen was produced in our laboratory.[46] Here we expanded that collection and synthesized an analog unnatural MUC1 library based on the natural one. Both libraries were highly diverse and included the following glycan decoration patterns: a) a natural library consisting of 1 non-glycosylated (Naked), 5 monoglycosylated, and 8 diglycosylated natural (N) Tn antigen-containing glycopeptides; b) and unnatural library consisting of 5 monoglycosylated and 8 diglycosylated unnatural (U) sp^2-iminosugar-based Tn antigen mimic-containing

glycopeptides (Figure 6). The whole (glyco)peptide collection was synthesized using different protocols of MW assisted SPPS, purified through RP-HPLC and characterized using RP-UPLC, ESI-HRMS and amino acid analysis.

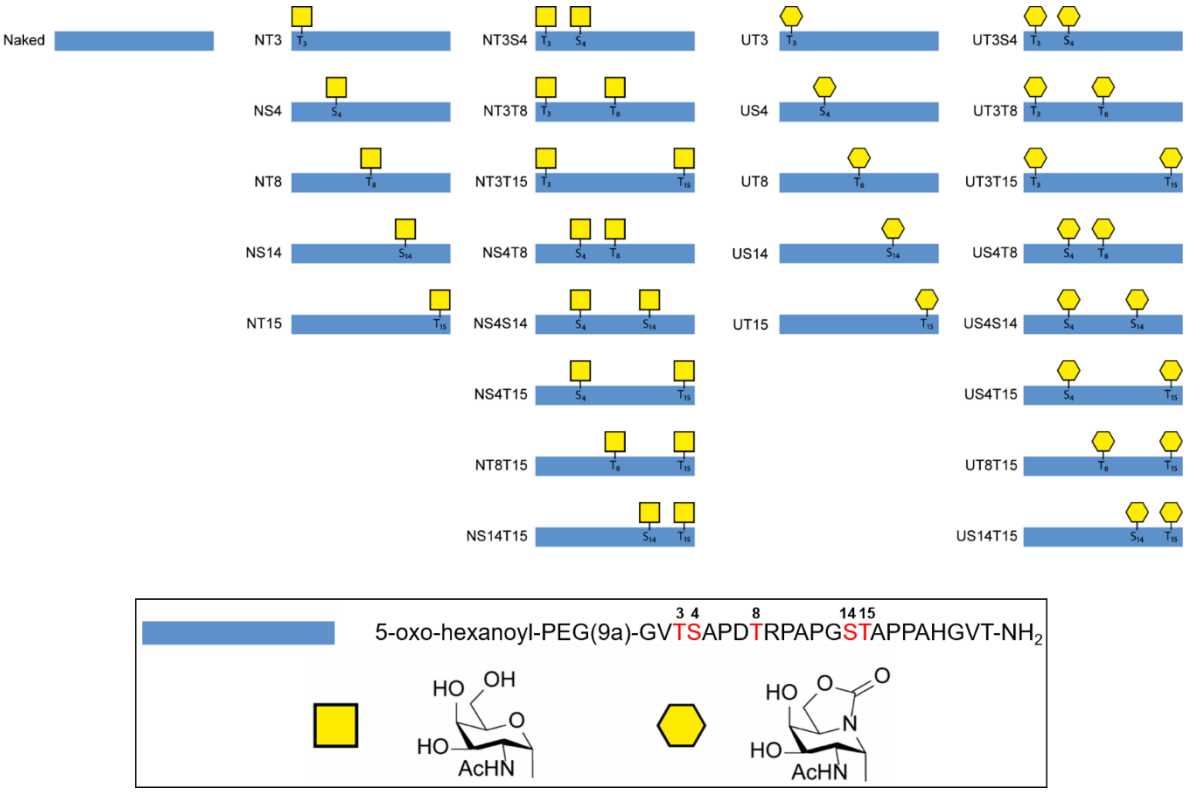

Figure 6. Complete glycopeptide library synthesized; potential glycosylation positions are shown in red; Threonine (T), Serine (S), the Tn antigen (N), and sp^2-iminosugar-based Tn antigen mimic (U).

2.3. Conclusion

The following table shows the (glyco)peptide library synthesized. The two different glycans, Tn antigen and *sp*^{2}-iminosugar glycomimetic were attached in different patterns to create a diverse collection. Glycosylation positions are marked in red. All the compounds were synthesized using MW assisted SPPS, purified through RP-HPLC and characterized using RP-UPLC, ESI-HRMS and amino acid analysis (for more details, see the Experimental section).

Code	Glycan	Sequence
Naked	None	5-oxo-hexanoyl-PEG(9a)-GVTSAPDTRPAPGSTAPPAHGVT-NH_2
NT3	Tn Antigen	5-oxo-hexanoyl-PEG(9a)-GV**T**SAPDTRPAPGSTAPPAHGVT-NH_2
UT3	*sp*^{2}-iminosugar	5-oxo-hexanoyl-PEG(9a)-GV**T**SAPDTRPAPGSTAPPAHGVT-NH_2
NS4	Tn Antigen	5-oxo-hexanoyl-PEG(9a)-GVT**S**APDTRPAPGSTAPPAHGVT-NH_2
US4	*sp*^{2}-iminosugar	5-oxo-hexanoyl-PEG(9a)-GVT**S**APDTRPAPGSTAPPAHGVT-NH_2
NT8	Tn Antigen	5-oxo-hexanoyl-PEG(9a)-GVTSAPD**T**RPAPGSTAPPAHGVT-NH_2
UT8	*sp*^{2}-iminosugar	5-oxo-hexanoyl-PEG(9a)-GVTSAPD**T**RPAPGSTAPPAHGVT-NH_2
NS14	Tn Antigen	5-oxo-hexanoyl-PEG(9a)-GVTSAPDTRPAPG**S**TAPPAHGVT-NH_2
US14	*sp*^{2}-iminosugar	5-oxo-hexanoyl-PEG(9a)-GVTSAPDTRPAPG**S**TAPPAHGVT-NH_2
NT15	Tn Antigen	5-oxo-hexanoyl-PEG(9a)-GVTSAPDTRPAPGS**T**APPAHGVT-NH_2
UT15	*sp*^{2}-iminosugar	5-oxo-hexanoyl-PEG(9a)-GVTSAPDTRPAPGS**T**APPAHGVT-NH_2
NT3S4	Tn Antigen	5-oxo-hexanoyl-PEG(9a)-GV**T**S**S**APDTRPAPGSTAPPAHGVT-NH_2
UT3S4	*sp*^{2}-iminosugar	5-oxo-hexanoyl-PEG(9a)-GV**T**S**S**APDTRPAPGSTAPPAHGVT-NH_2
NT3T8	Tn Antigen	5-oxo-hexanoyl-PEG(9a)-GV**T**SAPD**T**RPAPGSTAPPAHGVT-NH_2
UT3T8	*sp*^{2}-iminosugar	5-oxo-hexanoyl-PEG(9a)-GV**T**SAPD**T**RPAPGSTAPPAHGVT-NH_2
NT3T15	Tn Antigen	5-oxo-hexanoyl-PEG(9a)-GV**T**SAPDTRPAPGS**T**APPAHGVT-NH_2
UT3T15	*sp*^{2}-iminosugar	5-oxo-hexanoyl-PEG(9a)-GV**T**SAPDTRPAPGS**T**APPAHGVT-NH_2
NS4T8	Tn Antigen	5-oxo-hexanoyl-PEG(9a)-GVT**S**APD**T**RPAPGSTAPPAHGVT-NH_2
US4T8	*sp*^{2}-iminosugar	5-oxo-hexanoyl-PEG(9a)-GVT**S**APD**T**RPAPGSTAPPAHGVT-NH_2
NS4S14	Tn Antigen	5-oxo-hexanoyl-PEG(9a)-GVT**S**APDTRPAPG**S**TAPPAHGVT-NH_2
US4S14	*sp*^{2}-iminosugar	5-oxo-hexanoyl-PEG(9a)-GVT**S**APDTRPAPG**S**TAPPAHGVT-NH_2

NS4T15	Tn Antigen	5-oxo-hexanoyl-PEG(9a)-GVTSAPDTRPAPGSTAPPAHGVT-NH_2
US4T15	sp^2-iminosugar	5-oxo-hexanoyl-PEG(9a)-GVTSAPDTRPAPGSTAPPAHGVT-NH_2
NT8T15	Tn Antigen	5-oxo-hexanoyl-PEG(9a)-GVTSAPDTRPAPGSTAPPAHGVT-NH_2
UT8T15	sp^2-iminosugar	5-oxo-hexanoyl-PEG(9a)-GVTSAPDTRPAPGSTAPPAHGVT-NH_2
NS14T15	Tn Antigen	5-oxo-hexanoyl-PEG(9a)-GVTSAPDTRPAPGSTAPPAHGVT-NH_2
US14T15	sp^2-iminosugar	5-oxo-hexanoyl-PEG(9a)-GVTSAPDTRPAPGSTAPPAHGVT-NH_2

2.4. Experimental section

2.4.1. Materials

Commercially available reagents and solvents were used without further purification. Ac_2O, piperidine, hydrazine, MeOH, MTBE were purchased from Wako Pure Chemical Industries, Ltd. (Osaka, Japan). [*N*-*α*-(9-fluorenyl-methyloxycarbonyl) (Fmoc)]-L-amino acids were purchased from Watanabe Chemical Industries, Ltd. (Hiroshima, Japan) and Merck Schuchardt OHG (Hohenbrunn, Germany), while glycosylated amino acids Fmoc-α-*O*-(Ac_3GalNAc)-Ser/Thr[43,47–50] and Fmoc-α-*O*-(sp^2-Ac_2GalNAc)-Ser/Thr[17] were synthesized following previous reported protocols. DMF, DCM, HBTU and TFA were purchased from Watanabe Chemical Industries, Ltd. (Hiroshima, Japan). DIEA, HOBt and HOAt were manufactured by Kokusan Chemical Co., Ltd. (Tokyo, Japan). NovaPEG Rink Amide resin (loading 0.37 mmol/g) and PEG linker were supplied by Merck Schuchardt OHG (Hohenbrunn, Germany). The ketone linker was acquired from Tokyo Chemical Industry Co., Ltd. (Tokyo, Japan) and PyBOP was purchased from Merck KGaA (Darmstadt, Germany). SPPS reactions on resin were conducted in a polypropylene heat-resistant syringe equipped with thick filter (LibraTube®) Hipep Laboratories (Kyoto, Japan). SPPS coupling and deprotection reactions were performed through a Green Motif I microwave (IDX Corp., Tochigi, Japan) stirring the resin with a vortex shaker, wattage range 0-50 W and maintaining the temperature at 50°C. Semi-preparative RP-HPLC purifications were performed on a Prominence Shimadzu system (Shimadzu Corporation, Kyoto, Japan) equipped with two LC-6AD pumps, SPD-20A UV/VIS detector at 220 nm and Inertsil ODS-3 reversed-phase C18 column (250× 20 mm I.D.) Flow rate 5 mL/min; eluent A, H_2O (0.1% TFA) and eluent B, ACN (0.1% TFA) in a linear gradient (A/B) from 0.95:0.05 to 0.5:0.5 in 60 min. Analytical

RP-UPLC purifications were conducted on a Waters ACQUITY^{TM} Ultra Performance LC system (Waters Corporation, Massachusetts, United States) equipped with a binary solvent manager pump, auto sampler, TUV detector at 220 nm and ACQUITY UPLC® BEH C18 (1.7 µm, 2.1x50 mm Column, Waters). Flow rate 0.2 mL/min; eluent A, H_2O (0.1% TFA) and eluent B, ACN (0.1% TFA) in a linear gradient (A/B) from 0.98:0.02 to 0.7:0.3 in 12 min. MALDI-TOF MS were recorded on a Bruker Daltonics Ultraflex-III MALDI-TOF/TOF mass spectrometer using DHB–NaDHB (9:1) in H_2O–ACN (1:1). Amino acid analysis was performed by Global Facility Center at Hokkaido University using a JLC-500/V fully automatic amino acid analyzer (JEOL Ltd., Tokyo, Japan) and High-Speed Amino Acid Analyzer LA8080 AminoSAAYA (Hitachi, Ltd., Tokyo, Japan).

2.4.2. Methods

MUC1 VNTR based naked, natural and unnatural glycopeptides were manually synthesized on NovaPEG Rink Amide resin through MW assisted SPPS. Resin pre-washings were conducted inside the polypropylene syringe at room temperature with MeOH (2x1 min), DMF (2x1 min), DCM (3x1 min), TFA–DCM (1:99) (3x1 min), DIEA–DCM (1:99) (3x1 min), DCM (3x1 min) while solvents and soluble reagents were removed by vacuum. Standard coupling reactions were conducted pre-activating Fmoc-amino acids (4 eq) with HOBt (4 eq) and HBTU (4 eq) in DMF along DIEA (6 eq) followed by MW irradiation at 50°C for 10 min while shaking.[36,37,41] Fmoc protecting group removal was conducted using 20% piperidine in DMF at 50°C under MW irradiation for 3 min. Fmoc-His and Fmoc-Asp reactions were conducted at room temperature;[51] coupling (1 hour) and three steps deprotection (10 min, 5 min, 5 min). Slight adjustments were adopted after Pro couplings (15 minutes under MW) and for Pro-Pro we conducted a double coupling reaction for the incorporation of the second Pro. Fmoc-glycoamino acid reactions were conducted following previously reported double activation method,[44] in which the Fmoc-glycoamino acid (1.2 eq) is directly added over the resin followed by PyBOP (1.2 eq), HOAt (1.2 eq) and DIEA (3 eq) in DMF, placed 15 min at 50°C under MW irradiation and then, without filtering, PyBOP (1.2 eq), HOAt (1.2 eq) were added again followed by 15 min at 50°C. Free amino groups were capped by DMF–Ac_2O–DIEA (85:10:5) at room temperature during 3 min shaking. Washings after reactions were performed with DMF (3x1 min), DCM (3x1 min), DMF (3x1 min). PEG linker and ketone linker were added following the standard coupling protocol. Glycan acetyl groups[34] were removed by MeOH (3x1 min), Hydrazine–MeOH (7:3) (4x45 min), TFA–DCM (1:99) (3x1 min) on solid-phase, the reaction was followed by MS. Then,

to finish with resin cleavage treatment TFA–H_2O (95:5) at room temperature for 2 hours shaking vigorously. The resulting glycopeptide was collected in a Falcon tube while acetic acid was passed through the resin followed by evaporation, cold MTBE treatment, dissolved in H_2O–ACN (1:1) and then lyophilized. All compounds were purified by semi-preparative RP-HPLC and characterized by analytical RP-UPLC, MS, and amino acid analysis.

2.4.3. Supplementary information

Glycopeptides characterization

Experimental data of the currently used natural (glyco)peptide library data was previously reported:

a) Synthesis and characterization of Compounds **Naked** (5-oxo-hexanoyl-PEG (9a)GVTSAPDTRPAPGSTAPPAHGVT-NH2, purity 96%), **NS4** (5-oxo-hexanoyl-PEG(9a)-GVTS(**Tn**)APDTRPAPGSTAPPAHGVT-NH2, purity 98%), **NT8** (5-oxo-hexanoyl-PEG-GVTSAPDT(**Tn**)RPAPGSTAPPAHGVT-NH2, purity 98%), **NS4T8** (5-oxo-hexanoyl-PEG-GVTS(**Tn**)APDT(**Tn**)RPAPGSTAPPAHGVT-NH2, purity 98%).[52]

b) Synthesis and characterization of Compounds **NT3** (5-oxo-hexanoyl-PEG-GVT(**Tn**)SAPDTRPAPGSTAPPAHGVT-NH2, purity 100%), **NS14** (5-oxo-hexanoyl-PEG- GVTSAPDTRPAPGS(**Tn**)TAPPAHGVT-NH2, purity 99,9%), **NT15** (5-oxo-hexanoyl-PEG-GVTSAPDTRPAPGST(**Tn**)APPAHGVT-NH2, purity 99,9%) and **NT3T15** (5-oxo-hexanoyl-PEG-GVT(**Tn**)SAPDTRPAPGST(**Tn**)APPAHGVT-NH2, purity 99,9%).[16]

c) Synthesis and characterization of Compounds **NT3S4** (5-oxo-hexanoyl-PEG-GVT(**Tn**)S(**Tn**)APDTRPAPGSTAPPAHGVT-NH2, purity 98%), **NT3T8** (5-oxo-hexanoyl-PEG-GVT(**Tn**)SAPDT(**Tn**)RPAPGSTAPPAHGVT-NH2, purity 98%), **NS4T15** (5-oxo-hexanoyl-PEG-GVTS(**Tn**)APDTRPAPGST(**Tn**)APPAHGVT-NH2, purity 99%), **NT8T15** (5-oxo-hexanoyl-PEG-GVTSAPDT(**Tn**)RPAPGST(**Tn**)APPAHGVT-NH2, purity 99%), **NS14T15** (5-oxo-hexanoyl-PEG-GVTSAPDTRPAPGS(**Tn**)T(**Tn**)APPAHGVT-NH2, purity 99%).[46]

The compounds synthesized in this study were purified by semi-preparative RP-HPLC, analyzed by RP-UPLC and characterized by MS and amino acid analysis.

Compound UT3. Analytical UPLC: t_R = 8.047 min, peak area ratio 99.86%. MALDI-TOFMS: $C_{112}H_{178}N_{32}O_{41}$ $[M+H]^+$ calcd (m/z) 2628.2827, found (m/z) 2628.2443. Amino acid analysis (theoretical values in brackets): Asp (1) 1.0, Thr (4) 3.9, Ser (2) 1.8, Gly (3) 3.1, Ala (4) 4.1, Val (2) 2.1, His (1) 1.0, Arg (1) 1.0, Pro (5) 5.0.

Compound US4. Analytical UPLC: t_R = 8.037 min, peak area ratio 99.52%. MALDI-TOFMS: $C_{112}H_{178}N_{32}O_{41}$ $[M+H]^+$ calcd (m/z) 2628.2827, found (m/z) 2628.2775. Amino acid analysis (theoretical values in brackets): Asp (1) 1.0, Thr (4) 3.9, Ser (2) 1.8, Gly (3) 3.1, Ala (4) 4.1, Val (2) 2.1, His (1) 1.1, Arg (1) 1.0, Pro (5) 4.9.

Compound UT8. Analytical UPLC: t_R = 8.251 min, peak area ratio 100%. MALDI-TOFMS: $C_{112}H_{178}N_{32}O_{41}$ $[M+H]^+$ calcd (m/z) 2628.2827, found (m/z) 2628.2781. Amino acid analysis (theoretical values in brackets): Asp (1) 1.0, Thr (4) 3.9, Ser (2) 1.9, Gly (3) 3.1, Ala (4) 4.0, Val (2) 2.1, His (1) 1.0, Arg (1) 1.0, Pro (5) 5.0.

Compound US14. Analytical UPLC: t_R = 7.998 min, peak area ratio 100%. MALDI-TOFMS: $C_{112}H_{178}N_{32}O_{41}$ $[M+H]^+$ calcd (m/z) 2628.2827, found (m/z) 2628.2874. Amino acid analysis (theoretical values in brackets): Asp (1) 1.0, Thr (4) 3.9, Ser (2) 1.8, Gly (3) 3.1, Ala (4) 4.1, Val (2) 2.1, His (1) 1.1, Arg (1) 1.0, Pro (5) 4.8.

Compound UT15. Analytical UPLC: t_R = 8.058 min, peak area ratio 99.31%. MALDI-TOFMS: $C_{112}H_{178}N_{32}O_{41}$ $[M+H]^+$ calcd (m/z) 2628.2827, found (m/z) 2628.2851. Amino acid analysis (theoretical values in brackets): Asp (1) 1.0, Thr (4) 3.9, Ser (2) 1.8, Gly (3) 3.1, Ala (4) 4.1, Val (2) 2.1, His (1) 1.0, Arg (1) 1.0, Pro (5) 5.0.

Compound UT3S4. Analytical UPLC: t_R = 7.947 min, peak area ratio 100%. MALDI-TOFMS: $C_{121}H_{190}N_{34}O_{46}$ $[M+H]^+$ calcd (m/z) 2856.3573, found (m/z) 2856.3520. Amino acid analysis (theoretical values in brackets): Asp (1) 1.0, Thr (4) 3.9, Ser (2) 1.8, Gly (3) 3.1, Ala (4) 4.1, Val (2) 2.0, His (1) 1.0, Arg (1) 1.0, Pro (5) 5.1.

Compound UT3T8. Analytical UPLC: t_R = 7.950 min, peak area ratio 99.54%. MALDI-TOFMS: $C_{121}H_{190}N_{34}O_{46}$ $[M+H]^+$ calcd (m/z) 2856.3573, found (m/z) 2856.3580.Amino acid analysis (theoretical values in brackets): Asp (1) 1.0, Thr (4) 3.9, Ser (2) 1.9, Gly (3) 3.1, Ala (4) 4.0, Val (2) 2.0, His (1) 1.1, Arg (1) 1.0, Pro (5) 5.1.

Compound UT3T15. Analytical UPLC: t_R = 7.831 min, peak area ratio 100%. MALDI-TOFMS: $C_{121}H_{190}N_{34}O_{46}$ $[M+H]^+$ calcd (m/z) 2856.3573, found (m/z) 2856.3492.Amino acid analysis (theoretical values in brackets): Asp (1) 1.0, Thr (4) 3.8, Ser (2) 1.8, Gly (3) 3.1, Ala (4) 4.1, Val (2) 2.0, His (1) 1.0, Arg (1) 1.0, Pro (5) 5.2.

Compound US4T8. Analytical UPLC: t_R = 8.068 min, peak area ratio 99.20%. MALDI-TOFMS: $C_{121}H_{190}N_{34}O_{46}$ $[M+H]^+$ calcd (m/z) 2856.3573, found (m/z) 2856.3605. Amino acid analysis (theoretical values in brackets): Asp (1) 1.0, Thr (4) 3.9, Ser (2) 1.8, Gly (3) 3.1, Ala (4) 3.9, Val (2) 2.0, His (1) 1.0, Arg (1) 1.0, Pro (5) 5.1.

Compound NS4S14. Analytical UPLC: t_R = 7.732 min, peak area ratio 99.35%. MALDI-TOFMS: $C_{119}H_{192}N_{32}O_{46}$ $[M+H]^+$ calcd (m/z) 2806.3668, found (m/z) 2806.3629. Amino acid analysis (theoretical values in brackets): Asp (1) 1.0, Thr (4) 3.9, Ser (2) 1.8, Gly (3) 3.1, Ala (4) 4.0, Val (2) 2.0, His (1) 1.0, Arg (1) 1.0, Pro (5) 5.1.

Compound US4S14. Analytical UPLC: t_R = 8.002 min, peak area ratio 98.91%. MALDI-TOFMS: $C_{121}H_{190}N_{34}O_{46}$ $[M+H]^+$ calcd (m/z) 2856.3573, found (m/z) 2856.3654. Amino acid analysis (theoretical values in brackets): Asp (1) 1.0, Thr (4) 3.9, Ser (2) 1.8, Gly (3) 3.1, Ala (4) 4.0, Val (2) 2.1, His (1) 1.1, Arg (1) 1.0, Pro (5) 4.9.

Compound US4T15. Analytical UPLC: t_R = 8.069 min, peak area ratio 99.36%. MALDI-TOFMS: $C_{121}H_{190}N_{34}O_{46}$ $[M+H]^+$ calcd (m/z) 2856.3573, found (m/z) 2856.3579. Amino acid analysis (theoretical values in brackets): Asp (1) 1.0, Thr (4) 3.9, Ser (2) 1.8, Gly (3) 3.1, Ala (4) 4.0, Val (2) 2.0, His (1) 1.0, Arg (1) 1.0, Pro (5) 5.1.

Compound UT8T15. Analytical UPLC: t_R = 8.092 min, peak area ratio 100%. MALDI-TOFMS: $C_{121}H_{190}N_{34}O_{46}$ $[M+H]^+$ calcd (m/z) 2856.3573, found (m/z) 2856.3563. Amino acid analysis (theoretical values in brackets): Asp (1) 1.0, Thr (4) 3.9, Ser (2) 1.8, Gly (3) 3.1, Ala (4) 4.0, Val (2) 2.1, His (1) 1.0, Arg (1) 1.0, Pro (5) 5.1.

Compound US14T15. Analytical UPLC: t_R = 8.002 min, peak area ratio 99.77%. MALDI-TOFMS: $C_{121}H_{190}N_{34}O_{46}$ $[M+H]^+$ calcd (m/z) 2856.3573, found (m/z) 2856.3485. Amino acid analysis (theoretical values in brackets): Asp (1) 1.0, Thr (4) 3.9, Ser (2) 1.8, Gly (3) 3.1, Ala (4) 4.0, Val (2) 2.0, His (1) 1.0, Arg (1) 1.0, Pro (5) 5.1.

It is worth mentioning that in some mass spectra we have observed the appearance of another peak. This new peak is always 228 m/z less than the target compound. We investigated this phenomenon and it occurs only during the MALDI analysis. It is caused by the vaporization process and it shows the target compound plus related peaks corresponding to the removal of the *sp*^{2}-iminosugar. The purity and integrity of the synthesized compounds was checked by RP-UPLC. In addition, to support this statement, we conducted a MALDI-TOF experiment of the Fmoc-α-*O*-(*sp*^{2}-Ac$_2$GalNAc)-Thr-OH previously assessed as pure by NMR. In this experiment, we can observe how a new peak at 313 m/z corresponding to the loss of the glycan with two Ac protecting groups appears after the MALDI-TOF test. NMR spectra of the pure Fmoc-α-*O*-(*sp*^{2}-Ac$_2$GalNAc)-Thr-OH can be confirmed in the previous reference.[17]

MALDI-TOF experiment with Fmoc-α-*O*-(*sp*^{2}-Ac$_2$GalNAc)-Thr-OH

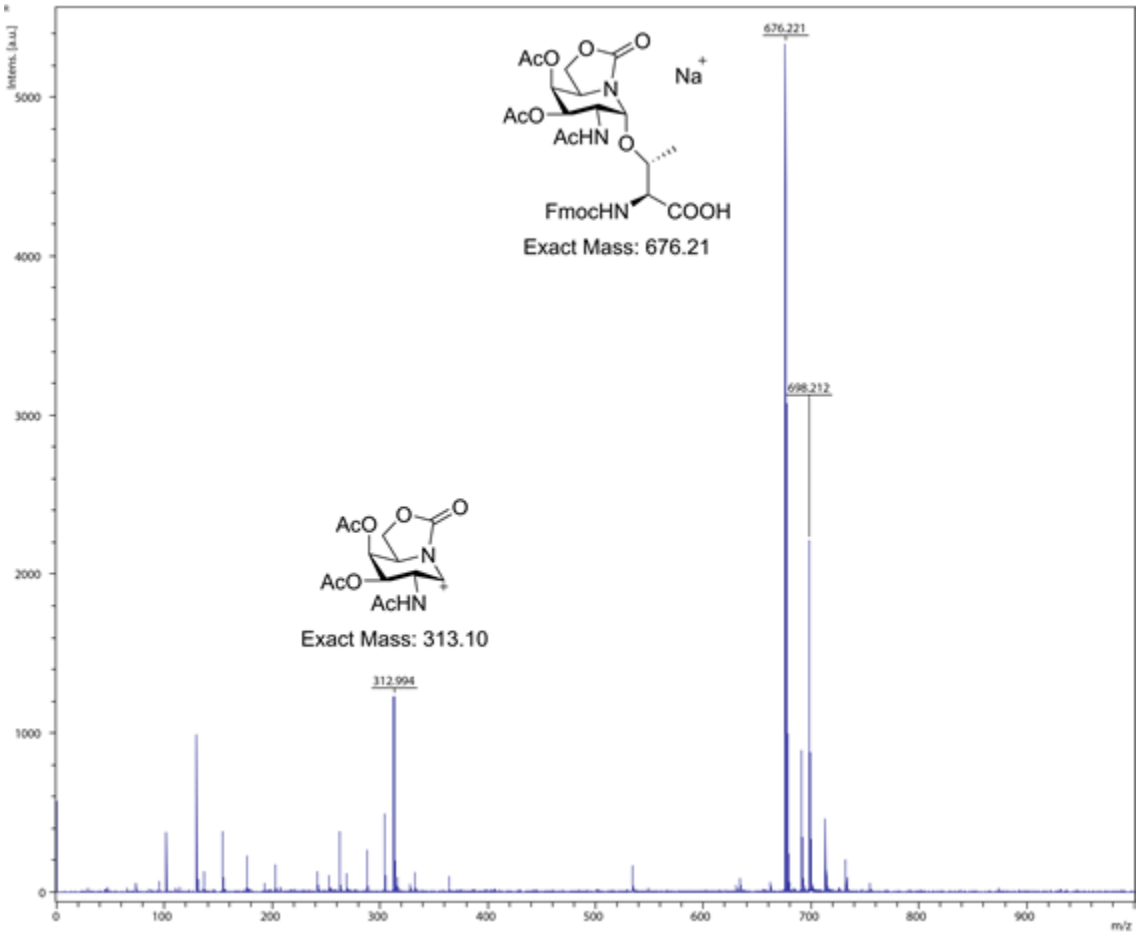

UPLC chromatograms and MS

UPLC profile (a) and ESI-HRMS mass spectrum (b) of **UT3**.

(a)

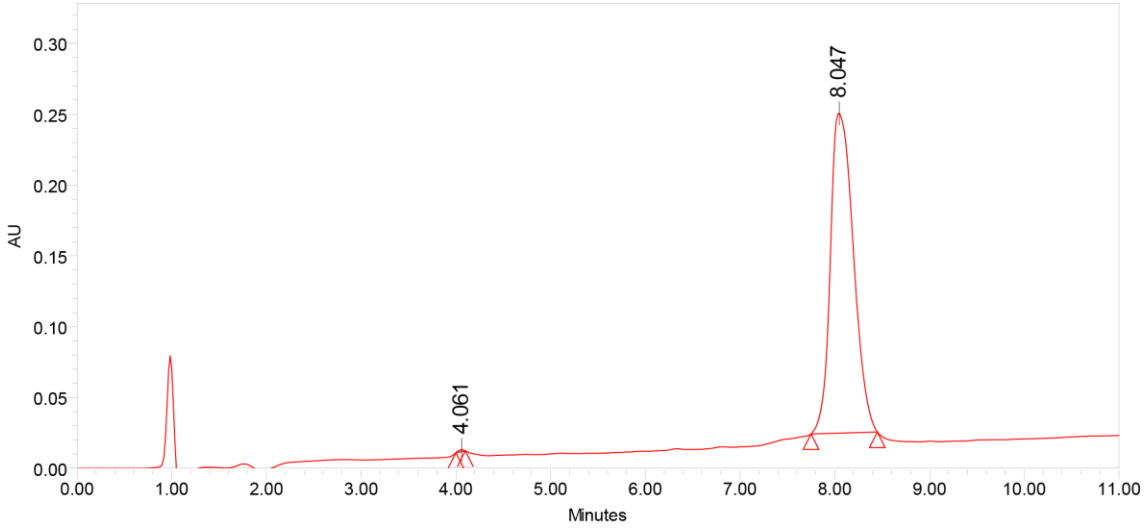

(b)

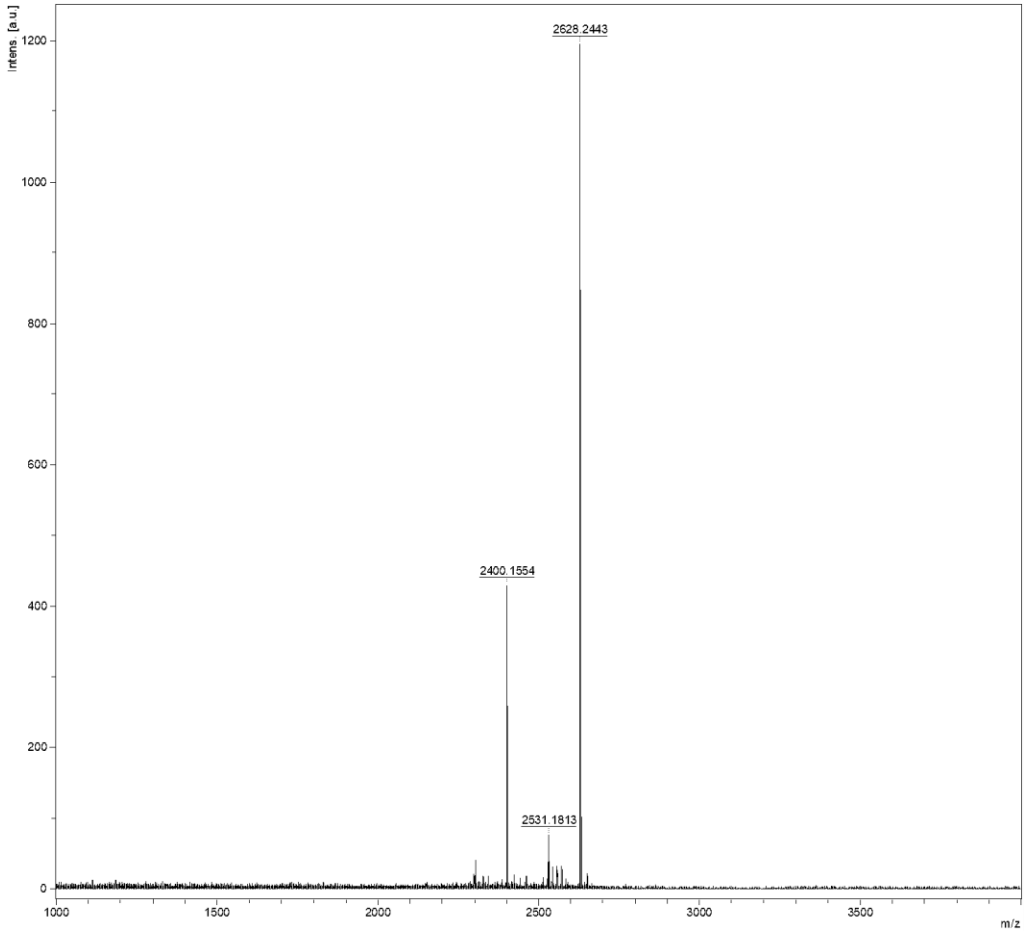

UPLC profile (a) and ESI-HRMS mass spectrum (b) of **US4**.

(a)

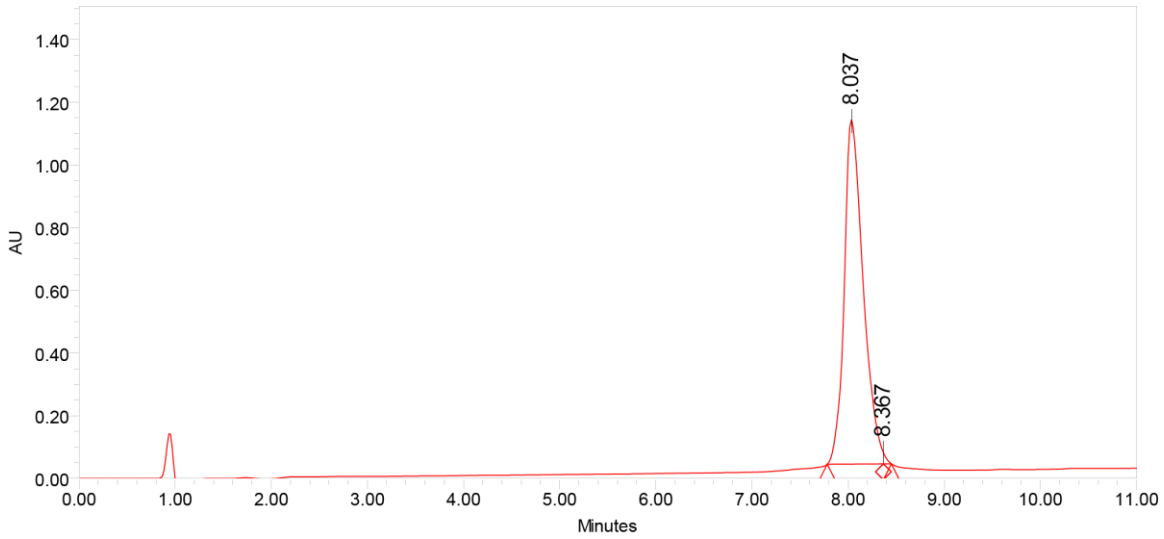

(b)

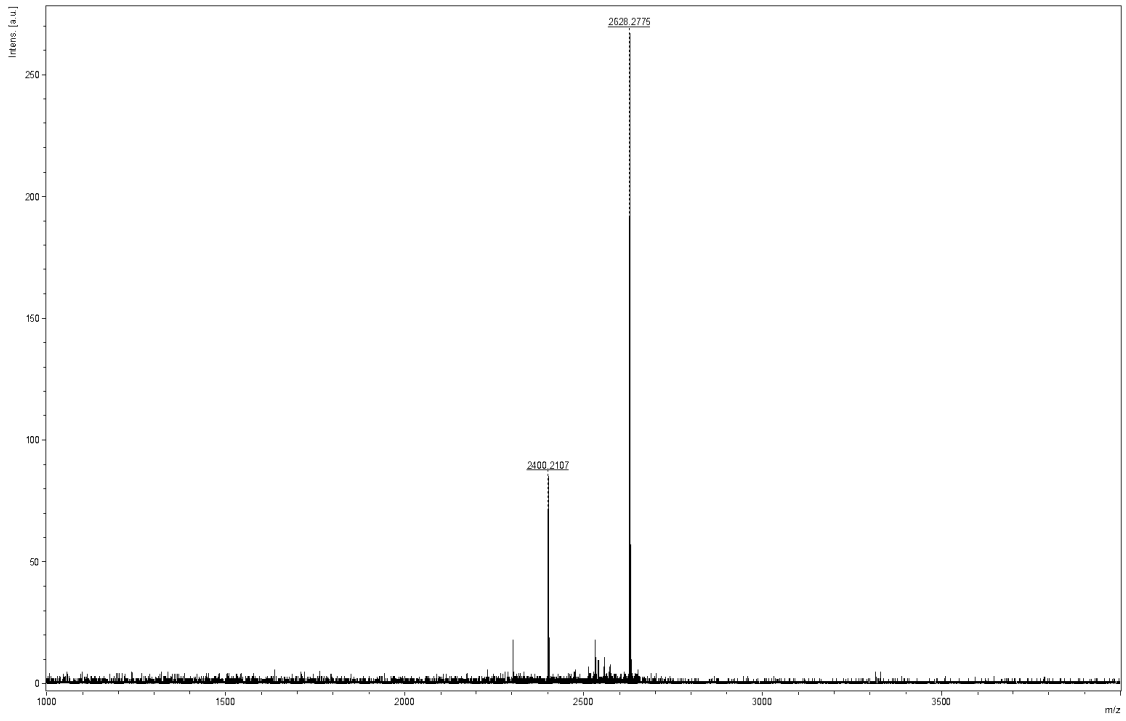

UPLC profile (a) and ESI-HRMS mass spectrum (b) of **UT8**.

(a)

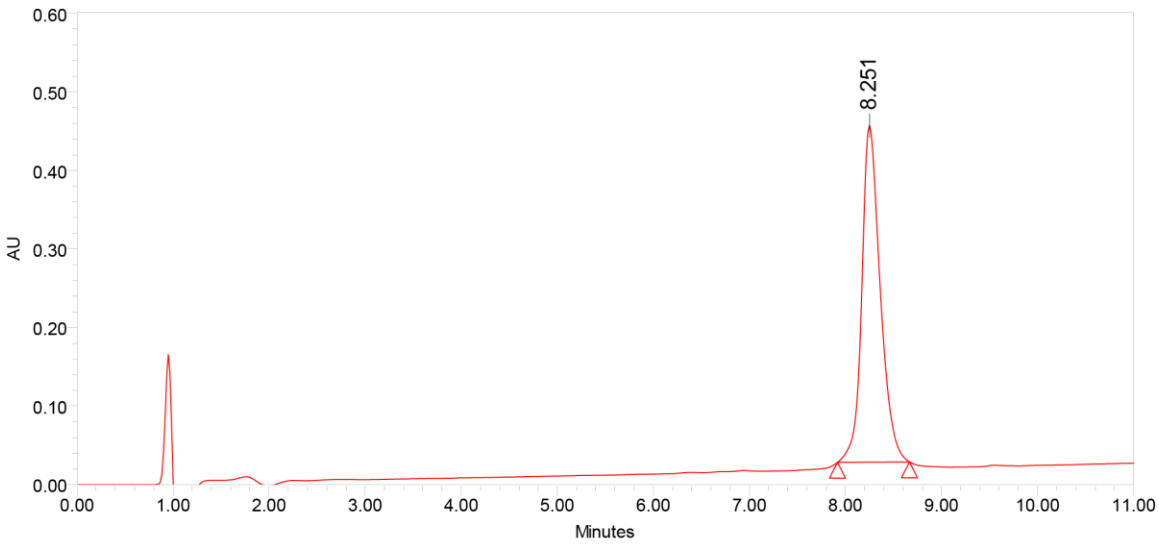

(b)

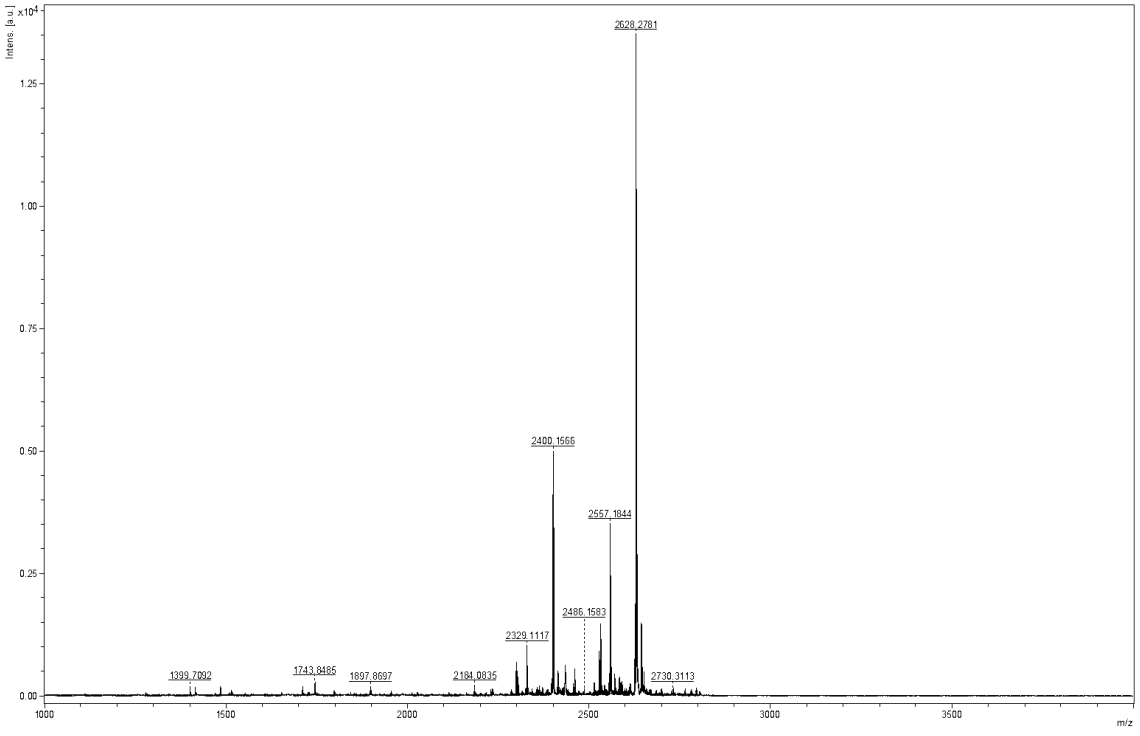

UPLC profile (a) and ESI-HRMS mass spectrum (b) of **US14**.

(a)

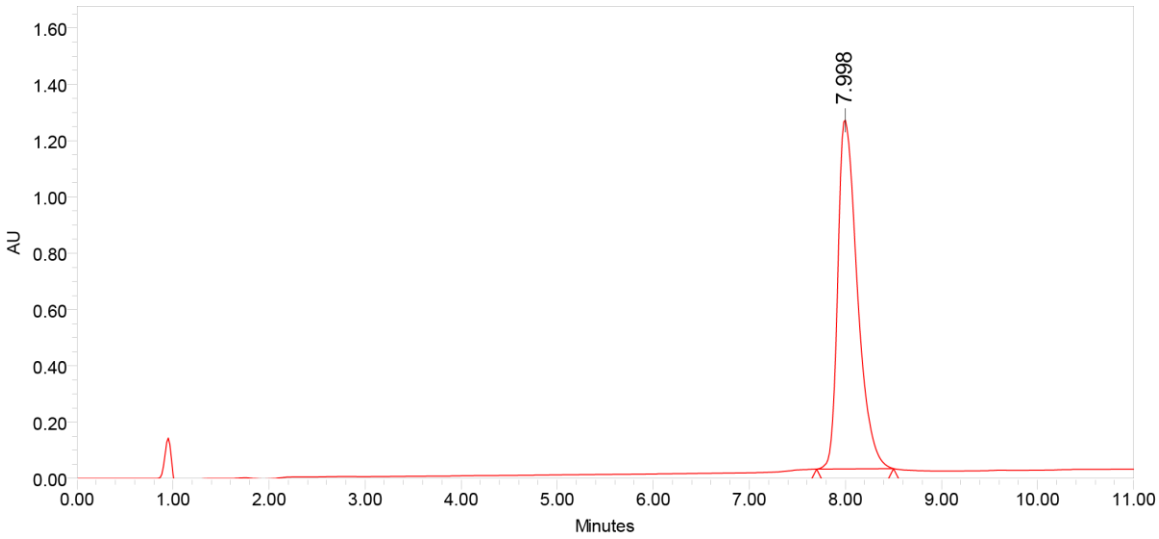

(b)

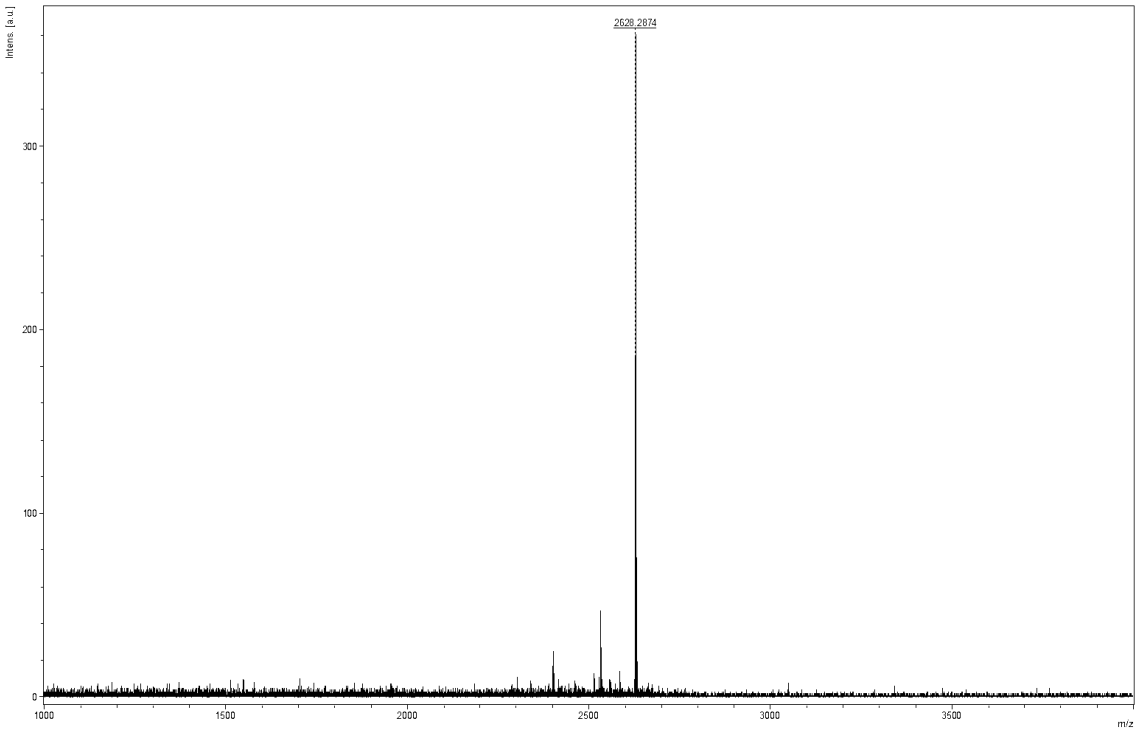

UPLC profile (a) and ESI-HRMS mass spectrum (b) of **UT15**.

(a)

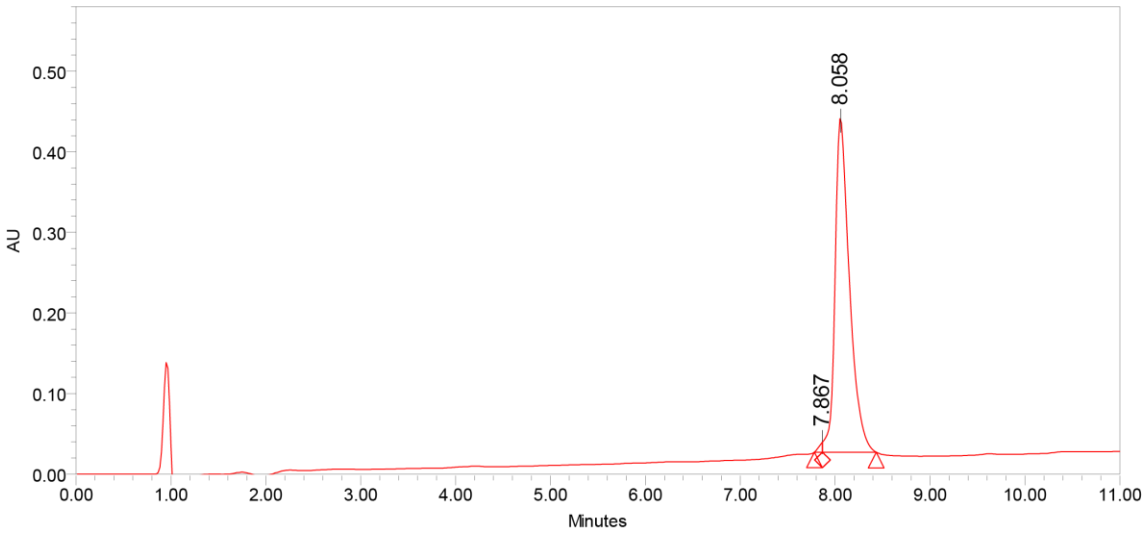

(b)

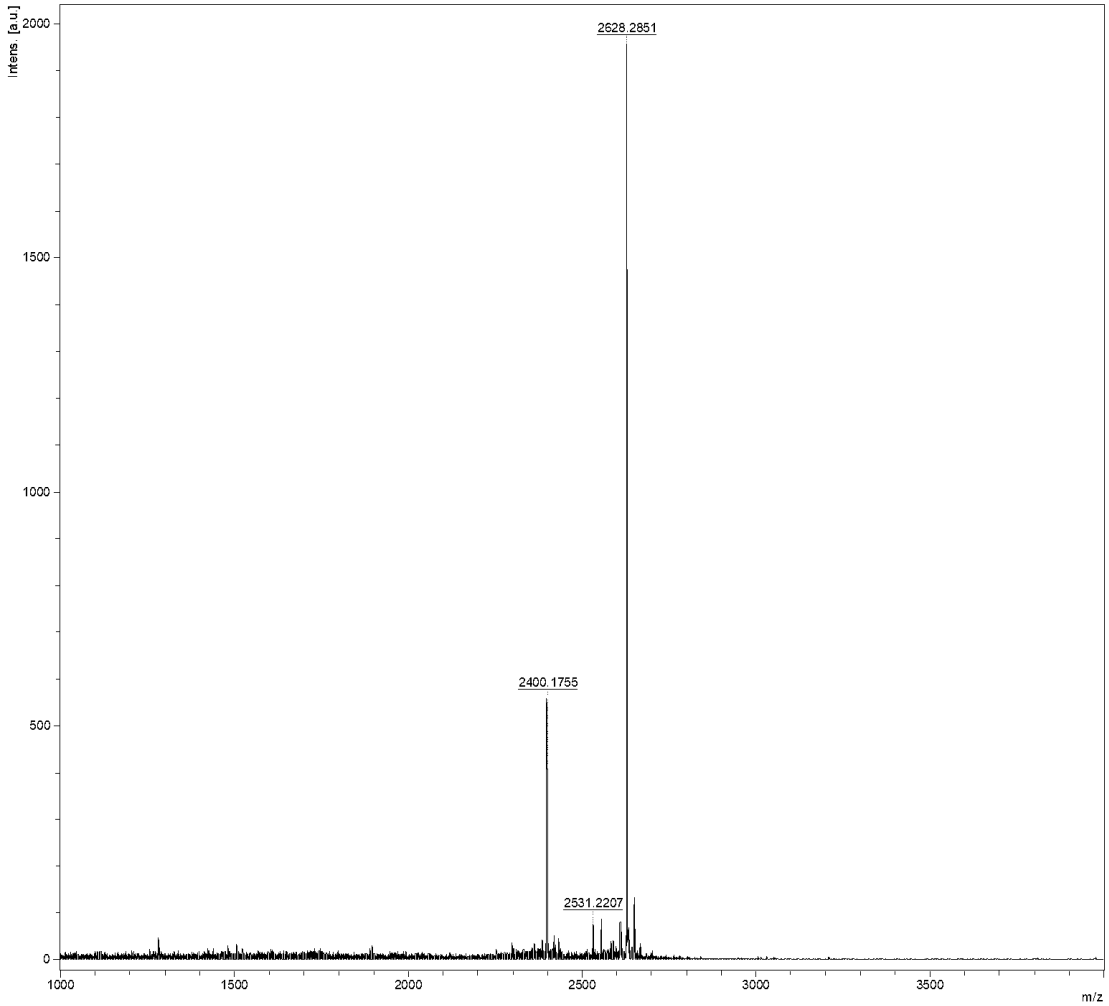

UPLC profile (a) and ESI-HRMS mass spectrum (b) of **UT3S4**.

(a)

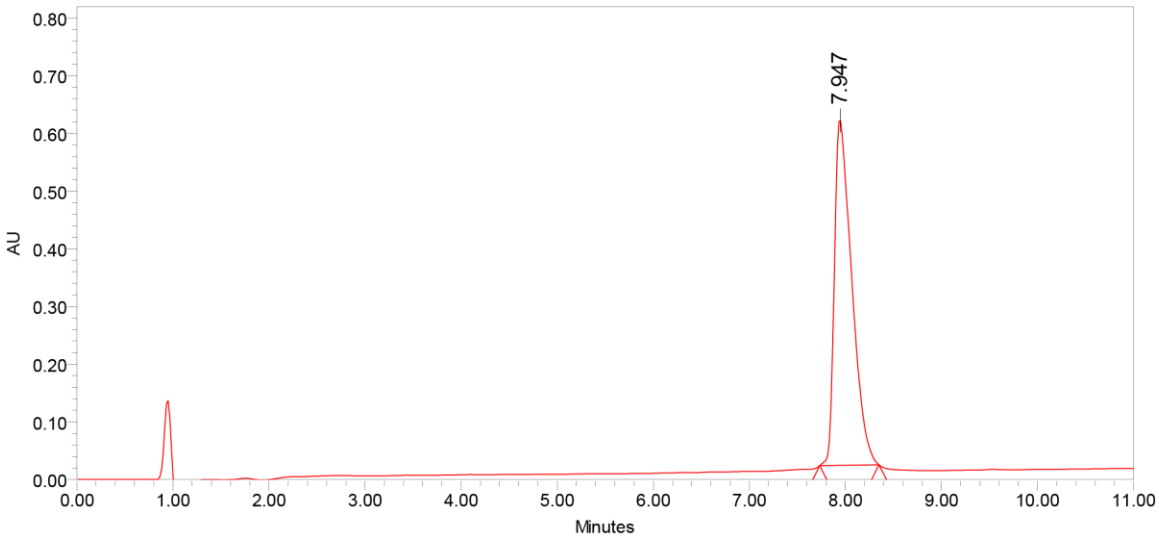

(b)

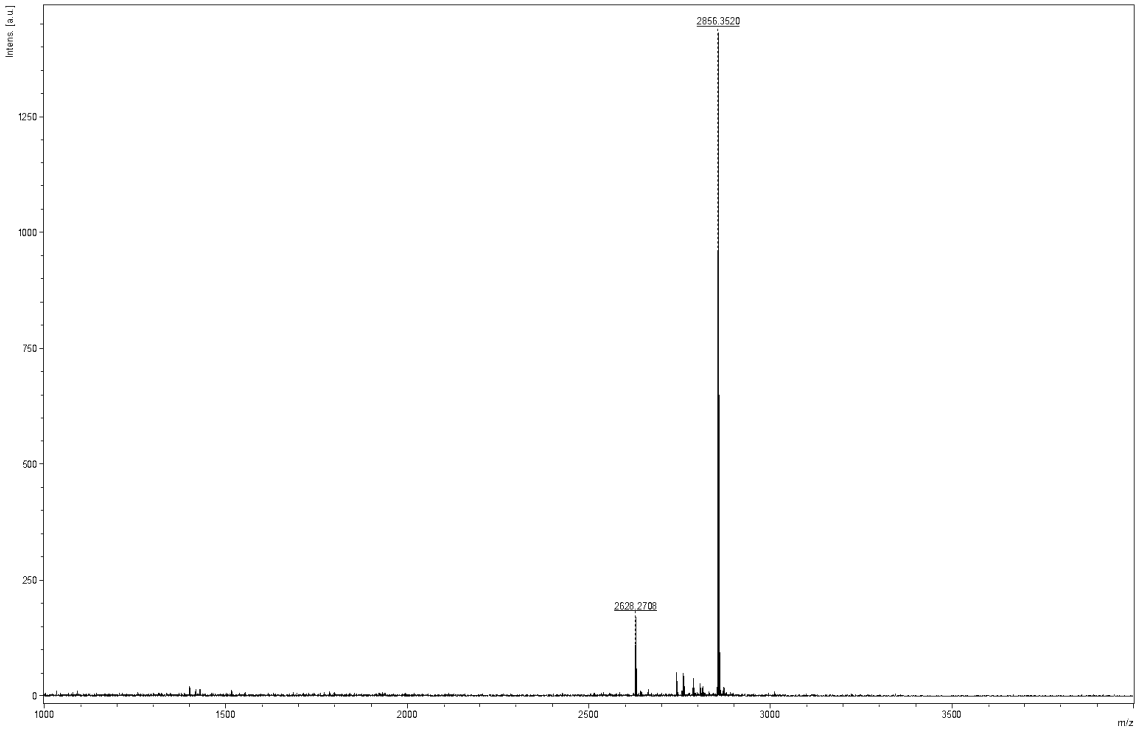

UPLC profile (a) and ESI-HRMS mass spectrum (b) of **UT3T8**.

(a)

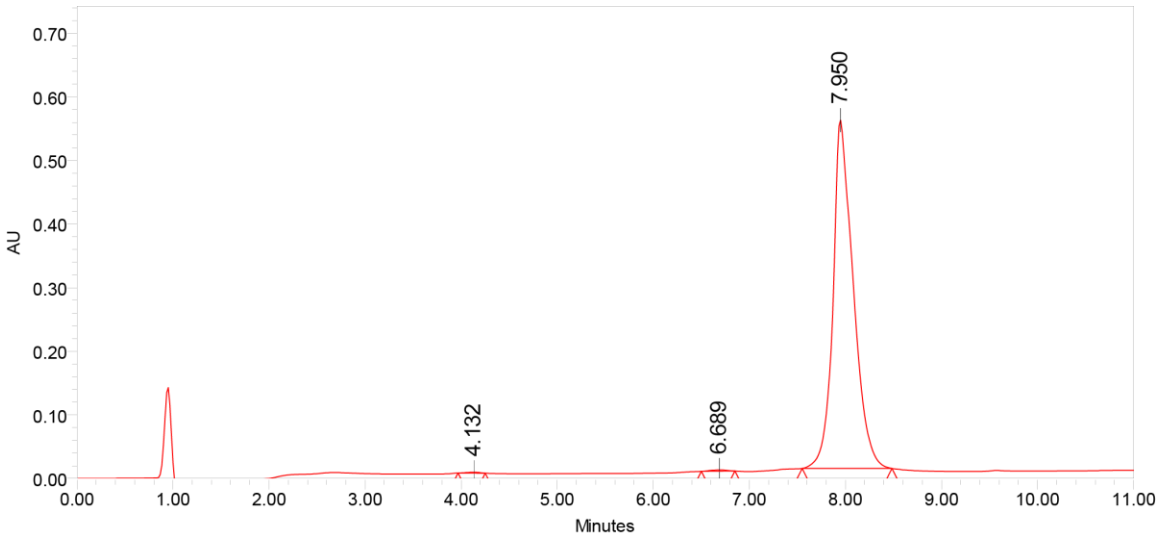

(b)

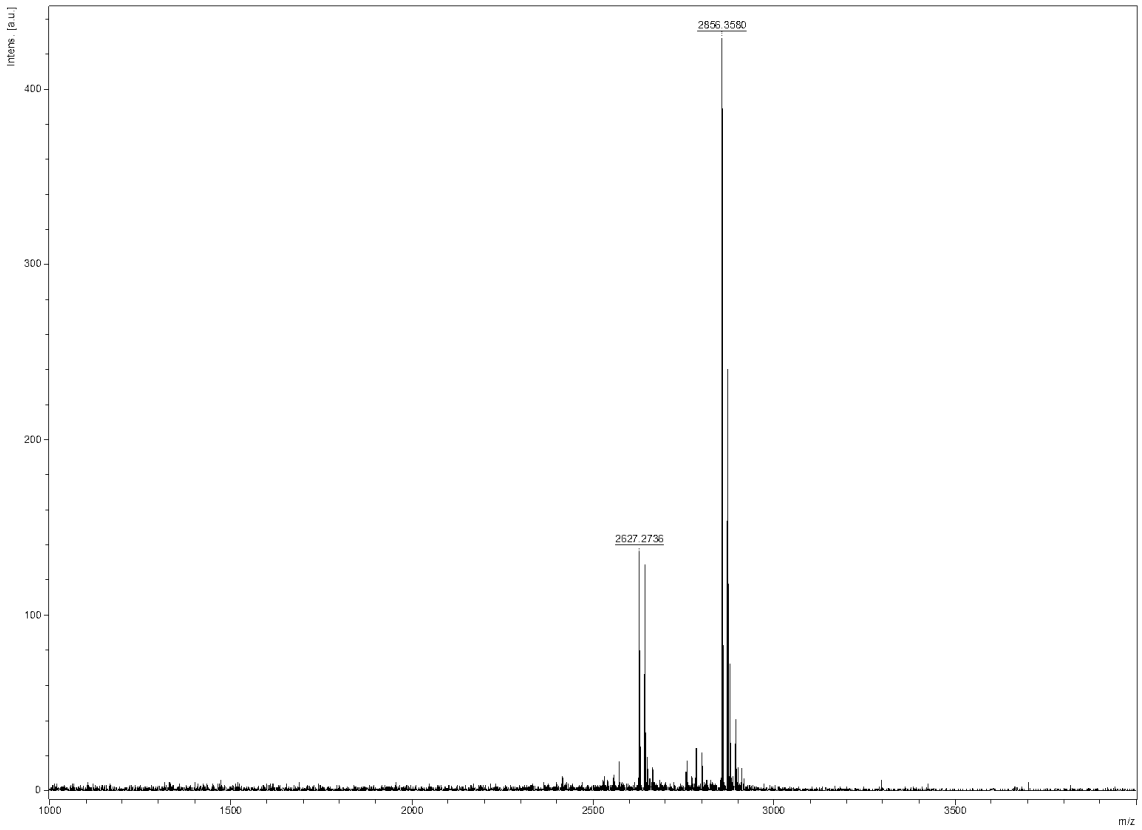

UPLC profile (a) and ESI-HRMS mass spectrum (b) of **UT3T15**.

(a)

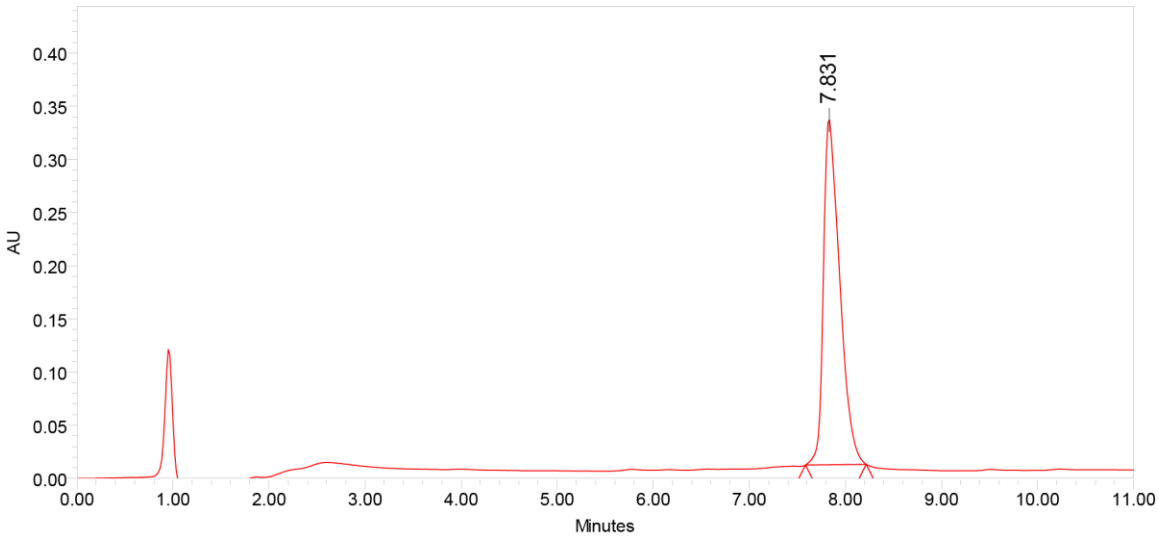

(b)

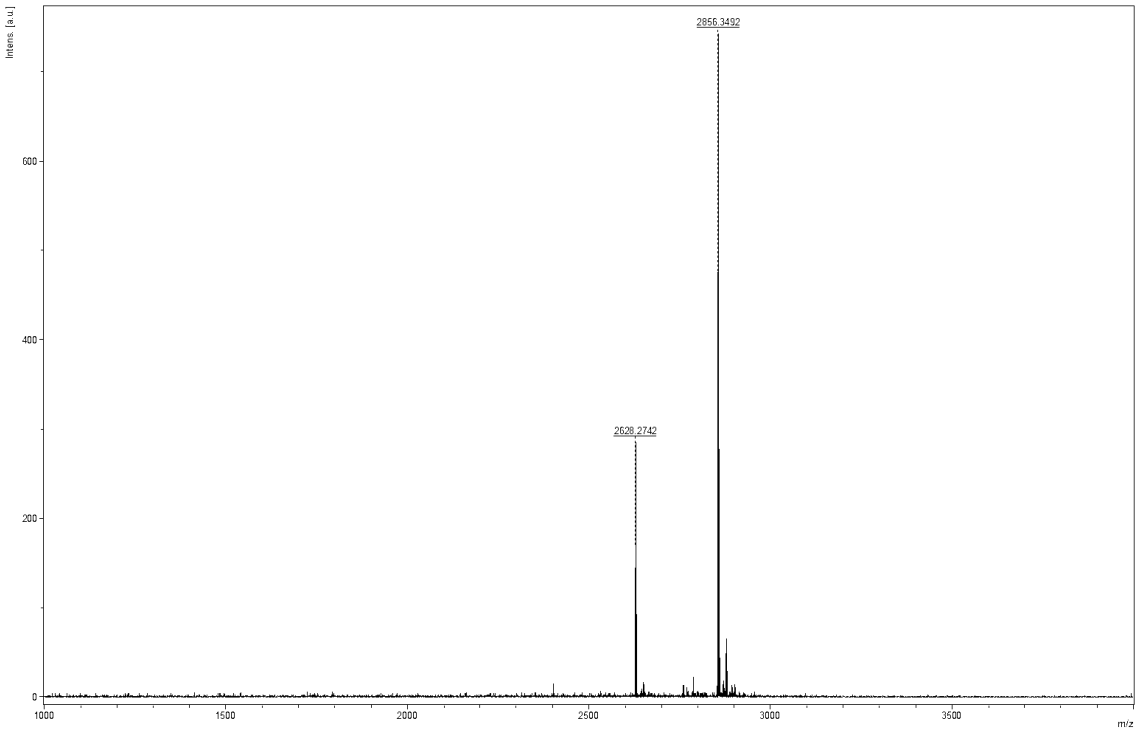

UPLC profile (a) and ESI-HRMS mass spectrum (b) of **US4T8**.

(a)

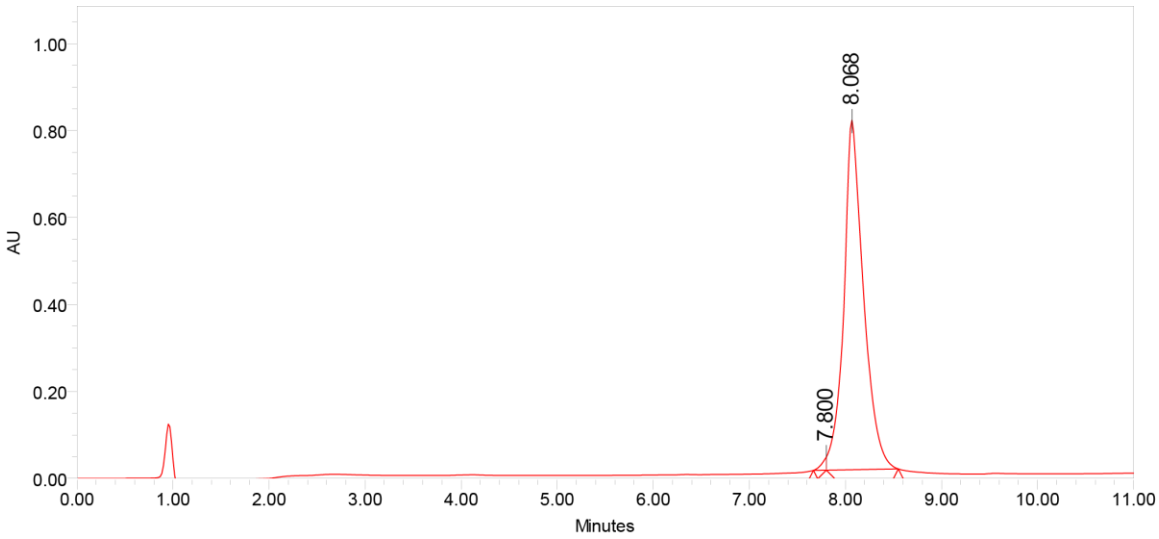

(b)

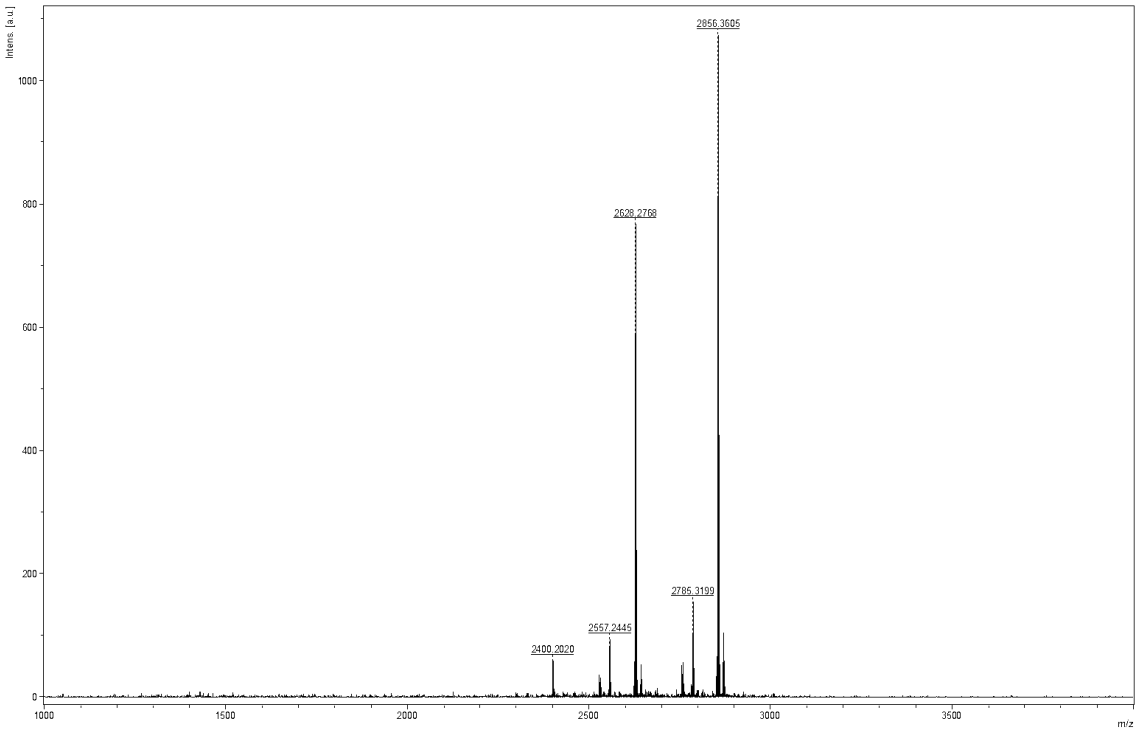

UPLC profile (a) and ESI-HRMS mass spectrum (b) of **NS4S14**.

(a)

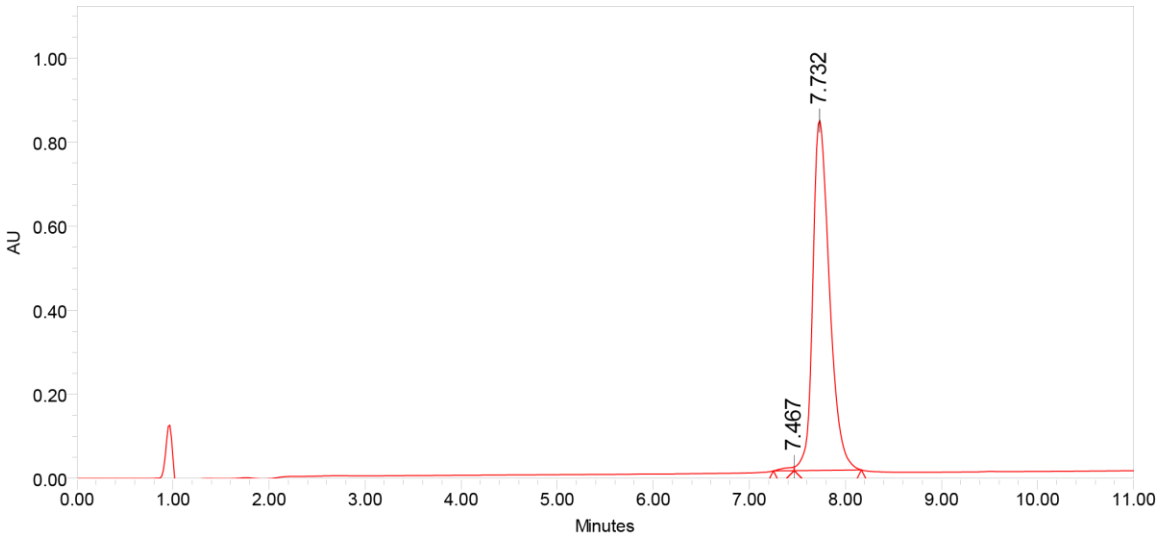

(b)

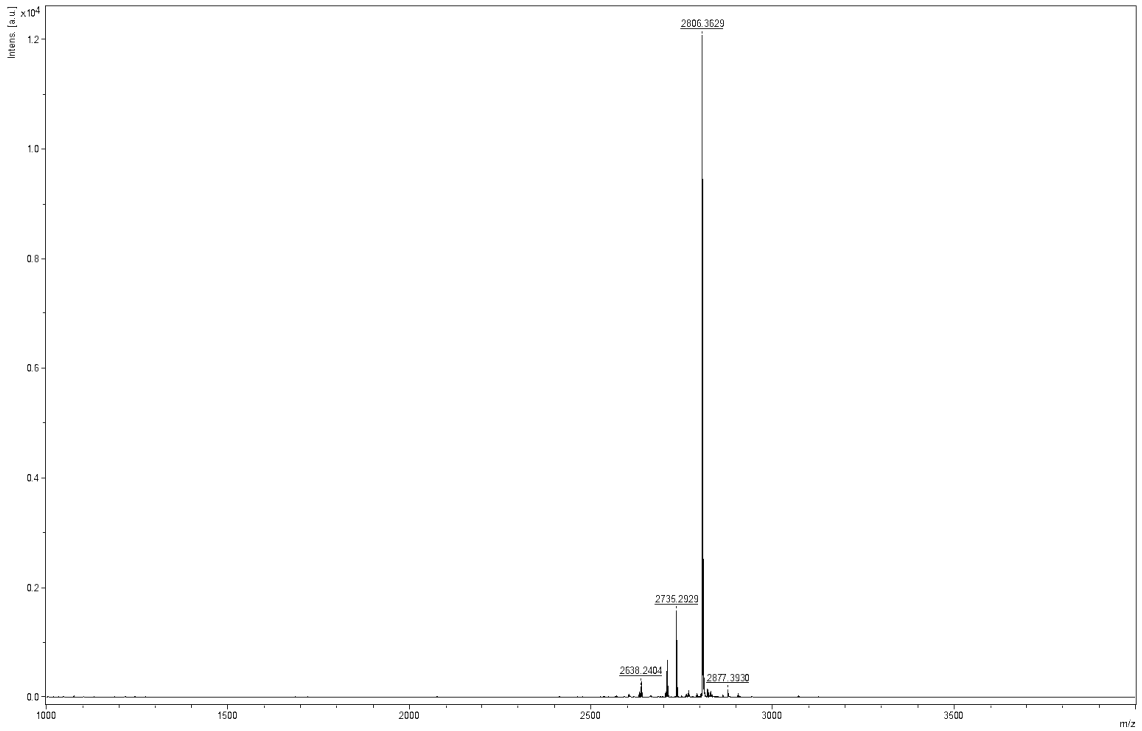

UPLC profile (a) and ESI-HRMS mass spectrum (b) of **US4S14**.

(a)

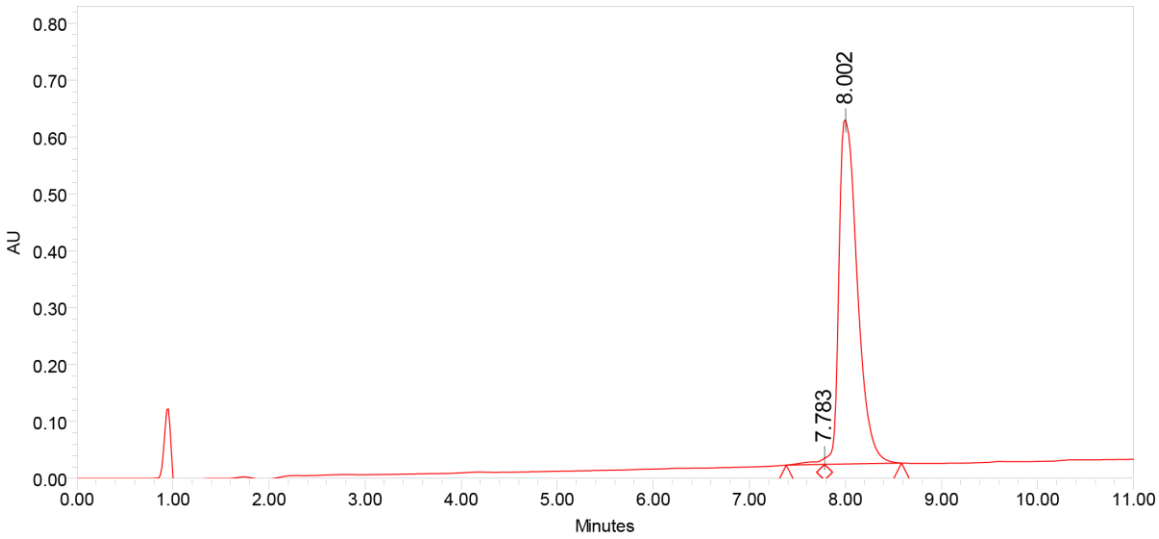

(b)

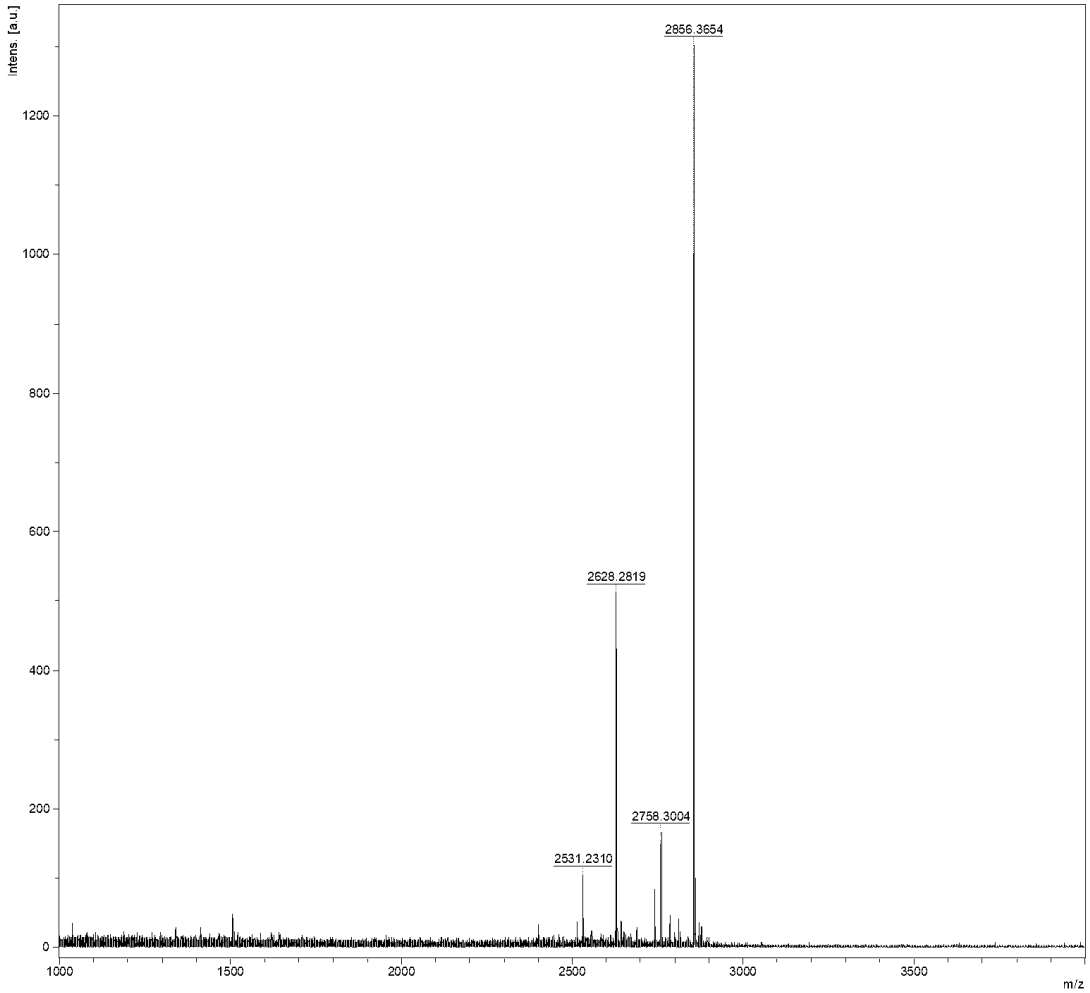

UPLC profile (a) and ESI-HRMS mass spectrum (b) of **US4T15**.

(a)

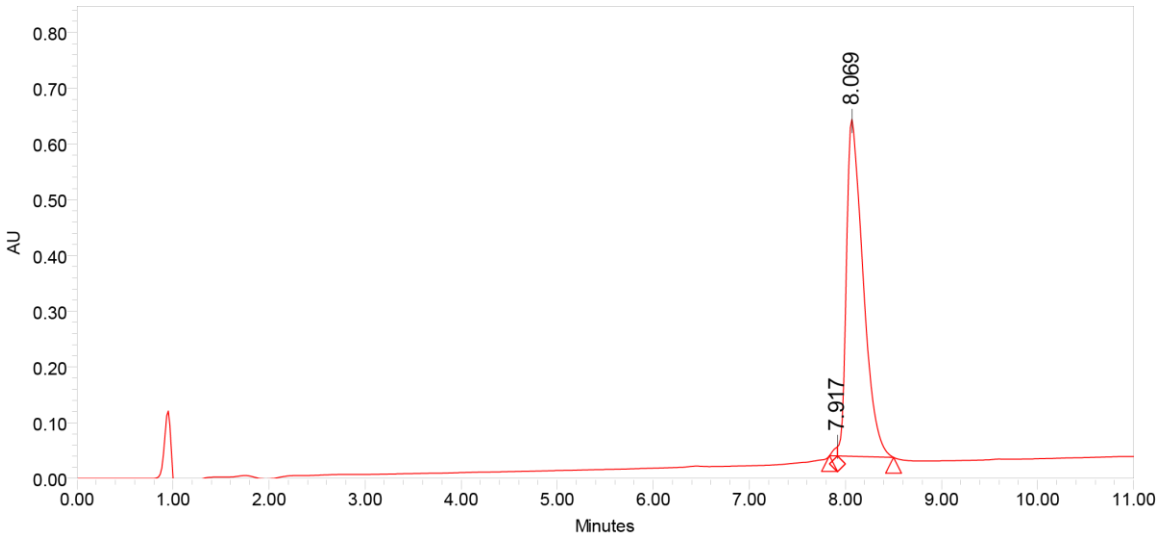

(b)

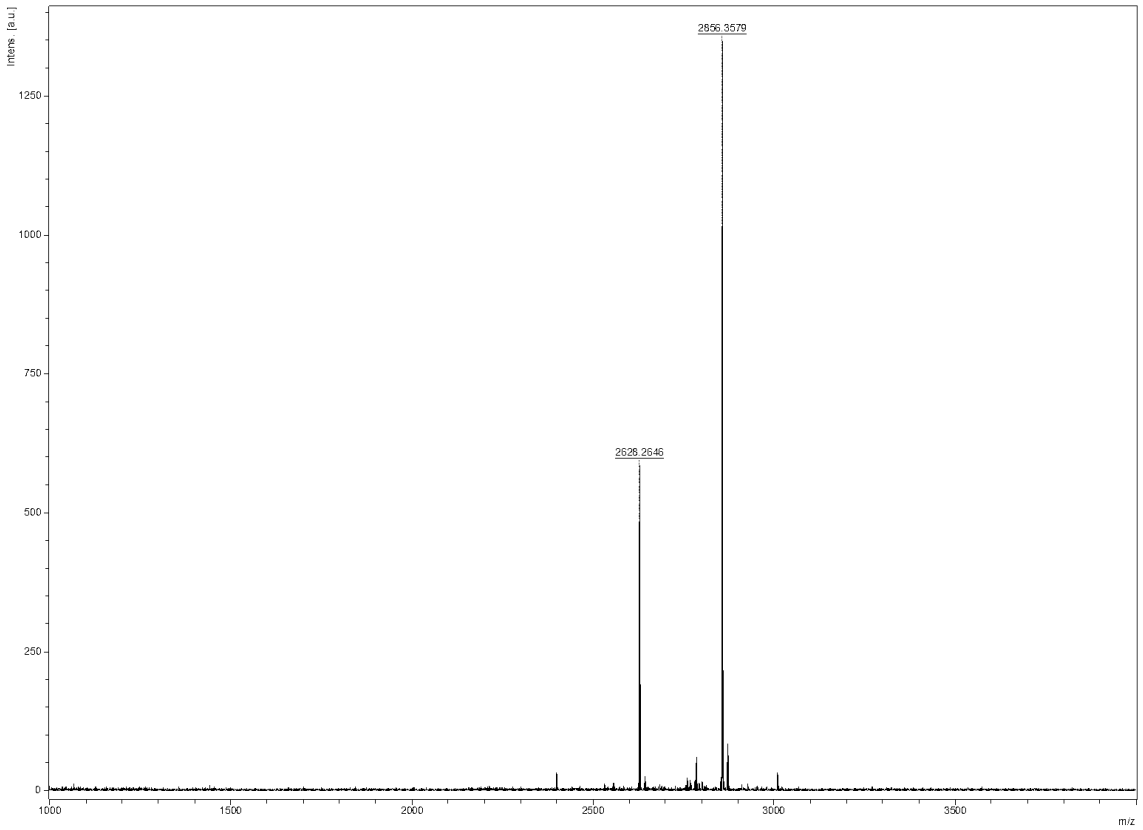

UPLC profile (a) and ESI-HRMS mass spectrum (b) of **UT8T15**.

(a)

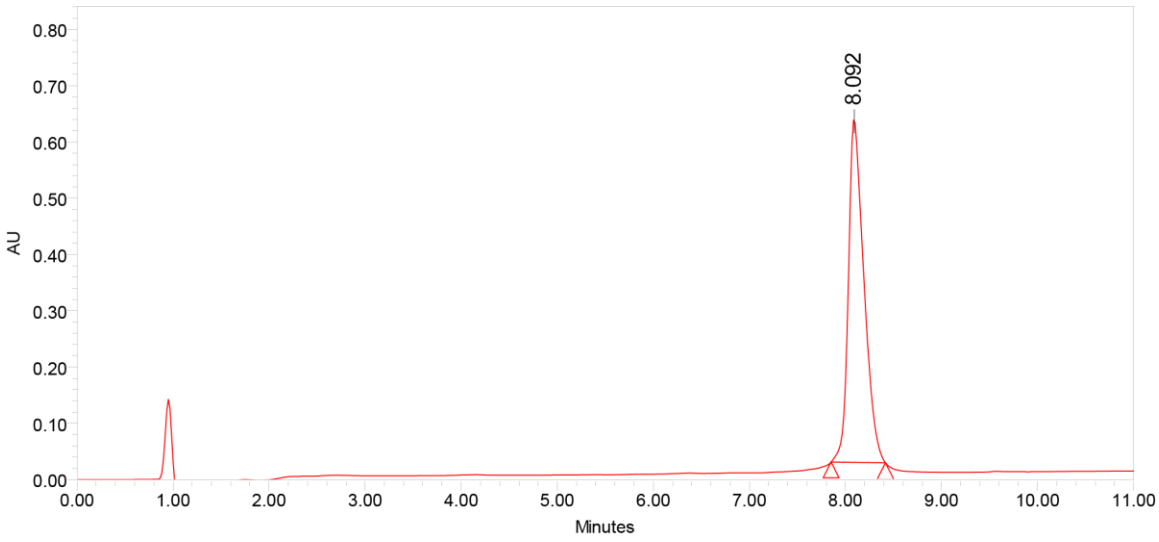

(b)

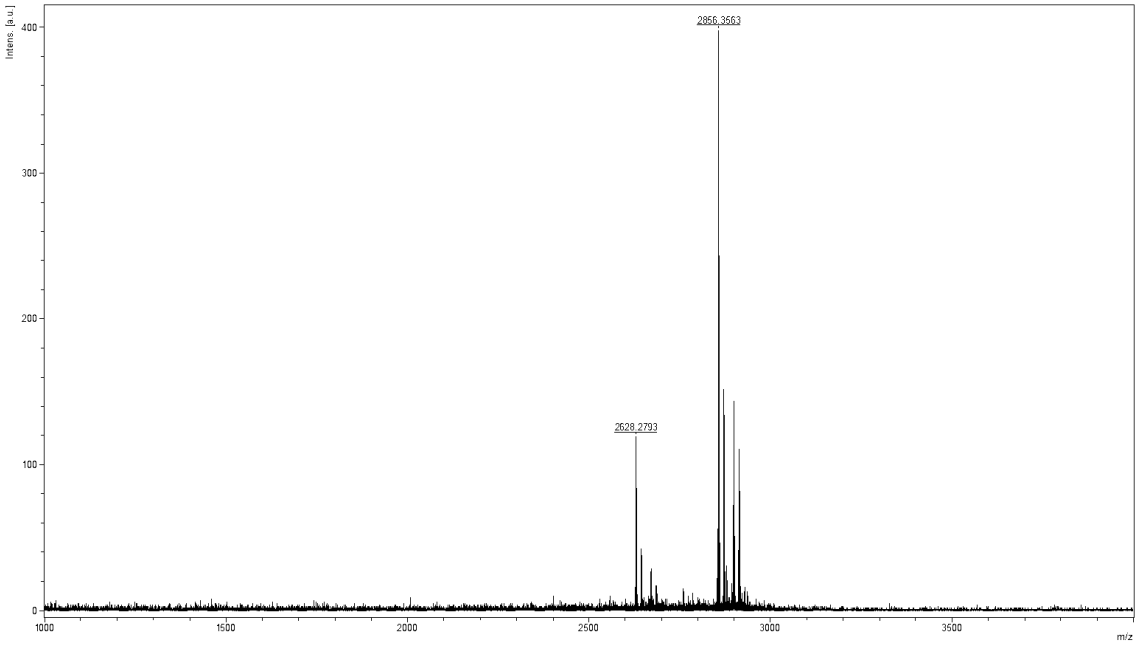

UPLC profile (a) and ESI-HRMS mass spectrum (b) of **US14T15**.

(a)

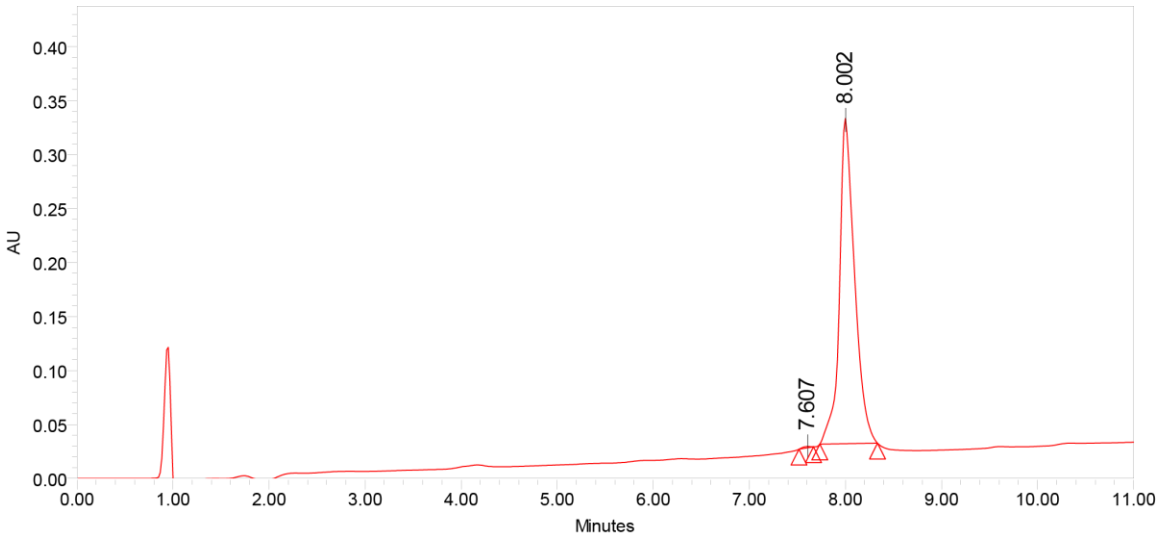

(b)

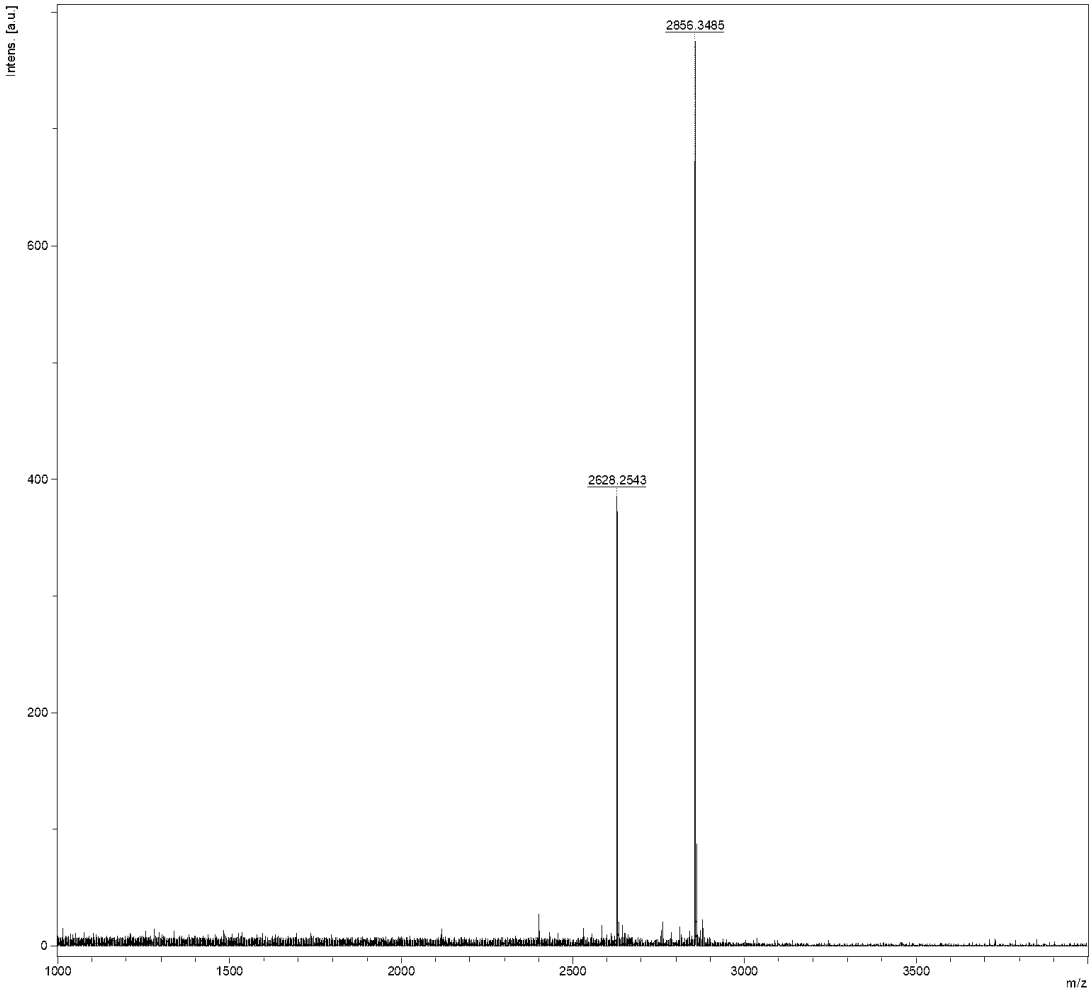

2.5. References

(1) Falzone, L.; Salomone, S.; Libra, M. Evolution of Cancer Pharmacological Treatments at the Turn of the Third Millennium. *Front. Pharmacol.* **2018**, *9* (NOV). https://doi.org/10.3389/fphar.2018.01300.

(2) Schirrmacher, V. From Chemotherapy to Biological Therapy: A Review of Novel Concepts to Reduce the Side Effects of Systemic Cancer Treatment (Review). *Int. J. Oncol.* **2019**, *54* (2), 407–419. https://doi.org/10.3892/ijo.2018.4661.

(3) Farkona, S.; Diamandis, E. P.; Blasutig, I. M. Cancer Immunotherapy: The Beginning of the End of Cancer? *BMC Med.* **2016**, *14* (1), 73. https://doi.org/10.1186/s12916-016-0623-5.

(4) Kennedy, L. B.; Salama, A. K. S. A Review of Cancer Immunotherapy Toxicity. *CA. Cancer J. Clin.* **2020**, *70* (2), 86–104. https://doi.org/10.3322/caac.21596.

(5) Ingale, S.; Wolfert, M. A.; Gaekwad, J.; Buskas, T.; Boons, G.-J. Robust Immune Responses Elicited by a Fully Synthetic Three-Component Vaccine. *Nat. Chem. Biol.* **2007**, *3* (10), 663–667. https://doi.org/10.1038/nchembio.2007.25.

(6) Palitzsch, B.; Hartmann, S.; Stergiou, N.; Glaffig, M.; Schmitt, E.; Kunz, H. A Fully Synthetic Four-Component Antitumor Vaccine Consisting of a Mucin Glycopeptide Antigen Combined with Three Different T-Helper-Cell Epitopes. *Angew. Chemie - Int. Ed.* **2014**, *53* (51), 14245–14249. https://doi.org/10.1002/anie.201406843.

(7) Krajmalnik-Brown, R.; Ilhan, Z.-E.; Kang, D.-W.; DiBaise, J. K. Effects of Gut Microbes on Nutrient Absorption and Energy Regulation. *Nutr. Clin. Pract.* **2012**, *27*

(2), 201–214. https://doi.org/10.1177/0884533611436116.

(8) Videira, P. A.; Julien, S.; Loureiro, L. R.; Sousa, D. P.; Carrascal, M. A.; Delannoy, P. Vaccine and Antibody Therapy Against Thomsen- Friedenreich Tumor-Associated Carbohydrate Antigens. In *Recent Advances in Biotechnology*; A. Videira, P., Julien, S., R. Loureiro, L., P. Sousa, D., A. Carrascal, M., Delannoy, P., Eds.; BENTHAM SCIENCE PUBLISHERS, **2016**; 3, 3–38. https://doi.org/10.2174/978168108391911603000 4.

(9) Slovin, S. F.; Keding, S. J.; Ragupathi, G. Carbohydrate Vaccines as Immunotherapy for Cancer. *Immunol. Cell Biol.* **2005**, *83* (4), 418–428. https://doi.org/10.1111/j.1440-1711.2005.01350.x.

(10) Taylor-Papadimitriou, J.; Burchell, J. M.; Graham, R.; Beatson, R. Latest Developments in MUC1 Immunotherapy. *Biochem. Soc. Trans.* **2018**, *46* (3), 659–668. https://doi.org/10.1042/BST20170400.

(11) Buettner, M. J.; Shah, S. R.; Saeui, C. T.; Ariss, R.; Yarema, K. J. Improving Immunotherapy Through Glycodesign. *Front. Immunol.* **2018**, *9* (NOV). https://doi.org/10.3389/fimmu.2018.02485.

(12) Ernst, B.; Magnani, J. L. From Carbohydrate Leads to Glycomimetic Drugs. *Nat. Rev. Drug Discov.* **2009**, *8* (8), 661–677. https://doi.org/10.1038/nrd2852.

(13) Hevey, R. Strategies for the Development of Glycomimetic Drug Candidates. *Pharmaceuticals* **2019**, *12* (2), 55. https://doi.org/10.3390/ph12020055.

(14) Tamburrini, A.; Colombo, C.; Bernardi, A. Design and Synthesis of Glycomimetics: Recent Advances. *Med. Res. Rev.* **2020**, *40* (2), 495–531.

https://doi.org/10.1002/med.21625.

(15) Nativi, C.; Papi, F.; Roelens, S. Tn Antigen Analogues: The Synthetic Way to "Upgrade" an Attracting Tumour Associated Carbohydrate Antigen (TACA). *Chem. Commun.* **2019**, *55* (54), 7729–7736. https://doi.org/10.1039/c9cc02920f.

(16) Coelho, H.; Matsushita, T.; Artigas, G.; Hinou, H.; Cañada, F. J.; Lo-Man, R.; Leclerc, C.; Cabrita, E. J.; Jiménez-Barbero, J.; Nishimura, S.-I.; Garcia-Martín, F.; Marcelo, F. The Quest for Anticancer Vaccines: Deciphering the Fine-Epitope Specificity of Cancer-Related Monoclonal Antibodies by Combining Microarray Screening and Saturation Transfer Difference NMR. *J. Am. Chem. Soc.* **2015**, *137* (39), 12438–12441. https://doi.org/10.1021/jacs.5b06787.

(17) Fernández, E. M. S.; Navo, C. D.; Martínez-Sáez, N.; Gonçalves-Pereira, R.; Somovilla, V. J.; Avenoza, A.; Busto, J. H.; Bernardes, G. J. L.; Jiménez-Osés, G.; Corzana, F.; Fernández, J. M. G.; Ortiz Mellet, C.; Peregrina, J. M. Tn Antigen Mimics Based on Sp 2 -Iminosugars with Affinity for an Anti-MUC1 Antibody. *Org. Lett.* **2016**, *18* (15), 3890–3893. https://doi.org/10.1021/acs.orglett.6b01899.

(18) Compain, P.; Martin, O. R. *Iminosugars*; Eds.; John Wiley & Sons, Ltd: Chichester, UK, **2007**. https://doi.org/10.1002/9780470517437.

(19) Paulsen, H. Carbohydrates Containing Nitrogen or Sulfur in the "Hemiacetal" Ring. *Angew. Chemie Int. Ed. English* **1966**, *5* (5), 495–510. https://doi.org/10.1002/anie.196604951.

(20) Inouye, S.; Tsuruoka, T.; Nida, T. The Structure of Nojirimycin, a Piperidinose Sugar Antibiotic. *J. Antibiot. (Tokyo).* **1966**, *19* (6), 288–292.

https://doi.org/10.7164/antibiotics.19.288.

(21) Hohenschutz, L. D.; Bell, E. A.; Jewess, P. J.; Leworthy, D. P.; Pryce, R. J.; Arnold, E.; Clardy, J. Castanospermine, A 1,6,7,8-Tetrahydroxyoctahydroindolizine Alkaloid, from Seeds of Castanospermum Australe. *Phytochemistry* **1981**, *20* (4), 811–814. https://doi.org/10.1016/0031-9422(81)85181-3.

(22) Díaz Pérez, V. M.; García Moreno, M. I.; Ortiz Mellet, C.; Fuentes, J.; Díaz Arribas, J. C.; Cañada, F. J.; García Fernández, J. M. Generalized Anomeric Effect in Action: Synthesis and Evaluation of Stable Reducing Indolizidine Glycomimetics as Glycosidase Inhibitors. *J. Org. Chem.* **2000**, *65* (1), 136–143. https://doi.org/10.1021/jo991242o.

(23) Sánchez-Fernández, E. M.; Gonçalves-Pereira, R.; Rísquez-Cuadro, R.; Plata, G. B.; Padrón, J. M.; García Fernández, J. M.; Ortiz Mellet, C. Influence of the Configurational Pattern of Sp2-Iminosugar Pseudo N-, S-, O- and C-Glycosides on Their Glycoside Inhibitory and Antitumor Properties. *Carbohydr. Res.* **2016**, *429*, 113–122. https://doi.org/10.1016/j.carres.2016.01.006.

(24) Bermejo, I. A.; Navo, C. D.; Castro-López, J.; Guerreiro, A.; Jiménez-Moreno, E.; Sánchez Fernández, E. M.; García-Martín, F.; Hinou, H.; Nishimura, S.-I.; García Fernández, J. M.; Mellet, C. O.; Avenoza, A.; Busto, J. H.; Bernardes, G. J. L.; Hurtado-Guerrero, R.; Peregrina, J. M.; Corzana, F. Synthesis, Conformational Analysis and in Vivo Assays of an Anti-Cancer Vaccine That Features an Unnatural Antigen Based on an Sp 2 -Iminosugar Fragment. *Chem. Sci.* **2020**, *11* (15), 3996–4006. https://doi.org/10.1039/C9SC06334J.

(25) Aguilar-Moncayo, M.; Díaz-Pérez, P.; García Fernández, J. M.; Ortiz Mellet, C.; García-Moreno, M. I. Synthesis and Glycosidase Inhibitory Activity of Isourea-Type Bicyclic Sp2-Iminosugars Related to Galactonojirimycin and Allonojirimycin. *Tetrahedron* **2012**, *68* (2), 681–689. https://doi.org/10.1016/j.tet.2011.10.091.

(26) Díaz Pérez, P.; García-Moreno, M. I.; Ortiz Mellet, C.; García Fernández, J. M. Synthesis and Comparative Glycosidase Inhibitory Properties of Reducing Castanospermine Analogues. *European J. Org. Chem.* **2005**, *2005* (14), 2903–2913. https://doi.org/10.1002/ejoc.200500071.

(27) Gueder, N.; Allan, G.; Telliez, M. S.; Hague, F.; Fernandez, J. M.; Sanchez-Fernandez, E. M.; Ortiz-Mellet, C.; Ahidouch, A.; Ouadid-Ahidouch, H. Sp2-Iminosugar α-Glucosidase Inhibitor 1-C-Octyl-2-Oxa-3-Oxocastanospermine Specifically Affected Breast Cancer Cell Migration through Stim1, B1-Integrin, and FAK Signaling Pathways. *J. Cell. Physiol.* **2017**, *232* (12), 3631–3640. https://doi.org/10.1002/jcp.25832.

(28) Sánchez-Fernández, E. M.; Gómez-Pérez, V.; García-Hernández, R.; García Fernández, J. M.; Plata, G. B.; Padrón, J. M.; Ortiz Mellet, C.; Castanys, S.; Gamarro, F. Antileishmanial Activity of Sp2-Iminosugar Derivatives. *RSC Adv.* **2015**, *5* (28), 21812–21822. https://doi.org/10.1039/c5ra02627j.

(29) Schaeffer, E.; Sánchez-Fernández, E. M.; Gonçalves-Pereira, R.; Flacher, V.; Lamon, D.; Duval, M.; Fauny, J.-D.; García Fernández, J. M.; Mueller, C. G.; Ortiz Mellet, C. Sp2-Iminosugar Glycolipids as Inhibitors of Lipopolysaccharide-Mediated Human Dendritic Cell Activation in Vitro and of Acute Inflammation in Mice in Vivo. *Eur. J.*

Med. Chem. **2019**, *169*, 111–120. https://doi.org/10.1016/j.ejmech.2019.02.078.

(30) Hussain, S.; Miller, J. L.; Harvey, D. J.; Gu, Y.; Rosenthal, P. B.; Zitzmann, N.; McCauley, J. W. Strain-Specific Antiviral Activity of Iminosugars against Human Influenza A Viruses. *J. Antimicrob. Chemother*. **2015**, *70* (1), 136–152. https://doi.org/10.1093/jac/dku349.

(31) Sánchez-Fernández, E. M.; Rísquez-Cuadro, R.; Chasseraud, M.; Ahidouch, A.; Mellet, C. O.; Ouadid-Ahidouch, H.; Fernández, J. M. G. Synthesis of N-, S-, and C-Glycoside Castanospermine Analogues with Selective Neutral α-Glucosidase Inhibitory Activity as Antitumour Agents. *Chem. Commun.* **2010**, *46* (29), 5328–5330. https://doi.org/10.1039/c0cc00446d.

(32) Allan, G.; Ouadid-Ahidouch, H.; Sanchez-Fernandez, E. M.; Risquez-Cuadro, R.; Fernandez, J. M. G.; Ortiz-Mellet, C.; Ahidouch, A. New Castanospermine Glycoside Analogues Inhibit Breast Cancer Cell Proliferation and Induce Apoptosis without Affecting Normal Cells. *PLoS One* **2013**, *8* (10), e76411. https://doi.org/10.1371/journal.pone.0076411.

(33) Hevey, R. Bioisosteres of Carbohydrate Functional Groups in Glycomimetic Design. *Biomimetics* **2019**, *4* (3), 53. https://doi.org/10.3390/biomimetics4030053.

(34) Sánchez-Fernández, E. M.; Rísquez-Cuadro, R.; Ortiz Mellet, C.; García Fernández, J. M.; Nieto, P. M.; Angulo, J. Sp2-Iminosugar O-, S-, and N-Glycosides as Conformational Mimics of α-Linked Disaccharides; Implications for Glycosidase Inhibition. *Chemistry* **2012**, *18* (27), 8527–8539. https://doi.org/10.1002/chem.201200279.

(35) Herrera-González, I.; Sánchez-Fernández, E. M.; Sau, A.; Nativi, C.; García Fernández, J. M.; Galán, M. C.; Ortiz Mellet, C. Stereoselective Synthesis of Iminosugar 2-Deoxy(Thio)Glycosides from Bicyclic Iminoglycal Carbamates Promoted by Cerium(IV) Ammonium Nitrate and Cooperative Brønsted Acid-Type Organocatalysis. *J. Org. Chem.* **2020**, *85* (7), 5038–5047. https://doi.org/10.1021/acs.joc.0c00324.

(36) Palomo, J. M. Solid-Phase Peptide Synthesis: An Overview Focused on the Preparation of Biologically Relevant Peptides. *RSC Adv.* **2014**, *4* (62), 32658–32672. https://doi.org/10.1039/C4RA02458C.

(37) Jaradat, D. M. M. Thirteen Decades of Peptide Synthesis: Key Developments in Solid Phase Peptide Synthesis and Amide Bond Formation Utilized in Peptide Ligation. *Amino Acids* **2018**, *50* (1), 39–68. https://doi.org/10.1007/s00726-017-2516-0.

(38) Merrifield, R. B. Solid Phase Peptide Synthesis. I. The Synthesis of a Tetrapeptide. *J. Am. Chem. Soc.* **1963**, *85* (14), 2149–2154. https://doi.org/10.1021/ja00897a025.

(39) García-Martín, F.; Quintanar-Audelo, M.; García-Ramos, Y.; Cruz, L. J.; Gravel, C.; Furic, R.; Côté, S.; Tulla-Puche, J.; Albericio, F. ChemMatrix, a Poly(Ethylene Glycol)-Based Support for the Solid-Phase Synthesis of Complex Peptides. *J. Comb. Chem.* **2006**, *8* (2), 213–220. https://doi.org/10.1021/cc0600019.

(40) Isidro-Llobet, A.; Álvarez, M.; Albericio, F. Amino Acid-Protecting Groups. *Chem. Rev.* **2009**, *109* (6), 2455–2504. https://doi.org/10.1021/cr800323s.

(41) El-Faham, A.; Albericio, F. Peptide Coupling Reagents, More than a Letter Soup. *Chem. Rev.* **2011**, *111* (11), 6557–6602. https://doi.org/10.1021/cr100048w.

(42) Erdélyi, M.; Gogoll, A. Rapid Microwave-Assisted Solid Phase Peptide Synthesis. *Synthesis (Stuttg).* **2002**, No. 11, 1592–1596. https://doi.org/10.1055/s-2002-33348.

(43) Matsushita, T.; Hinou, H.; Kurogochi, M.; Shimizu, H.; Nishimura, S. I. Rapid Microwave-Assisted Solid-Phase Glycopeptide Synthesis. *Org. Lett.* **2005**, *7* (5), 877–880. https://doi.org/10.1021/ol0474352.

(44) Garcia-Martin, F.; Hinou, H.; Matsushita, T.; Hayakawa, S.; Nishimura, S. I. An Efficient Protocol for the Solid-Phase Synthesis of Glycopeptides under Microwave Irradiation. *Org. Biomol. Chem.* **2012**, *10* (8), 1612–1617. https://doi.org/10.1039/c2ob06532k.

(45) Pedersen, S. L.; Tofteng, A. P.; Malik, L.; Jensen, K. J. Microwave Heating in Solid-Phase Peptide Synthesis. *Chem. Soc. Rev.* **2012**, *41* (5), 1826–1844. https://doi.org/10.1039/c1cs15214a.

(46) Artigas, G.; Hinou, H.; Garcia-Martin, F.; Gabius, H. J.; Nishimura, S. I. Synthetic Mucin-Like Glycopeptides as Versatile Tools to Measure Effects of Glycan Structure/Density/Position on the Interaction with Adhesion/Growth-Regulatory Galectins in Arrays. *Chem. - An Asian J.* **2017**, *12* (1), 159–167. https://doi.org/10.1002/asia.201601420.

(47) Peters, S.; Bielfeldt, T.; Meldal, M.; Bock, K.; Paulsena, H. Multiple Column Solid Phase Glycopeptide Synthesis. *Tetrahedron Lett.* **1991**, *32* (38), 5067–5070. https://doi.org/10.1016/S0040-4039(00)93429-4.

(48) Tachibana, Y.; Matsubara, N.; Nakajima, F.; Tsuda, T.; Tsuda, S.; Monde, K.; Nishimura, S. I. Efficient and Versatile Synthesis of Mucin-like Glycoprotein Mimics.

Tetrahedron **2002**, *58* (51), 10213–10224. https://doi.org/10.1016/S0040-4020(02)01359-5.

(49) Fumoto, M.; Hinou, H.; Ohta, T.; Ito, T.; Yamada, K.; Takimoto, A.; Kondo, H.; Shimizu, H.; Inazu, T.; Nakahara, Y.; Nishimura, S. I. Combinatorial Synthesis of MUC1 Glycopeptides: Polymer Blotting Facilitates Chemical and Enzymatic Synthesis of Highly Complicated Mucin Glycopeptides. *J. Am. Chem. Soc.* **2005**, *127* (33), 11804–11818. https://doi.org/10.1021/ja052521y.

(50) Matsushita, T.; Hinou, H.; Fumoto, M.; Kurogochi, M.; Fujitani, N.; Shimizu, H.; Nishimura, S. I. Construction of Highly Glycosylated Mucin-Type Glycopeptides Based on Microwave-Assisted Solid-Phase Syntheses and Enzymatic Modifications. *J. Org. Chem.* **2006**, *71* (8), 3051–3063. https://doi.org/10.1021/jo0526643.

(51) Palasek, S. A.; Cox, Z. J.; Collins, J. M. Limiting Racemization and Aspartimide Formation in Microwave-Enhanced Fmoc Solid Phase Peptide Synthesis. *J. Pept. Sci.* **2007**, *13* (3), 143–148. https://doi.org/10.1002/psc.804.

(52) Garcia-Martin, F.; Matsushita, T.; Hinou, H.; Nishimura, S. I. Fast Epitope Mapping for the Anti-MUC1 Monoclonal Antibody by Combining a One-Bead-One-Glycopeptide Library and a Microarray Platform. *Chemistry* **2014**, *20* (48), 15891–15902. https://doi.org/10.1002/chem.201403239.

Chapter 3.
Microarray platform with monoclonal antibodies

3.1. Introduction

3.1.1. Microarray platform

The microarray platform technology started in the early 90s to answer the need for genomic and postgenomic high throughput data compilation techniques. Peptide microarrays involve the presentation of a collection of samples immobilized on a plane solid surface, thereby allowing multiple interaction events to be monitored simultaneously (Figure 1).[1] This platform requires a very low volume of sample and allows the screening of multiple antigen epitopes at the same time. It provides relevant information regarding binding properties which can positively contribute to different medical and pharmaceutical fields, from basic research to clinical applications.[2,3]

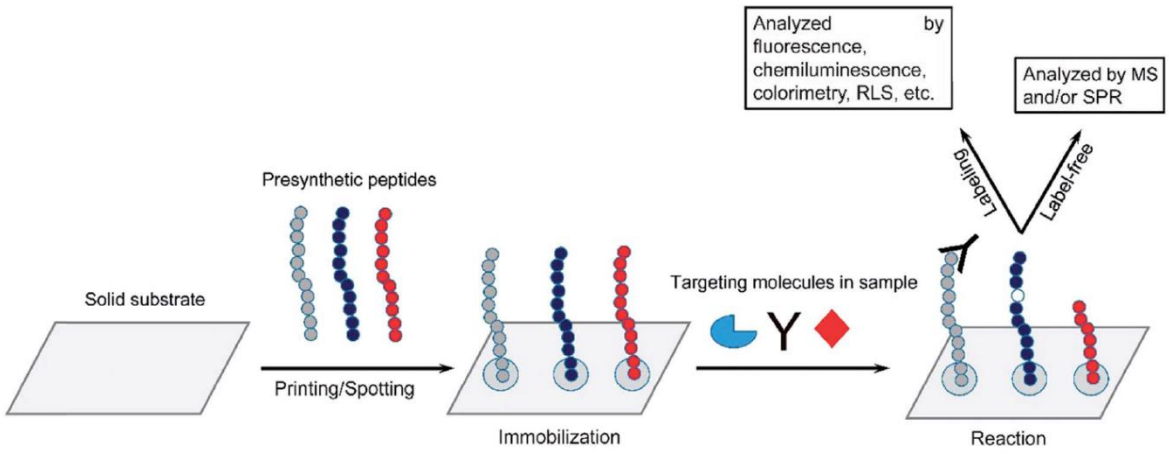

Figure 1. Schematic representation of a peptide microarray.[4]

The microscopic printed peptides are usually pre-synthesized by SPPS and spotted by a robotic arrayer. There are three major immobilization methods: physical absorption, covalent reaction and specific biorecognition. Covalent bond formation between the planar surface and the peptides was the strategy selected for this study. The reasons to support this

decision are: the stable linkage formation allowing washing steps, defined peptide orientation and reproducibility.[4,5]

Since the contribution of the MUC1 glycan portion to the antibody binding is crucial, we conceived a strategy based on the rational design of unnatural Tn antigen glycopeptide mimic motifs for anti-MUC1 mAbs detection. Our approach relies on the use of a microarray platform to assess mAbs selectivity and glycan pattern discrimination between natural and unnatural MUC1 based glycopeptides.

3.2. Results and discussion

This high throughput technique allowed us to compare our previously synthesized MUC1 glycopeptide library containing the natural Tn antigen and the novel sp^2-iminosugar attached glycopeptide library. Both families of glycopeptides were printed on top of the microarray slides, followed by incubation with mAbs (SM3, VU-11E2 and VU-3C6) and then incubation with the Cy™3-labeled secondary antibody. Finally, fluorescence intensity was assessed using GlycoStation™ Reader 1200 and analyzed by ArrayVision™ software (Figure 2).

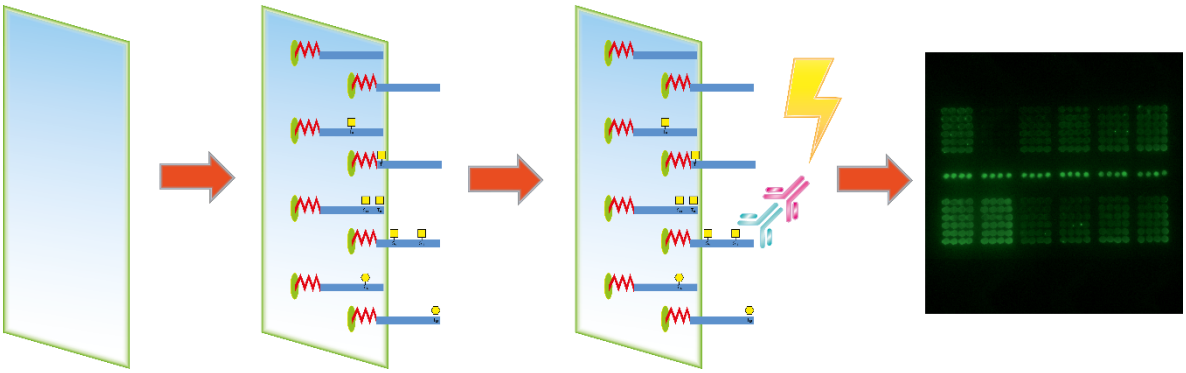

Figure 2. Microarray experiment workflow description. Slide deprotection, glycopeptide attachment, antibodies binding and fluorescence analysis.

Regarding the results obtained, the three mAbs used in the present study were specific to the MUC1 VNTR peptide with a preference for epitopes at the APDTRP region (Table 1).[6] Furthermore, the presence of short glycans increased affinity with mAbs, particularly for VU-11E2 and VU-3C6.

mAbs clone	Epitopes
SM3	APDTRP
VU-11E2	TSAPDTRP
VU-3C6	GVTSAPDTRPAP

Table 1. Anti-MUC1 mAbs used and recognition epitopes associated.[6]

Microarray binding results for the three mAbs are shown in Figure 3, including the non-glycosylated peptide MUC1 (in red), the MUC1 sequence with the natural Tn antigen (in blue), and the same glycopeptide library with the Tn antigen replaced by the unnatural sp^2-iminosugar-based mimetic (in green). We also included a blank as the control for microarray experiments.

The results obtained for the mAb SM3 (Figure 3A) showed a slight preference for the S4 and T8 pairs (both N and U) between the 10 monoglycosylated compounds. In comparisons, the intensity of the non-glycosylated (Naked) sequence signal (Figure 3A, in red) was stronger than the corresponding monoglycosylated signal intensities. This is consistent with previous findings suggesting that SM3 binds preferentially to the peptide sequence.[7] In contrast, in comparisons of diglycosylated sequences, the T3T8 and T8T15 pairs showed the strongest intensities, surpassing the Naked peptide. We also observed strong signal intensity for the pair S4T8 as well as a significant binding difference between NT3T15 and UT3T15, with the unnatural sequence providing better results. In the case of the VU-3C6 mAb (Figure 3B), the NT8 sequence exhibited the highest binding profile in the monoglycosylated series and surpassed UT8. The diglycosylated natural and unnatural T3T8, T3T15, and S4T8 pairs exhibited very strong signal intensities. The natural NT8T15 sequence was an exceptional ligand of this antibody and also markedly better than its unnatural counterpart UT8T15. In this set of measurements, the RFU value of the Naked

sample (Figure 3B, in red), was lower than that of glycopeptides, indicating the important contribution of the glycan part in binding with the mAb VU-3C6. The results obtained with the mAb VU-11E2 were of interest (Figure 3C) due to its stronger ability to distinguish between different glycosylation patterns. In this case, the RFU value of the Naked peptide (Figure 3C, in red) was lower than those of the two previous mAbs, implying the important contribution of the glycan part in the VU-11E2–MUC1 complex and high specificity for the glycosylation pattern. Binding values for monoglycosylated compounds showed a clear preference for the T8 pair. Consistent with other results (SM3 mAb in Figure 3A and VU-3C6 in Figure 3B), diglycosylated structures containing a glycan at Thr-8, similar to the pairs T3T8 and T8T15 as well as US4T8, showed the highest binding efficiencies (Figure 3C). Interestingly, we observed a prominent contrast between NS4T8 low signal intensity and the strong response for its unnatural sp^2-iminosugar analogue US4T8. The molecular basis for this discrepancy has not yet been elucidated and warrants further study, which is currently in progress.

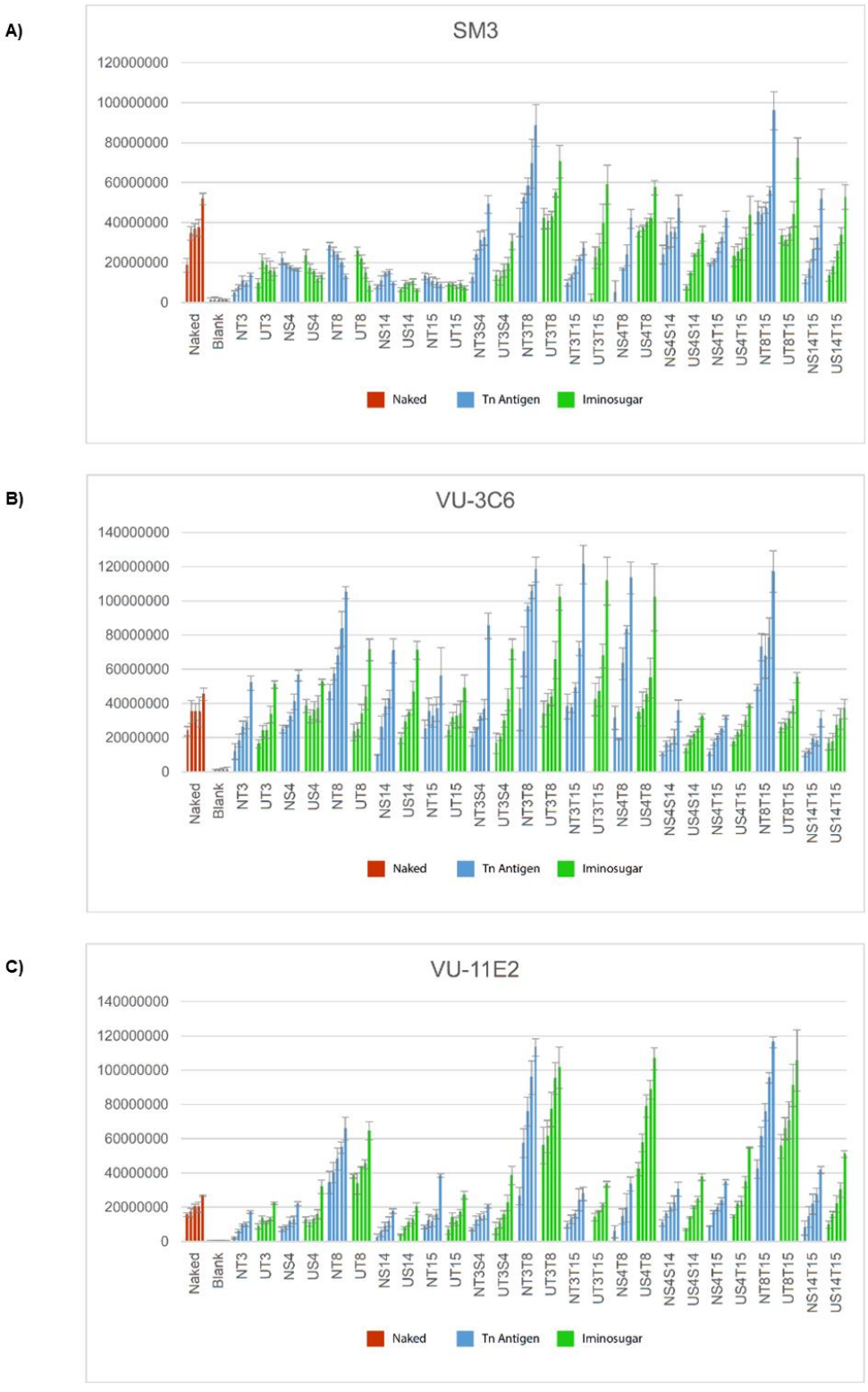

Figure 3. This collection of graphs represent the correlation between the different samples in a concentration gradient style (25, 50, 100, 200 and 400 µM) in the horizontal axis and their

corresponding microarray RFU (reference fluorescence unit) values in the vertical axis for (A) mAb SM3 (25 μg/mL); (B) mAb VU-3C6 (25 μg/mL); (C) mAb VU-11E2 (25 μg/mL). For comparison purposes, samples are organized in Natural (blue) and Unnatural (green) pairs.

One of the main conclusions reached from the results shown in Figure 3 is that the Thr-8 position plays an important role in binding between glycopeptides and the three mAbs. These results are consistent with previous findings identifying the PDTR region as the MUC1 epitope exhibiting the highest affinity against a number of antibodies and lectins such as the Macrophage Galactose-Type Lectin.[8–10] The RFU values for glycopeptides with two glycosylated positions were generally better than those of monoglycosylated compounds when referring to SM3 and VU-3C6 mAbs. In contrast, mAb VU-11E2 binding results were strongly dependent on the glycan pattern. Based on a complete analysis of the binding results obtained, we concluded that a strong correlation existed, which demonstrated that sp^2-iminosugar-based glycopeptides are suitable Tn antigen mimics for the recognition of anti-Tn antigen-directed antibodies.

3.3. Conclusion

To assess the mimic capabilities of the sp^2-iminosugar as Tn antigen equivalent, the previously synthesized library was tested using a microarray platform. Immunological evaluations were conducted using anti-MUC1 mAbs SM3, VU-3C6 and VU-11E2. The binding information obtained showed a clear glycan patter dependency. The overall results collected can be compiled as follows:

The Threonine in position 8 plays an important role in binding between glycopeptides and the three mAbs. This concurs with previous findings identifying the PDTR region as the MUC1 epitope exhibiting the highest affinity against a number of antibodies and lectins.

Binding results were generally better with two glycans attached, suggesting that two glycans modify the peptide conformation improving the binding.

The monoclonal antibody VU-11E2 presented the best ability to discriminate between glycosylation patterns.

The results obtained confirmed the suitability of the sp^2-iminosugar analog as Tn antigen mimic.

3.4. Experimental section

3.4.1. Materials

Microarray slides (75x25x1 mm) made of cyclic polyolefin were covered with methacrylic *N*-protected AO/PC-copolymer and hybridization covers (60x25x0.7 mm) were manufactured by Sumitomo Bakelite Co., Ltd. (Tokyo, Japan). Silicon separating rubbers (60x24x0.1 mm) were supplied by Fuso Rubber Co., Ltd. (Hiroshima, Japan) and micro glass covers (18x18 mm) were purchased from Matsunami Glass Ind., Ltd. (Osaka, Japan). Anti-MUC1 mouse mAbs clones SM3 (0.2 mg/mL), VU-11E2 (0.10 mg/mL) and VU-3C6 (0.86 mg/mL) were purchased from Santa Cruz Biotechnology, Inc. (Texas, United States), Monosan (Uden, The Netherlands) and Exalpha Biological Inc. (Massachusetts, United States) respectively. Secondary antibody FluoroLink™ Cy™3-labeled goat anti-mouse IgG (H + L) was purchased from Amersham Biosciences (Buckinghamshire, United Kingdom). Fluorescence intensity measures were obtained through GlycoStation™ Reader 1200 (GlycoTechnica Ltd., Yokohama, Japan), analyzed by ArrayVision™ software V8.0 (GE Healthcare, Tokyo, Japan) and the resulting data was processed employing Grubbs's test statistical analysis for outliers.[11]

3.4.2. Methods

Following a previous optimized microarray protocol, *N*-protected AO/PC-copolymer slides were deprotected by 2N HCl treatment at room temperature overnight, rinsed with MilliQ H_2O (3×1 min), and dried by centrifugation.[1,12] The printing process was performed using a MicroSys 5100 Microarrayer (Cartesian Technologies, Inc., California, United States) robot in a six-concentration (400, 200, 100, 50, 25, and 12.5 µM) quadruplicate pattern, discarding the lower concentration results due to artifact. Samples were placed in a 384-well plate along with 25 mM AcOH–Pyr and 0.0025% (v/v) Triton X-100, printed, incubated at 80°C for 1 hour to attach the sample though an oxime bond to the microarray slide surface, washed gently with MilliQ H_2O (1x1 min), and dried.[13] In mAbs evaluation assays, each slide contained three chambers with identical printing. Slides were then treated with aqueous succinic anhydride (10 mg/mL) at room temperature for 4 hours, gently shaken to block the remaining free aminooxy groups, rinsed with MilliQ H_2O (2x1 min), and dried. Regarding the mAbs incubation, a three- or six- chamber silicone rubber was placed on the slide, followed by micro glass cover attachment over each chamber. The anti-MUC1 mouse mAbs clones SM3, VU-11E2, and VU-3C6 (all of which are the mouse mAbs IgG1 type) were separately mixed with reaction buffer[1] to obtain 40µL at 25 µg/mL, added to the pertinent chamber, and maintained at room temperature for 2 hours. After completion of the reaction, the slide was rinsed with washing buffer[1] (3x1 min), MilliQ H_2O (1x1 min), dried by centrifugation, and again covered with a hybridization cover. The secondary antibody Cy™3-labeled anti-mouse IgG and reaction buffer (1 µg/mL) were added to the whole slide (100 µL), placed under dark conditions at room temperature for 1 hour, followed by a

washing buffer (3x1 min) treatment and drying by centrifugation. Fluorescence analyses were then conducted. Slides were stored in vacuum at -4°C for preservation.

3.4.3. Supplementary information

Microarray design and sample correlation for mAbs

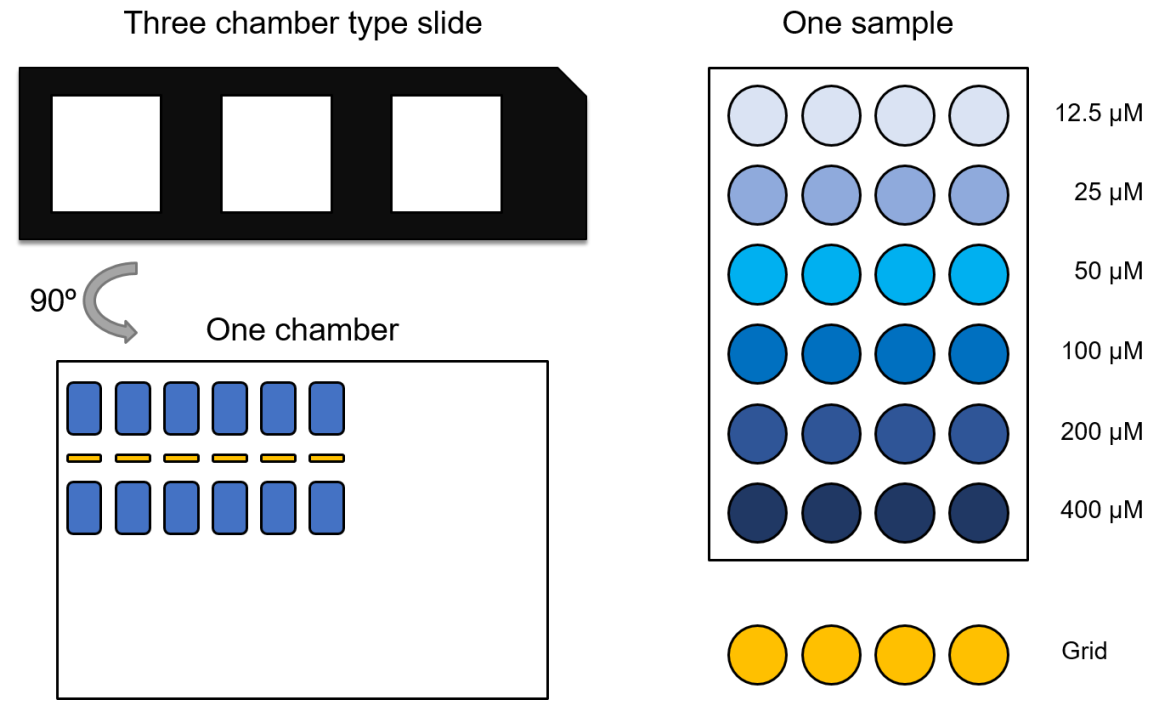

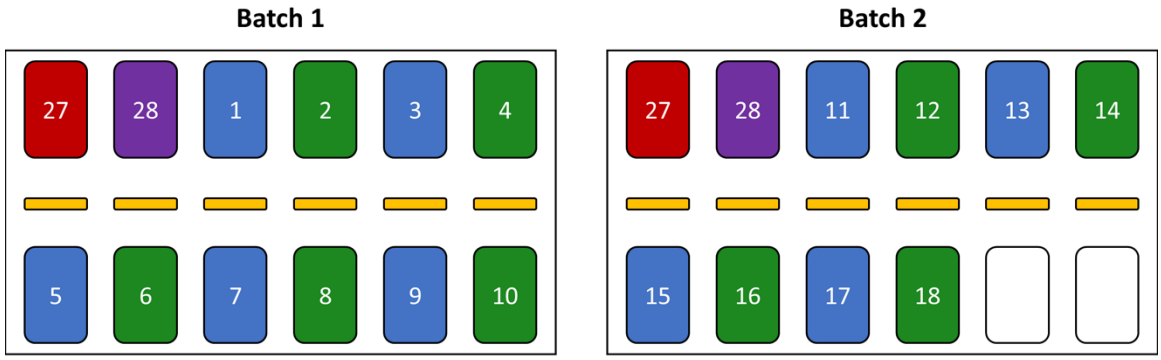

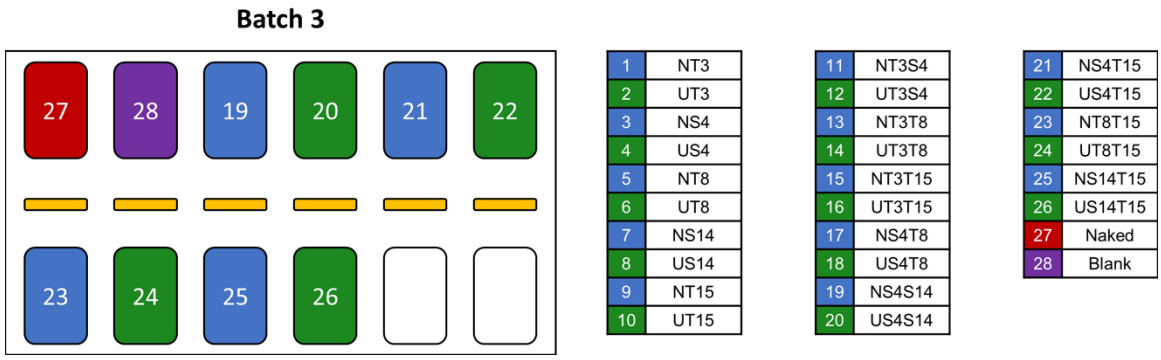

1	NT3
2	UT3
3	NS4
4	US4
5	NT8
6	UT8
7	NS14
8	US14
9	NT15
10	UT15

11	NT3S4
12	UT3S4
13	NT3T8
14	UT3T8
15	NT3T15
16	UT3T15
17	NS4T8
18	US4T8
19	NS4S14
20	US4S14

21	NS4T15
22	US4T15
23	NT8T15
24	UT8T15
25	NS14T15
26	US14T15
27	Naked
28	Blank

Microarray results for mAb SM3

Fluorescence intensity measures were obtained through GlycoStationTM Reader 1200 (GlycoTechnica Ltd., Yokohama, Japan) and analyzed by ArrayVision™ software V8.0 (GE Healthcare, Tokyo, Japan). The software measures the fluorescence intensity signal and the background of the sample. The RFU is calculated by subtracting the sample background from the sample fluorescence to get the actual value. In order to improve statistical correlation, 12.5 μM concentration results were discharged despite appearing in the slide picture. The experiment was conducted 4 times, the results showed reproducibility and the example displayed is one of the cases. Microarray slide sample position correlation: a) Batch 1; b) Batch 2; c) Batch 3

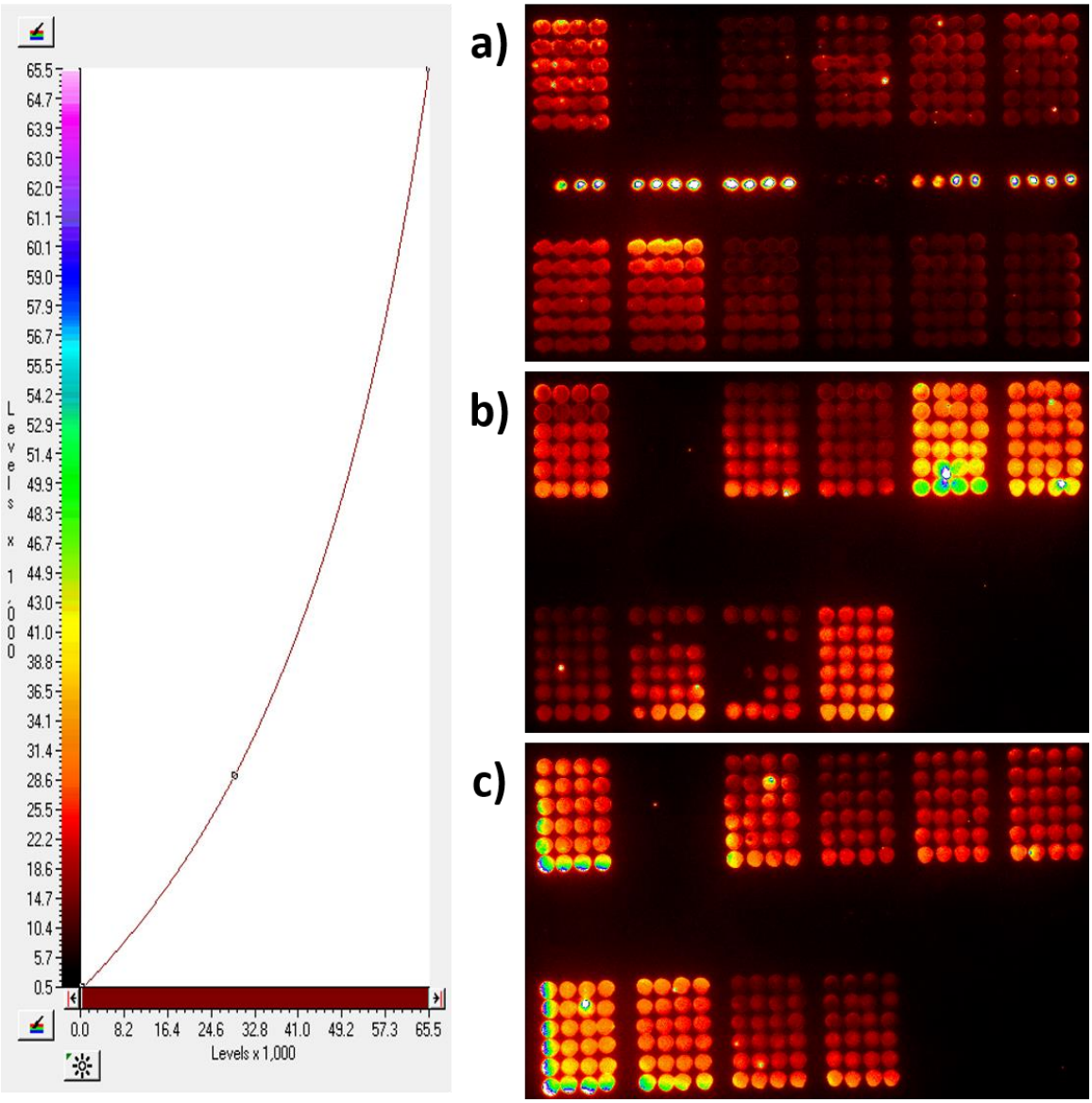
a)
b)
c)
Levels x 1,000
65.5
64.7
63.9
63.0
62.0
61.1
60.1
59.0
57.9
56.7
55.5
54.2
52.9
51.4
49.9
48.3
46.7
44.9
43.0
41.0
38.8
36.5
34.1
31.4
28.6
25.5
22.2
18.6
14.7
10.4
5.7
0.5
0.0
8.2
16.4
24.6
32.8
41.0
49.2
57.3
65.5

Microarray results for mAb VU-3C6

Fluorescence intensity measures were obtained through GlycoStationTM Reader 1200 (GlycoTechnica Ltd., Yokohama, Japan) and analyzed by ArrayVision™ software V8.0 (GE Healthcare, Tokyo, Japan). The software measures the fluorescence intensity signal and the background of the sample. The RFU is calculated by subtracting the sample background from the sample fluorescence to get the actual value. In order to improve statistical correlation, 12.5 μM concentration results were discharged despite appearing in the slide picture. The experiment was conducted 4 times, the results showed reproducibility and the example displayed is one of the cases. Microarray slide sample position correlation: a) Batch 1; b) Batch 2; c) Batch 3

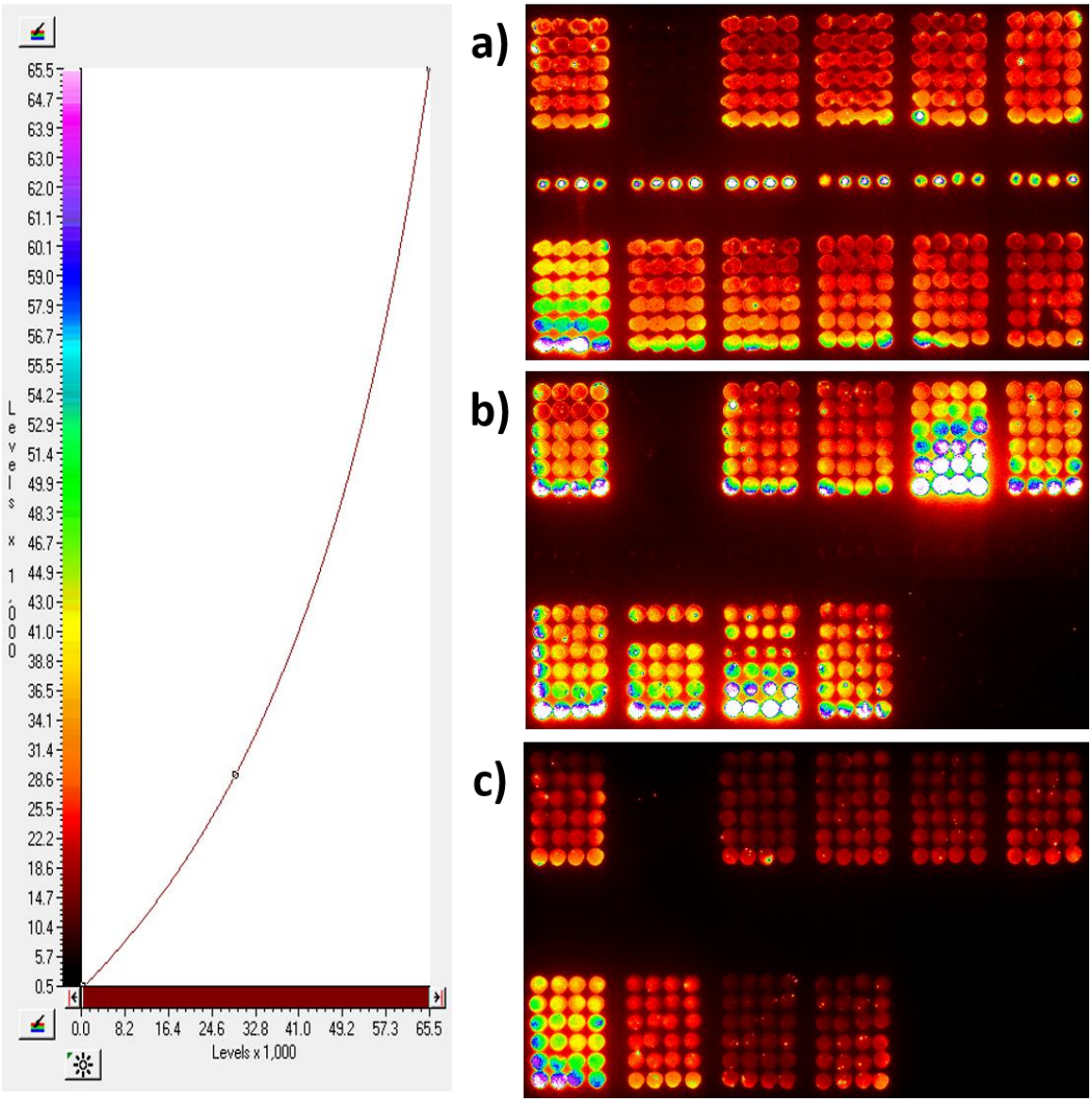
65.5
64.7
63.9
63.0
62.0
61.1
60.1
59.0
57.9
56.7
55.5
54.2
52.9
51.4
49.9
48.3
46.7
44.9
43.0
41.0
38.8
36.5
34.1
31.4
28.6
25.5
22.2
18.6
14.7
10.4
5.7
0.5
Levels x 1,000
0.0 8.2 16.4 24.6 32.8 41.0 49.2 57.3 65.5
Levels x 1,000
a)
b)
c)

Microarray results for mAb VU-11E2

Fluorescence intensity measures were obtained through GlycoStationTM Reader 1200 (GlycoTechnica Ltd., Yokohama, Japan) and analyzed by ArrayVision™ software V8.0 (GE Healthcare, Tokyo, Japan). The software measures the fluorescence intensity signal and the background of the sample. The RFU is calculated by subtracting the sample background from the sample fluorescence to get the actual value. In order to improve statistical correlation, 12.5 μM concentration results were discharged despite appearing in the slide picture. The experiment was conducted 4 times, the results showed reproducibility and the example displayed is one of the cases. Microarray slide sample position correlation: a) Batch 1; b) Batch 2; c) Batch 3

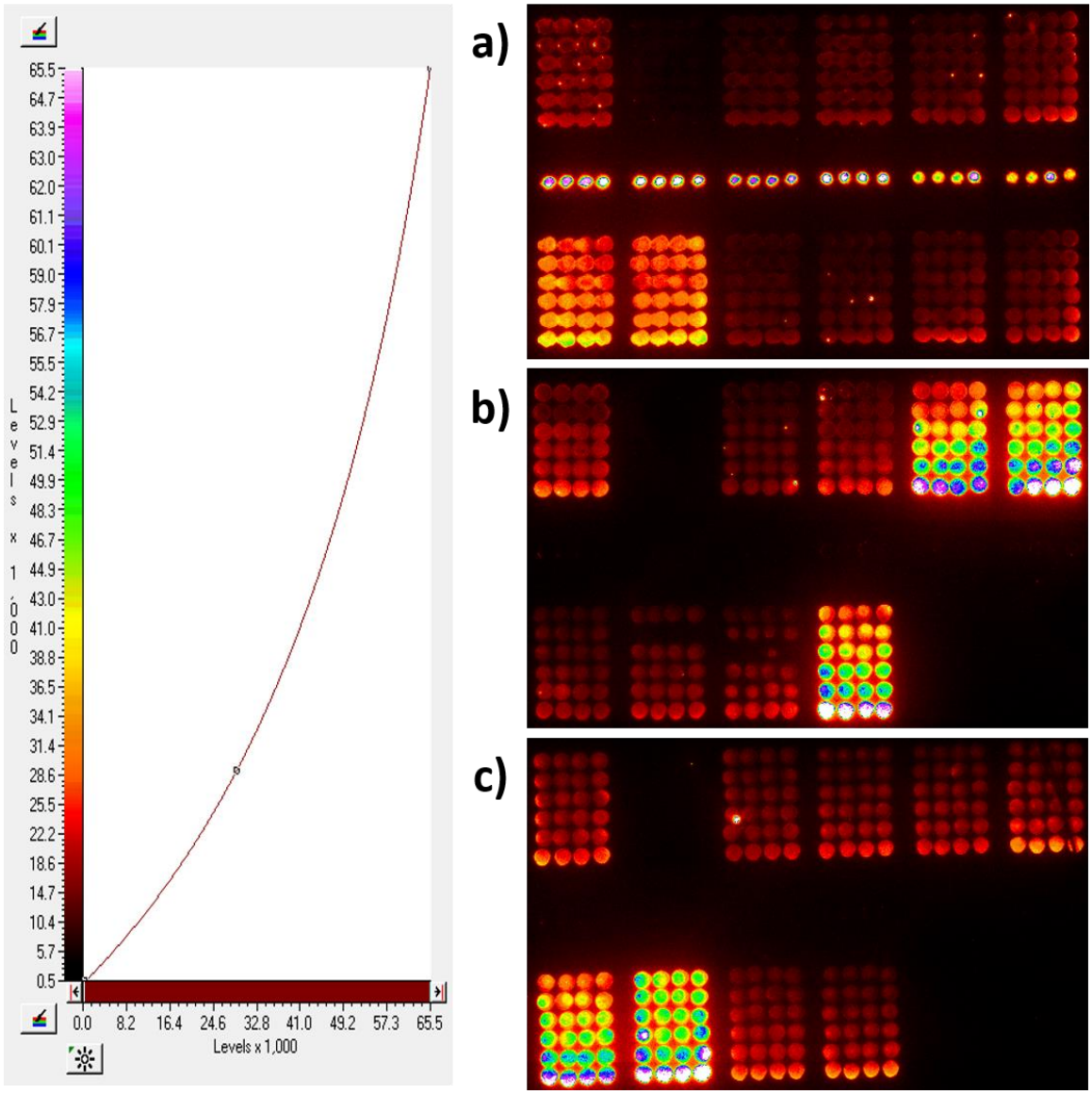
a)
b)
c)
65.5
64.7
63.9
63.0
62.0
61.1
60.1
59.0
57.9
56.7
55.5
54.2
52.9
51.4
49.9
48.3
46.7
44.9
43.0
41.0
38.8
36.5
34.1
31.4
28.6
25.5
22.2
18.6
14.7
10.4
5.7
0.5
Levels x 1,000
0.0
8.2
16.4
24.6
32.8
41.0
49.2
57.3
65.5
Levels x 1,000

3.5. References

(1) Matsushita, T.; Takada, W.; Igarashi, K.; Naruchi, K.; Miyoshi, R.; Garcia-Martin, F.; Amano, M.; Hinou, H.; Nishimura, S. I. A Straightforward Protocol for the Preparation of High Performance Microarray Displaying Synthetic MUC1 Glycopeptides. *Biochim. Biophys. Acta - Gen. Subj.* **2014**, *1840* (3), 1105–1116. https://doi.org/10.1016/j.bbagen.2013.11.009.

(2) Zhou, X.; Zhou, J. Oligosaccharide Microarrays Fabricated on Aminooxyacetyl Functionalized Glass Surface for Characterization of Carbohydrate–Protein Interaction. *Biosens. Bioelectron.* **2006**, *21* (8), 1451–1458. https://doi.org/10.1016/j.bios.2005.06.008.

(3) Wang, C.-C.; Huang, Y.-L.; Ren, C.-T.; Lin, C.-W.; Hung, J.-T.; Yu, J.-C.; Yu, A. L.; Wu, C.-Y.; Wong, C.-H. Glycan Microarray of Globo H and Related Structures for Quantitative Analysis of Breast Cancer. *Proc. Natl. Acad. Sci.* **2008**, *105* (33), 11661–11666. https://doi.org/10.1073/pnas.0804923105.

(4) Meng, X.; Wei, J.; Wang, Y.; Zhang, H.; Wang, Z. The Role of Peptide Microarrays in Biomedical Research. *Anal. Methods* **2018**, *10* (38), 4614–4624. https://doi.org/10.1039/C8AY01442F.

(5) Tateno, H.; Mori, A.; Uchiyama, N.; Yabe, R.; Iwaki, J.; Shikanai, T.; Angata, T.; Narimatsu, H.; Hirabayashi, J. Glycoconjugate Microarray Based on an Evanescent-Field Fluorescence-Assisted Detection Principle for Investigation of Glycan-Binding Proteins. *Glycobiology* **2008**, *18* (10), 789–798. https://doi.org/10.1093/glycob/cwn068.

(6) Karsten, U.; Serttas, N.; Paulsen, H.; Danielczyk, A.; Goletz, S. Binding Patterns of DTR-Specific Antibodies Reveal a Glycosylation-Conditioned Tumor-Specific Epitope of the Epithelial Mucin (MUC1). *Glycobiology* **2004**, *14* (8), 681–692. https://doi.org/10.1093/glycob/cwh090.

(7) Price, M. R.; Rye, P. D.; Petrakou, E.; Murray, A.; Brady, K.; Imai, S.; Haga, S.; Kiyozuka, Y.; Schol, D.; Meulenbroek, M. F. A.; Snijdewint, F. G. M.; von Mensdorff-Pouilly, S.; Verstraeten, R. A.; NIL, K.; Blockzjil, A.; NIL, N.; Nilsson, O.; NIL, R.; Suresh, M. R.; NIL, K.; Fortier, S.; NIL, B.; Berg, A.; Longenecker, M. B.; NIL, H.; Boer, M.; NIL, K.; McKenzie, I. F. C.; NIL, G.; Simeoni, L. A.; Ter-Grigoryan, A. G.; Belyanchikov, I. M.; Bovin, N. V.; Cao, Y.; Karsten, U.; Dai, J.; Allard, W. J.; Davis, G.; Yeung, K. K.; Hanisch, F.-G.; Lloyd, K. O.; Kudryashov, V.; Sikut, R.; Sikut, A.; Zhang, K.; Baeckström, D.; Hansson, G. C.; Reis, C. A.; Hassan, H.; Bennett, E. P.; Claussen, H.; Norum, L.; Varaas, T.; Kierulf, B.; Nustad, K.; Ciborowski, P.; Konitzki, W. M.; Magarian- Blander, J.; Finn, O. J.; Hilgers, J. Summary Report on the ISOBM TD-4 Workshop: Analysis of 56 Monoclonal Antibodies against the MUC1 Mucin. *Tumor Biol.* **1998**, *19* (Suppl. 1), 1–20. https://doi.org/10.1159/000056500.

(8) Garcia-Martin, F.; Matsushita, T.; Hinou, H.; Nishimura, S. I. Fast Epitope Mapping for the Anti-MUC1 Monoclonal Antibody by Combining a One-Bead-One-Glycopeptide Library and a Microarray Platform. *Chemistry* **2014**, *20* (48), 15891–15902. https://doi.org/10.1002/chem.201403239.

(9) Coelho, H.; Matsushita, T.; Artigas, G.; Hinou, H.; Cañada, F. J.; Lo-Man, R.; Leclerc, C.; Cabrita, E. J.; Jiménez-Barbero, J.; Nishimura, S.-I.; Garcia-Martín, F.; Marcelo,

F. The Quest for Anticancer Vaccines: Deciphering the Fine-Epitope Specificity of Cancer-Related Monoclonal Antibodies by Combining Microarray Screening and Saturation Transfer Difference NMR. *J. Am. Chem. Soc.* **2015**, *137* (39), 12438–12441. https://doi.org/10.1021/jacs.5b06787.

(10) Artigas, G.; Monteiro, J. T.; Hinou, H.; Nishimura, S.-I.; Lepenies, B.; Garcia-Martin, F. Glycopeptides as Targets for Dendritic Cells: Exploring MUC1 Glycopeptides Binding Profile toward Macrophage Galactose-Type Lectin (MGL) Orthologs. *J. Med. Chem.* **2017**, *60* (21), 9012–9021. https://doi.org/10.1021/acs.jmedchem.7b01242.

(11) Tietjen, G. L.; Moore, R. H. Some Grubbs-Type Statistics for the Detection of Several Outliers. *Technometrics* **1972**, *14* (3), 583–597. https://doi.org/10.1080/00401706.1972.10488948.

(12) Artigas, G.; Hinou, H.; Garcia-Martin, F.; Gabius, H. J.; Nishimura, S. I. Synthetic Mucin-Like Glycopeptides as Versatile Tools to Measure Effects of Glycan Structure/Density/Position on the Interaction with Adhesion/Growth-Regulatory Galectins in Arrays. *Chem. - An Asian J.* **2017**, *12* (1), 159–167. https://doi.org/10.1002/asia.201601420.

(13) Uchiyama, N.; Kuno, A.; Tateno, H.; Kubo, Y.; Mizuno, M.; Noguchi, M.; Hirabayashi, J. Optimization of Evanescent-Field Fluorescence-Assisted Lectin Microarray for High-Sensitivity Detection of Monovalent Oligosaccharides and Glycoproteins. *Proteomics* **2008**, *8* (15), 3042–3050. https://doi.org/10.1002/pmic.200701114.

Chapter 4.
Early stage breast cancer autoantibodies exploration

4.1. Introduction

4.1.1. Autoantibodies as biomarkers discovery

In the battle against breast cancer, an early diagnosis represents the most auspicious approach for a successful treatment. The exceptional technological advances in the last 20 years have made possible the development of diverse diagnostic platforms. At present, the most prominent approach is the use of non-invasive imaging test. This includes the use of different techniques like breast ultrasounds,[1] screening and diagnostic mammography[2] or magnetic resonance imaging.[3] On the other hand, a blood test may be conducted before or after surgery and different types of biopsies may be required to make a definite diagnosis. However, the continuous use of these intrusive procedures will derive in unnecessary stress and discomfort for patients.[4] Thus, the development of new analytic resources to expand actual diagnostic tests is essential.

Biosensors are sensitive and specific analytical devices used for the detection of a particular substance. High-sensitive, rapid and standardized methodologies would result in accessible testing, faster treatment implementation and a patient's prognosis improvement.[5–8] An effective and accurate biosensor requires a well-defined target molecule. Therefore, an early stage breast cancer biosensor requires an appropriate cancer biomarker target.

The classical strategy for cancer detection consists in the serological search of tumor associated biomarkers. Several tumor markers have been proposed as tumor biomarkers including MUC1.[9,10] Unfortunately, the detection of cancer antigens directly from serum presents low sensitivity. The low concentration of tumor antigens produced is hardly measurable, specially at early stages, hampering clinical relevance and exploitation.[11,12] In

order to overcome this limitation, instead of the traditional use of antigens, we propose the use of autoAbs directed to those antigens for cancer detection. [13]

Natural antibodies, also referred as autoAbs, are immunoglobulins produced by the immune system directed against self-antigens. Although autoAbs have been considered associated with the development of autoimmune diseases, these antibodies play an important role in tolerance regulation, autoimmune diseases prevention and innate immune system homeostasis. [14,15] Analysis of serum autoAbs in clinical practice has recently become an attractive diagnostic tool for detection. In contrast to the challenges associated to low levels of cancer antigens at early stage detection, cancer-associated autoAbs represent attractive biomarkers because they may start to develop early in carcinogenesis and can be potentially detected. [16] This is due to the immune system antibody amplification phenomenon, through B cells specific autoAbs production against cancer antigens (Figure 1).[17–20]

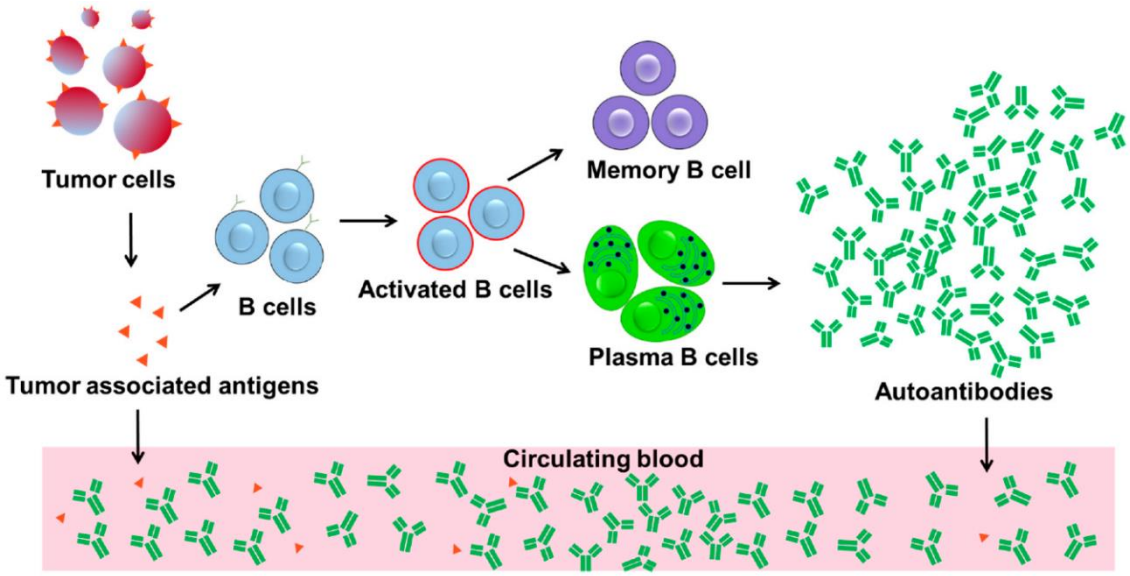

Figure 1. Immune amplification of AutoAbs from tumor associated antigens.[19]

As previously mentioned, early cancer detection ensures a treatment improvement as well as a survival enhancement. Rapid determination and discrimination between cancer stages with only a blood test will be advantageous for patients and will have positive consequences on the health system. The encouraging results with anti-MUC1 mAbs, in which some non-natural glycopeptides interacted at an equal or higher affinity level than their natural counterparts, prompted us to test their potential to sense autoAbs in breast cancer patients. The immune system acts against malignant cells on a daily basis and, consequently, healthy individuals also have autoAbs that recognize aberrant glycosylated MUC1. An ideal diagnostic tool needs to exhibit the ability to discriminate between healthy and malignant states and also differentiate among the different stages of cancer.

4.2. Results and discussion

In the present study, we challenged a selection of MUC1-related glycopeptides from our chemical library with healthy serum (He), stage I breast cancer serum (I), and metastatic stage IV breast cancer serum (IV). Based on mAbs results, the unglycosylated MUC1 sequence (Naked), monoglycosylated derivatives bearing the natural GalNAc and the unnatural sp^2-iminosugar glycomimetic in the PDTR region (NT8 and UT8, respectively), and two pairs of diglycosylated peptides (NS4T8/US4T8 and NT8T15/UT8T15) were selected for this purpose. The microarray slide incubation was performed using healthy serum, and sera from stage I and stage IV breast cancer patients, followed by the Cy™3-labeled anti-human IgG secondary antibody (Figure 2).

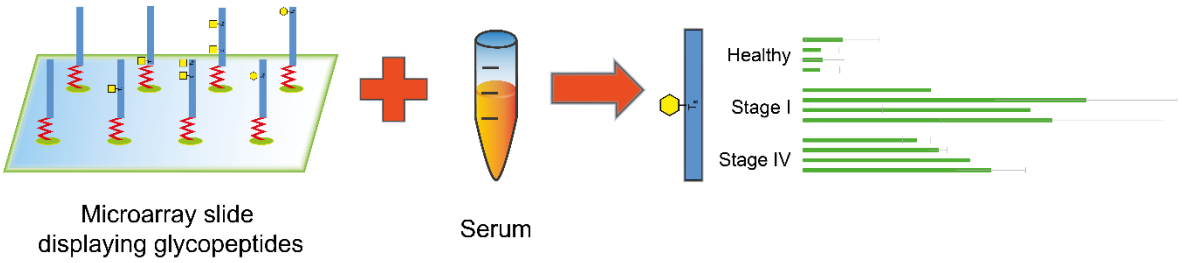

Figure 2. Summary diagram of the autoAbs exploration using the microarray platform.

We specifically tagged human IgG because it is the most abundant antibody in serum. Furthermore, IgG levels are higher in patients with malignant breast cancer and are induced by cytokines related to cancer immunosurveillance, such as IFN-γ.[21,22] Fluorescence intensity results for the three stages described above are shown in Figure 3.

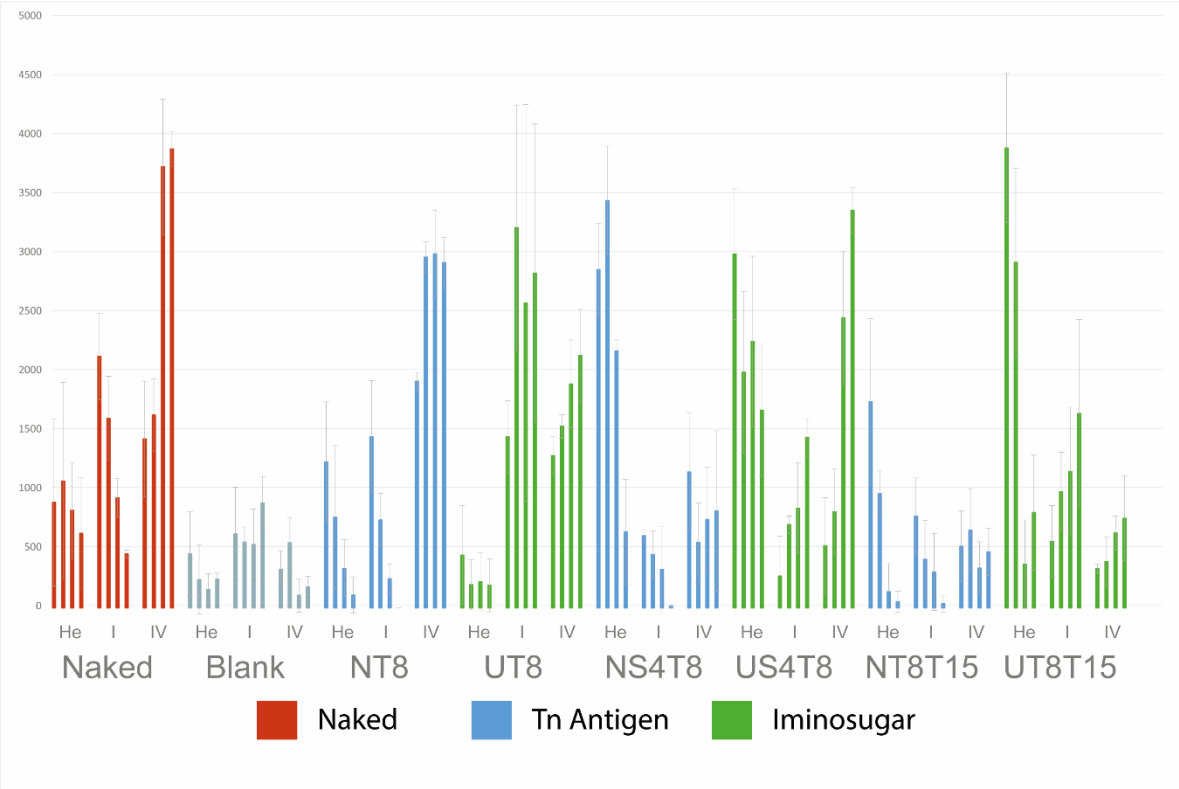

Figure 3. This graph shows the correlation between the different samples in a concentration gradient style (1, 10, 100, and 1000 μM) in the horizontal axis and their corresponding microarray RFU (reference fluorescence unit) values in the vertical axis for the different sera: Healthy (He), Stage I (I), and Stage IV (IV). For comparison purposes, samples are organized in Natural (blue) and Unnatural (green) pairs.

It is noteworthy that the natural and unnatural (glyco)peptides were all able to detect MUC1-related autoAbs in the different samples, with binding patterns that varied as a function of their structure. Most importantly, we further found significant affinity differences that were dependent on whether serum was obtained from healthy individuals, stage I or IV cancer patients.

First, we discuss the differences in responses depending on the serum pool. Focusing on the healthy serum pool, autoAbs mainly recognized Naked MUC1, NT8 and the diglycosylated peptides NS4T8, US4T8 and UT8T15. In stage I serum, malignant cells may display other antigens, resulting in different immune system recognition affinities. This explains the epitope recognition profile change observed, with the Naked sequence, monoglycosylated compounds NT8 and U8, and diglycosylated UT8T15 derivative showing the highest affinities. During stage IV or metastatic breast cancer, complex interactions between the immune system cells and the tumor microenvironment occur[23] leading to a change in epitope recognition with a preference for the Naked, followed by NT8, US4T8 and UT8 sequences.

A focus on individual epitopes revealed that the diglycosylated compounds NS4T8, NT8T15, and UT8T15 show a decreasing tendency from healthy condition to stage IV, while US4T8 shows a U-shaped affinity curve with higher affinity for healthy serum and stage IV. These binding profiles correlated with previous findings demonstrating the presence of anti-MUC1 autoAbs presence in healthy sera,[24] but do not allow an accurate early stage diagnosis. Naked and monoglycosylated NT8 showed increasing trends, with the highest affinity being observed at stage IV. The most promising results were obtained with the unnatural monoglycosylated glycopeptide UT8, which displayed the ability to discriminate between sera from healthy individuals and stage I patients (over 10-fold difference in RFU). To the best of our knowledge, this is the first example of a MUC1-related glycopeptide mimetic enabling the differential detection of autoAbs in healthy and early breast cancer scenarios.

4.3. Conclusion

The majority of the compounds were able to recognize and bind breast cancer associated autoAbs from the different serum specimens used. Some of the major findings are recapitulated as follow:

Binding with autoAbs from healthy serum could be observed. This correlates with previous data, supporting the presence of anti-MUC1 autoAbs presence in healthy sera.

In stage I sera, malignant cells display different antigens. This elicits different recognition affinities by immune system, explaining the epitope recognition profile changes.

In the case of metastatic or stage IV, the tumor environment produces a big impact on the immune system. This overwhelming destabilization of the immune system response can again generate new epitope recognition profile changes.

From among all the compounds studied, the most outstanding candidate was UT8. This promising candidate displayed low binding with healthy serum but a strong affinity for stage I cancer, becoming a potential early breast cancer diagnostic tool.

To the best of our knowledge, this is the first example of a MUC1-related glycopeptide mimetic enabling the differential detection of autoAbs in healthy and early breast cancer scenarios.

4.4. Experimental section

4.4.1. Materials

Microarray slides (75x25x1 mm) made of cyclic polyolefin were covered with methacrylic *N*-protected AO/PC-copolymer and hybridization covers (60x25x0.7 mm) were manufactured by Sumitomo Bakelite Co., Ltd. (Tokyo, Japan). Silicon separating rubbers (60x24x0.1 mm) were supplied by Fuso Rubber Co., Ltd. (Hiroshima, Japan), micro glass covers (18x18 mm) were purchased from Matsunami Glass Ind., Ltd. (Osaka, Japan) and Amicon® Ultra-0.5 mL 50k Molecular weight cut-off Centrifugal Filters were supplied by Merck Millipore Ltd. (County Cork, Ireland). Secondary antibody Cy™3-conjugated AffiniPure goat anti-human IgG (H+L) was purchased from Jackson ImmunoResearch Laboratories, Inc. (Pennsylvania, United States) respectively. Stage I and IV breast cancer human serum samples were obtained from BioIVT (New York, United States). Fluorescence intensity measures were obtained through GlycoStation™ Reader 1200 (GlycoTechnica Ltd., Yokohama, Japan), analyzed by ArrayVision™ software V8.0 (GE Healthcare, Tokyo, Japan) and the resulting data was processed employing Grubbs's test statistical analysis for outliers.[25]

4.4.2. Methods

Following a previous optimized microarray protocol, *N*-protected AO/PC-copolymer slides were deprotected by 2N HCl treatment at room temperature overnight, rinsed with MilliQ H_2O (3×1 min), and dried by centrifugation.[24,26] The printing was conducted by an Arduino-based CNC machine hand-crafted robot (Nishimura Laboratory, Hokkaido, Japan) in a four-concentration (1000, 100, 10, and 1 µM) quadruplicate pattern. Samples were placed in a 384-well plate along with 25 mM AcOH–Pyr and 0.0025% (v/v) Triton X-100, printed, incubated at 80°C for 1 hour to attach the sample though an oxime bond to the microarray slide surface, washed gently with MilliQ H_2O (1x1 min), and dried.[27] Slides were then treated with aqueous succinic anhydride (10 mg/mL) at room temperature for 4 hours, gently shaken to block the remaining free aminooxy groups, rinsed with MilliQ H_2O (2x1 min), and dried. To evaluate binding properties, an incubation with a pool of healthy samples and a pool of four different human stage I and a pool of four IV breast cancer serum samples were performed. Each pool sera were filtered through an Amicon centrifugal filter with a pore size of 50 kDa to concentrate the number of antibodies present in the sample. The resultant serum was mixed with reaction buffer (1:3) and added to the slide for an incubation under dark conditions. After two hours, the slide was gently rinsed with washing buffer (3x1 min), and then MilliQ H_2O (1x1 min) and dried by centrifugation. The slide was covered with a hybridization cover and a Cy™3-labeled goat anti-human IgG secondary antibody combined with reaction buffer (0.5µg/mL) was added to the slide and placed at room temperature under dark conditions for 1 hour. After completion, the slide was treated with washing buffer (3x1 min) to directly conduct fluorescence analyses. Slides were stored in vacuum at -4°C for preservation.

4.4.3. Supplementary information

Microarray design and sample correlation for autoAbs

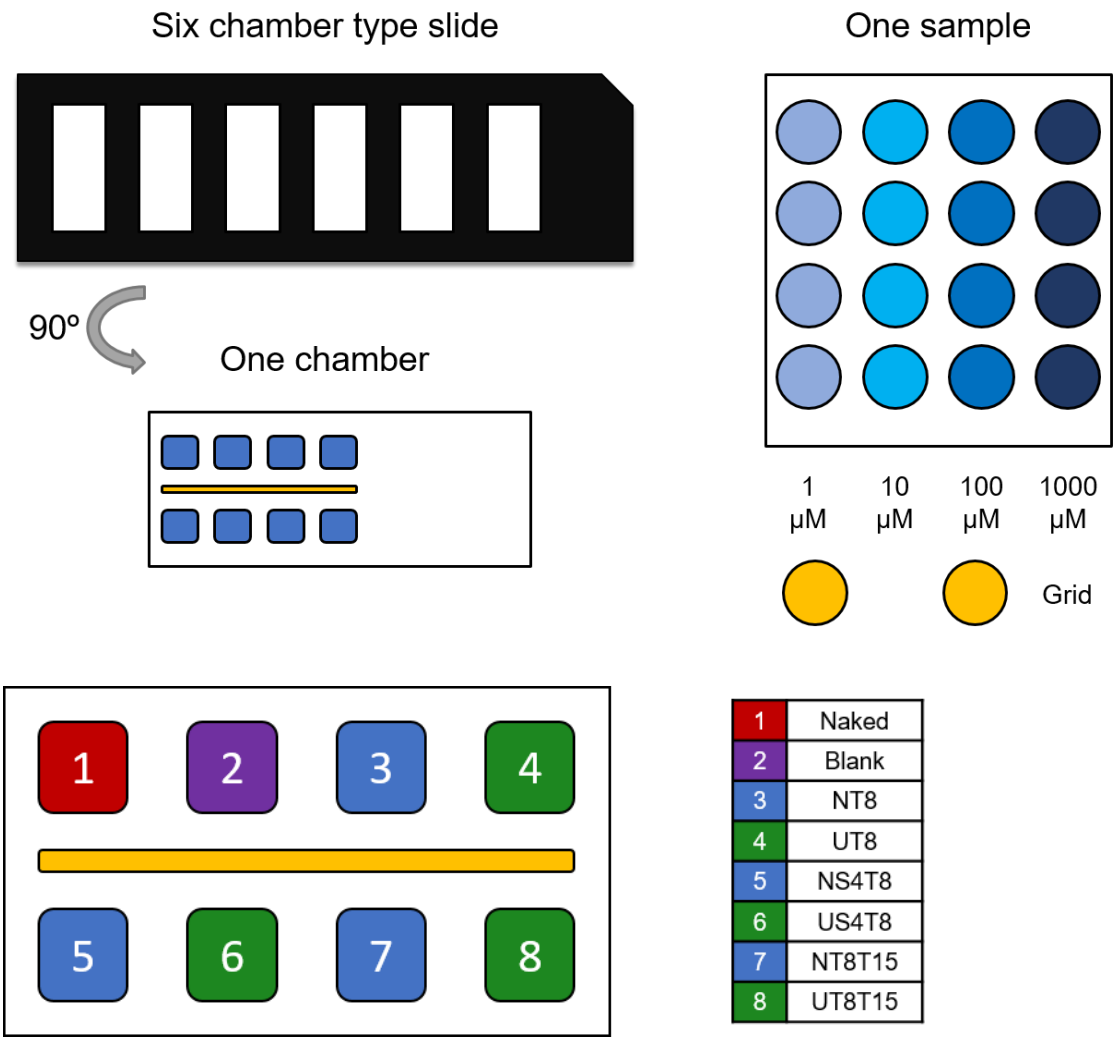

Microarray results for autoAbs

Fluorescence intensity measures were obtained through GlycoStationTM Reader 1200 (GlycoTechnica Ltd., Yokohama, Japan) and analyzed by ArrayVision™ software V8.0 (GE Healthcare, Tokyo, Japan). The software measures the fluorescence intensity signal and the background of the sample. The RFU is calculated by subtracting the sample background from the sample fluorescence to get the actual value. Sample printing on the microarray slide surface was conducted in the same conditions but with a different robot and a different type of pin (changing from a solid pin to a split pin), resulting in printing volume and RFU scale changes with no tendency between samples alteration. The experiment was conducted 3 times, the results showed reproducibility and the example displayed is one of the cases. Serum sample correlation: a) Healthy patient sera; b) Stage I human breast cancer serum; c) Stage IV human breast cancer serum.

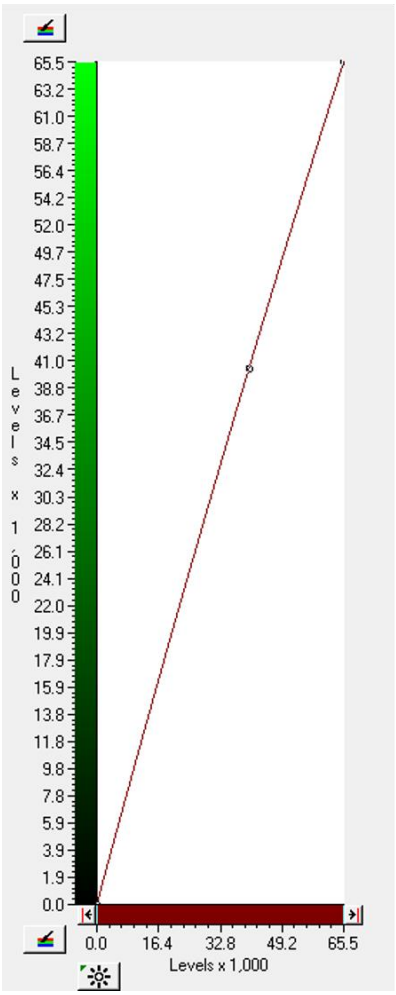
65.5
63.2
61.0
58.7
56.4
54.2
52.0
49.7
47.5
45.3
43.2
41.0
38.8
36.7
34.5
32.4
30.3
28.2
26.1
24.1
22.0
19.9
17.9
15.9
13.8
11.8
9.8
7.8
5.9
3.9
1.9
0.0
Levels x 1,000
0.0
16.4
32.8
49.2
65.5
Levels x 1,000

a)

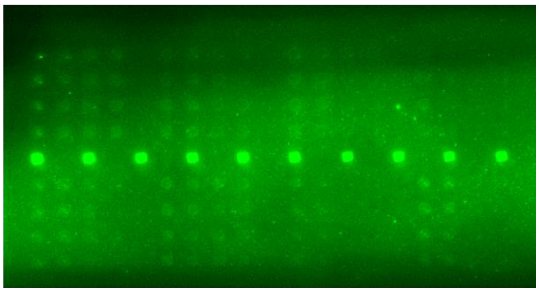

b)

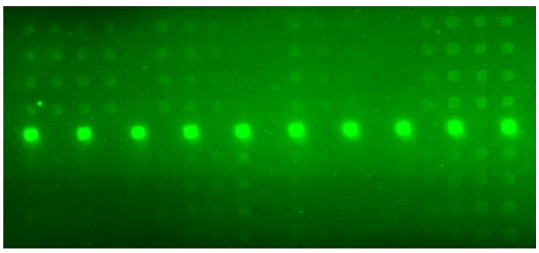

c)

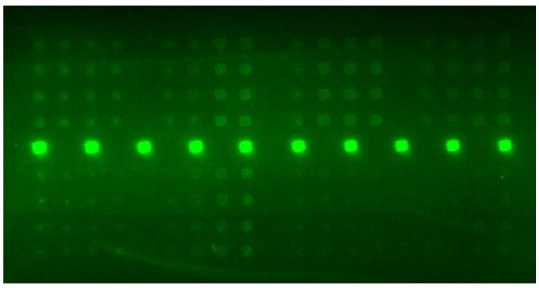

4.5. References

(1) Sehgal, C. M.; Weinstein, S. P.; Arger, P. H.; Conant, E. F. A Review of Breast Ultrasound. *J. Mammary Gland Biol. Neoplasia* **2006**, *11* (2), 113–123. https://doi.org/10.1007/s10911-006-9018-0.

(2) Carney, P. A.; Parikh, J.; Sickles, E. A.; Feig, S. A.; Monsees, B.; Bassett, L. W.; Smith, R. A.; Rosenberg, R.; Ichikawa, L.; Wallace, J.; Tran, K.; Miglioretti, D. L. Diagnostic Mammography: Identifying Minimally Acceptable Interpretive Performance Criteria. *Radiology* **2013**, *267* (2), 359–367. https://doi.org/10.1148/radiol.12121216.

(3) Jafari, S. H.; Saadatpour, Z.; Salmaninejad, A.; Momeni, F.; Mokhtari, M.; Nahand, J. S.; Rahmati, M.; Mirzaei, H.; Kianmehr, M. Breast Cancer Diagnosis: Imaging Techniques and Biochemical Markers. *J. Cell. Physiol.* **2018**, *233* (7), 5200–5213. https://doi.org/10.1002/jcp.26379.

(4) Waks, A. G.; Winer, E. P. Breast Cancer Treatment. *JAMA* **2019**, *321* (3), 288–300. https://doi.org/10.1001/jama.2018.19323.

(5) Tothill, I. E. Biosensors for Cancer Markers Diagnosis. *Semin. Cell Dev. Biol.* **2009**, *20* (1), 55–62. https://doi.org/10.1016/j.semcdb.2009.01.015.

(6) Mousa, S. Biosensors: The New Wave in Cancer Diagnosis. *Nanotechnol. Sci. Appl.* **2010**, *4* (1), 1–10. https://doi.org/10.2147/NSA.S13465.

(7) Wang, L. Early Diagnosis of Breast Cancer. *Sensors* **2017**, *17* (7), 1572. https://doi.org/10.3390/s17071572.

(8) Dincer, C.; Bruch, R.; Costa-Rama, E.; Fernández-Abedul, M. T.; Merkoçi, A.; Manz, A.; Urban, G. A.; Güder, F. Disposable Sensors in Diagnostics, Food, and Environmental Monitoring. *Adv. Mater.* **2019**, *31* (30), 1806739. https://doi.org/10.1002/adma.201806739.

(9) Basil, C. F.; Zhao, Y.; Zavaglia, K.; Jin, P.; Panelli, M. C.; Voiculescu, S.; Mandruzzato, S.; Lee, H. M.; Seliger, B.; Freedman, R. S.; Taylor, P. R.; Hu, N.; Zanovello, P.; Marincola, F. M.; Wang, E. Common Cancer Biomarkers. *Cancer Res.* **2006**, *66* (6), 2953–2961. https://doi.org/10.1158/0008-5472.CAN-05-3433.

(10) Duffy, M. J. J.; Harbeck, N.; Nap, M.; Molina, R.; Nicolini, A.; Senkus, E.; Cardoso, F. Clinical Use of Biomarkers in Breast Cancer: Updated Guidelines from the European Group on Tumor Markers (EGTM). *Eur. J. Cancer* **2017**, *75*, 284–298. https://doi.org/10.1016/j.ejca.2017.01.017.

(11) Basil, C. F.; Zhao, Y.; Zavaglia, K.; Jin, P.; Panelli, M. C.; Voiculescu, S.; Mandruzzato, S.; Lee, H. M.; Seliger, B.; Freedman, R. S.; Taylor, P. R.; Hu, N.; Zanovello, P.; Marincola, F. M.; Wang, E. Common Cancer Biomarkers. *Cancer Res.* **2006**, *66* (6), 2953–2961. https://doi.org/10.1158/0008-5472.CAN-05-3433.

(12) Lumachi, F.; Basso, S. M. M.; Marzano, B.; Bonamini, M.; Milan, E.; Chiara, G. B. 159 Relationship between Hormone Receptors, MIB-1 Index and Serum Tumour Markers CEA and CA 15–3 in Patients with PT1–2 Breast Cancer. *Eur. J. Cancer Suppl.* **2010**, *8* (3), 104–105. https://doi.org/10.1016/s1359-6349(10)70190-7.

(13) Wandall, H. H.; Blixt, O.; Tarp, M. A.; Pedersen, J. W.; Bennett, E. P.; Mandel, U.; Ragupathi, G.; Livingston, P. O.; Hollingsworth, M. A.; Taylor-Papadimitriou, J.;

Burchell, J.; Clausen, H. Cancer Biomarkers Defined by Autoantibody Signatures to Aberrant O-Glycopeptide Epitopes. *Cancer Res.* **2010**, *70* (4), 1306–1313. https://doi.org/10.1158/0008-5472.CAN-09-2893.

(14) Sauerborn, M.; Schellekens, H. B-1 Cells and Naturally Occurring Antibodies: Influencing the Immunogenicity of Recombinant Human Therapeutic Proteins? *Curr. Opin. Biotechnol.* **2009**, *20* (6), 715–721. https://doi.org/10.1016/j.copbio.2009.10.007.

(15) Lleo, A.; Invernizzi, P.; Gao, B.; Podda, M.; Gershwin, M. E. Definition of Human Autoimmunity — Autoantibodies versus Autoimmune Disease. *Autoimmun. Rev.* **2010**, *9* (5), A259–A266. https://doi.org/10.1016/j.autrev.2009.12.002.

(16) Zaenker, P.; Ziman, M. R. Serologic Autoantibodies as Diagnostic Cancer Biomarkers—A Review. *Cancer Epidemiol. Biomarkers Prev.* **2013**, *22* (12), 2161–2181. https://doi.org/10.1158/1055-9965.EPI-13-0621.

(17) Blixt, O.; Bueti, D.; Burford, B.; Allen, D.; Julien, S.; Hollingsworth, M.; Gammerman, A.; Fentiman, I.; Taylor-Papadimitriou, J.; Burchell, J. M. Autoantibodies to Aberrantly Glycosylated MUC1 in Early Stage Breast Cancer Are Associated with a Better Prognosis. *Breast Cancer Res.* **2011**, *13* (2), 1–16. https://doi.org/10.1186/bcr2841.

(18) Burford, B.; Gentry-Maharaj, A.; Graham, R.; Allen, D.; Pedersen, J. W.; Nudelman, A. S.; Blixt, O.; Fourkala, E. O.; Bueti, D.; Dawnay, A.; Ford, J.; Desai, R.; David, L.; Trinder, P.; Acres, B.; Schwientek, T.; Gammerman, A.; Reis, C. A.; Silva, L.; Osório, H.; Hallett, R.; Wandall, H. H.; Mandel, U.; Hollingsworth, M. A.; Jacobs, I.;

Fentiman, I.; Clausen, H.; Taylor-Papadimitriou, J.; Menon, U.; Burchell, J. M. Autoantibodies to MUC1 Glycopeptides Cannot Be Used as a Screening Assay for Early Detection of Breast, Ovarian, Lung or Pancreatic Cancer. *Br. J. Cancer* **2013**, *108* (10), 2045–2055. https://doi.org/10.1038/bjc.2013.214.

(19) Qiu, J.; Keyser, B.; Lin, Z.-T.; Wu, T. Autoantibodies as Potential Biomarkers in Breast Cancer. *Biosensors* **2018**, *8* (3), 67. https://doi.org/10.3390/bios8030067.

(20) Kobayashi, T. A Blood Tumor Marker Combination Assay Produces High Sensitivity and Specificity for Cancer According to the Natural History. *Cancer Med.* **2018**, *7* (3), 549–556. https://doi.org/10.1002/cam4.1275.

(21) Alsabti, E. A. K. Serum Immunoglobulins in Breast Cancer. *J. Surg. Oncol.* **1979**, *11* (2), 129–133. https://doi.org/10.1002/jso.2930110206.

(22) Nimmerjahn, F. Divergent Immunoglobulin G Subclass Activity Through Selective Fc Receptor Binding. *Science (80-.).* **2005**, *310* (5753), 1510–1512. https://doi.org/10.1126/science.1118948.

(23) Edechi, C. A.; Ikeogu, N.; Uzonna, J. E.; Myal, Y. Regulation of Immunity in Breast Cancer. *Cancers (Basel).* **2019**, *11* (8), 1–18. https://doi.org/10.3390/cancers11081080.

(24) Matsushita, T.; Takada, W.; Igarashi, K.; Naruchi, K.; Miyoshi, R.; Garcia-Martin, F.; Amano, M.; Hinou, H.; Nishimura, S. I. A Straightforward Protocol for the Preparation of High Performance Microarray Displaying Synthetic MUC1 Glycopeptides. *Biochim. Biophys. Acta - Gen. Subj.* **2014**, *1840* (3), 1105–1116. https://doi.org/10.1016/j.bbagen.2013.11.009.

(25) Tietjen, G. L.; Moore, R. H. Some Grubbs-Type Statistics for the Detection of Several Outliers. *Technometrics* **1972**, *14* (3), 583–597. https://doi.org/10.1080/00401706.1972.10488948.

(26) Artigas, G.; Hinou, H.; Garcia-Martin, F.; Gabius, H. J.; Nishimura, S. I. Synthetic Mucin-Like Glycopeptides as Versatile Tools to Measure Effects of Glycan Structure/Density/Position on the Interaction with Adhesion/Growth-Regulatory Galectins in Arrays. *Chem. - An Asian J.* **2017**, *12* (1), 159–167. https://doi.org/10.1002/asia.201601420.

(27) Uchiyama, N.; Kuno, A.; Tateno, H.; Kubo, Y.; Mizuno, M.; Noguchi, M.; Hirabayashi, J. Optimization of Evanescent-Field Fluorescence-Assisted Lectin Microarray for High-Sensitivity Detection of Monovalent Oligosaccharides and Glycoproteins. *Proteomics* **2008**, *8* (15), 3042–3050. https://doi.org/10.1002/pmic.200701114.

Chapter 5.
Final conclusions

A glycopeptide library containing 27 different compounds was successfully synthesized. This library was created using microwave assisted solid-phase peptide synthesis technology with some protocol modifications for optimization purposes.

The glycopeptides synthesized presented the Tn antigen or the sp^2-iminosugar-based Tn antigen mimic attached in different glycosylation patterns. The complete library consists of 1 non-glycosylated peptide, 5 natural monoglycosylated and 8 diglycosylated Tn antigen-containing glycopeptides, 5 monoglycosylated and 8 diglycosylated unnatural sp^2-iminosugar-based Tn antigen mimic-containing glycopeptides.

Previous samples were evaluated with monoclonal antibodies SM3, VU-3C6 and VU-11E2 in a microarray platform. The results can be summarized as follow:

The Threonine in position 8 plays an important role in binding between glycopeptides and the three mAbs. The binding was generally stronger with diglycosylated compounds than with compounds presenting just one glycan. The monoclonal antibody VU-11E2 was the most specific when referring to distinguish between different glycosylation patterns. The results obtained confirmed the suitability of the sp^2-iminosugar as Tn antigen mimic.

After microarray optimization to work with serum, the most promising compounds were tested with three different human serum samples from healthy individuals, stage I breast cancer patients and stage IV breast cancer patients.

The results obtained for autoantibodies showed different binding profiles. However, we observed one compound which displayed low affinity with healthy serum but a strong binding with stage I cancer serum. The mentioned compound is the sp^2-iminosugar-bearing

glycopeptide UT8 which can be considered as a promising early stage breast cancer biomarker candidate.

To the best of our knowledge, this is the first example of a MUC1-related glycopeptide mimetic enabling differential detection of autoantibodies in healthy and early breast cancer scenarios.

Acknowledgments

I would like to express my most sincere gratitude to my thesis supervisors, Professor Shin-Ichiro Nishimura, Professor Hiroshi Hinou, Professor Kenji Monde and Professor Fayna García-Martín of the Graduate School of Life Science at Hokkaido University. Their door was always open for discussion and they guided me in the right the direction. It was a great privilege and honor to work and study under their guidance.

I would like to personally thank Hokkaido University, the International Graduate Program and the Japanese Ministry of Education, Culture, Sports, Science and Technology for the scholarship that allowed me to conduct my doctoral program. Also, to the contributions of the Naito Foundation, the Spanish Ministerio de Ciencia, Innovación y Universidades, the Agencia Estatal de Investigación (project RTI2018-097609-B-C21), the Ministerio de Economía y Competitividad (SAF2016-76083-R) and the European Regional Development Funds (FEDER-UE) for their research grants that partly supported this work.

I cannot express enough thanks to our collaborators from Carmen Ortiz Mellet's group from the University of Seville (Spain) and the Institute for Chemical Research (Seville, Spain) for their contribution in my education and their continuous guidance. I would also like to acknowledge the service provided by the experts from the Hokkaido University Global Facility Center involved in the amino acid analysis measures. In addition, I am gratefully indebted to all my research colleagues and all the Nishimura laboratory members for all their help and years together and alto to all the people who have supported me to complete my research.

Last but not least, I must express my deepest gratitude to my wife for providing me with unfailing support and continuous encouragement throughout all my years of study. To my mother, for her love, caring and sacrifices for educating and preparing me for the future. To my all my friends who taught so much and their priceless advice. This accomplishment would not have been possible without them.